MODELS FOR THE MORPHOLOGY AND MORPHOGENESIS OF THE AMMONOID SHELL

By

RAUL VICENCIO

A thesis
Submitted to the School of Graduate Studies
in Partial Fulfilment of the Requirements
for the Degree
Doctor of Philosophy
McMaster University
(May 1973)

MODELS FOR THE AMMONOID SHELL

DOCTOR OF PHILOSOPHY (1973)
(Geology)

McMASTER UNIVERSITY
Hamilton, Ontario

TITLE: Models for the morphology and morphogenesis of the ammonoid shell

AUTHOR: Raul Vicencio

SUPERVISOR: Professor G.E.G. Westermann

NUMBER OF PAGES: ix + 116 + Appendix

SCOPE AND CONTENTS: The process of accretionary growth in molluscs is examined and a new growth equation suitable for accretionary growth is proposed and derived. The morphology of the shell in the Ammonoidea (Mollusca, Cephalopoda) is described and the morphogenesis simulated by means of theoretical models. In the case of the characterization of morphology, the shell is described by a set of objective descriptors that can be used in taxonomy. The morphogenesis of the ammonoid shell is explained in terms of static equilibrium of the secreting mantle and a diffusive process that mediates the actual precipitation of shell material on the growing edge of the shell. Different morphologies arise from varying the boundary conditions in the resulting differential equations.

ABSTRACT

A new theoretical equation for growth, suitable for accretionary growth, is developed. Allometric growth is a special case of the phenomenon of anisometry and is probably produced by the combination of two or more growth processes governed by exponential laws.

The morphology of the molluscan shell in general, and of the ammonoid cephalopods in particular, is represented by a set of descriptive models that emphasise the instantaneous cross-section rather than the total accretionary form. A measure of complication for non-rectifiable curves (of which the ammonoid suture line is an example) is proposed. A mechanistic model for the morphogenesis of the shell simulates the rates at which shell material is accreted and the static equilibrium of the mantle-shell edge and reproduces morphologies that closely resemble those of actual fossil ectocochliate cephalopods. A possible explanation of the phenomena of homeomorphy and iterative evolution, common in ammonoids, lies in their ability to produce similar morphologies with different sets of morphogenetic instructions.

ACKNOWLEDGEMENTS

Many people helped in diverse ways to the completion of this thesis: G.E.G. Westermann, my thesis supervisor, provided constant encouragement; the following individuals gave helpful criticism of some of the ideas presented here, some of which have been incorporated in the body of the thesis: J.C. Chamberlain, Jr., D.M. Davies, R.H. Hall, G.V. Middleton, H. Robinson and H.M. Verma, all then of McMaster University; D.M. Raup, University of Rochester; R.A. Reyment, Universitet Uppsala; and A. Seilacher, Universität Tübingen; J. Coward at McMaster gave advice on computer programming; G. Winton made the drawings; Helen Elliott typed the manuscript. To all of them I give sincere thanks.
I am grateful for financial assistance received from McMaster University, the Geological Survey of Canada and the National Research Council (grants to G.E.G. Westermann).

TABLE OF CONTENTS

LIST OF TABLES

LIST OF FIGURES

CHAPTER 1

INTRODUCTION

The ectocochliate cephalopods, all extinct with the exception of the Indo-Pacific genus Nautilus, constitute a remarkably homogeneous group, as far as their natural history is concerned. Exclusively marine and largely nektonic, they dominated the seas during most of the Palaeozoic and all the Mesozoic, when they form a substantial portion of the fossil invertebrate faunas of all marine zoogeographical regions and environments; their ubiquity was increased by the widespread post-mortem dispersal of their shells, most of which could be transported by drift far beyond the area of their living range (Reyment, 1958, 1970). In a similar manner, the dead shells of present day Nautilus drift to the Gulf of Siam and the shores of the Japanese islands, more than 2000 km away from the nearest extension of the live animal's range (Stenzel, 1965).

The morphology of the shell is relatively simple and probably for this reason the literature on its geometry is extensive (see Thompson, 1942, and Raup, 1966 for reviews). Raup (1966, 1967) produced a model that accounts for the coiling geometry of accretionary shells in an illuminating way; as he points out, however (Raup, 1966, p.1181), the total morphology of any given shell comprises many other characters not considered

by the model. Some of those characters are analyzed in the present work (Chapters 3 and 4) and some have escaped a systematic treatment (Chapter 5).

Among the ectocochliate cephalopods, the Ammonoidea are striking because of the variety of their external shell morphology. Many different combinations of their morphological attributes were produced in the course of their evolution, and since most of these attributes are easily measured, the taxonomy of the ammonoids and then their phylogeny, have been the subject of intensive study for the last one hundred years. This study has been extremely rewarding from the viewpoint of biostratigraphy, but much less so for the study of evolution, a field to which ammonoids promised to give much useful evidence.

In biostratigraphy, the discriminatory power of ammonoids as time markers remains unexcelled. This is particularly true of the Mesozoic, where although biostratigraphic frameworks based on faunal successions of other fossil groups are practicable, "... such schemes of classification and correlation are makeshifts and liable to be overthrown by the discovery of a single ammonite". (Arkell, 1956, p.13).

The biostratigraphic zonation of the Mesozoic is accordingly based entirely on ammonite successions and it allows a time resolution in worldwide biostratigraphic correlation of the order of one million years; finer resolutions are attainable in local successions.

In evolutionary palaeontology, on the other hand, far less success has been forthcoming. We know that these animals evolved fast, (ca. one species per half million years), but the significance of most of their adaptations is obscure, as is the function of the details of their morphology. Or, if a function is suspected, its mechanics are unclear and remain to be worked out. Although something is known about the hydrostatics (Trueman, 1941; Reyment, 1958; Raup, 1973) and the hydrodynamics (Kummel and Lloyd, 1955; Chamberlain, 1971) of the shell, these factors do not seem to have played a very important role in the evolution of the ammonoids, and certainly are not reflected in their taxonomy or their inferred phylogenetic lineages. In the Ammonitina, the mode of variation, origin and significance of the three most significant morphologic characters used in the taxonomy of the group, namely the coiling geometry, ribbing and septal structure, are the subject of varying interpretations; some mechanical interpretations are available (Pfaff, 1911), including some based on experiment (Chamberlain, 1971), but their significance is contested and is at best unclear (Mutvei, 1967; Westermann, 1971).

From a methodological viewpoint, since the function of the structure is not well known, no optimal configuration, or paradigm, for it has been devised (Rudwick, 1964); nor is it evident that one can be calculated, on mechanical grounds, for the several alternative and concurrent functions proposed. Even

if a paradigm can be set up, there is a distinct possibility that it may not be unique (Chapter 4).

In the evolution of many ammonoid lineages, particularly in the Mesozoic, a phenomenon, which has been called iterative evolution (Salfeld, 1913) is conspicuous: at the start of a new lineage (usually at the taxonomic rank of a family), a certain set succession of morphologic changes takes place. This succession affects particularly the degree of inflation and the ribbing style (see examples in Arkell et al., 1957). The repetition of the series of changes in shape and ornamentation in succeeding or unrelated lineages awaits a complete explanation; one is attempted in Chapter 4.

We can divide the main problems facing the student of ammonoid morphology then, into those of the attainment of the shell dimensions and proportions, the objective characterization of the resulting morphology, the mechanistic problem of morphogenesis, and the adaptive significance of the morphologic features of the shell. This thesis attempts to provide answers to these questions in the following three chapters, as follows: Chapter 2, growth; Chapter 3, characterization of shell morphology; and Chapter 4, morphogenesis of the shell.

CHAPTER 2

GROWTH AND RELATIVE GROWTH: SOME ANALYTIC MODELS

2.1 Size and growth

To contrast the situation with that in the physical sciences (Weaver, 1955), progress in the field of developmental morphology has been impeded, to a greater extent than in other fields of biology, by three main factors: (a) growth phenomena seem to be strongly coupled; in general, a study of the different variables in isolation reveals different functional relationships than a consideration of several or many of them in concert would, the total appearing greater than the sum of its parts. (b) In general, growth seems to have strong nonlinear components. It is only by simplifying growth processes beyond recognition that one can represent them by linear approximations. Some degree of success in the simplest cases is possible, but the explanatory power of the resulting functional relationships is questionable. This is apparently the case with Huxley's (or Nomura's) allometry equation, as shown below. (c) Many morphogenetic processes can, and apparently do, develop instability, that is, once small perturbations, random or otherwise, occur, they tend to propagate. As a result, fairly small causes can account for important effects; this is familiar to the student of phenomena regulated by exponential laws.

Both size and growth are continuous scalar quantities and by their nature should be measured on ratio scales. The most appropriate dimensions for size (y) are: length, area, volume and mass. Since mass usually assumes a constant density, the last two are roughly equivalent and one uses whichever is easier.

When measuring changes in dimension, whether ontogenetic or phylogenetic, caused by adaption or randomly, one must clearly separate effects due to Galileo's "principle of similitude" from those due to other causes (changes in function, innovations, etc.). The "principle of similitude" should be broadly understood in order to encompass changes in dimensions needed to comply with the laws of physics and chemistry (mechanical constraints being the most common, but those arising from fluid dynamics, diffusion, etc. being by no means rare). As it will become evident, these changes account for much of what is usually called allometry, heterauxesis, and heterogonic growth (also individual allomorphosis).

2.2 Previous work

The literature on the growth of organisms is enormous. No attempt at a revision shall be made here, except as it pertains to some of the models that will be formulated in this chapter. Comprehensive works and reviews include: Huxley (1932), Thompson (1942), Clark and Medawar, eds. (1945), Brody (1945), Zuckerman,

ed. (1950), Teissier (1960), Needham (1964), Bonner (1968) and Gould (1966, 1971).

Throughout the history of the subject, two main approaches have characterized it; on the one hand, the study of relative growth, that is, the increase in size of some organ or part of an organism with respect to another or to the whole organism; on the other, absolute growth, that is, the increase in size with age. Although the latter is a subject of everyday experience, the former is not intuitively obvious; one of the earliest clear statements of the change in proportions with increase in size was given by Galileo (1638). The "principle of similitude" (Thompson, 1942), is demonstrated on the Second Day of his dialogue, using the example of the bones (femora) of animals, and man-made structures. He correctly recognized that the ratio stress: length is not constant for constant proportions, but increases proportionally to size. As Thompson (1942) points out, Galileo was also aware of the increase in bending moments in longitudinal structures with increased length, as proved by his discussion of beams supported in one end.

Quantitative results obtained from actual measurements of brain and body weights were fitted by Snell (1891) to a bivariate power law,

$$y = bx^{\alpha} \qquad (2.2.1)$$

or, in its logarithmic form, the straight line,

$$\log y = \alpha \log x + \log b \qquad (2.2.2)$$

where x = body weight and y = brain weight, with α = slope and $b = y_{x=1}$.

Several others (Dubois, 1897, 1922; Lapicque, 1907) also made use of the power law, but all of them, as did Snell, assumed the same value for the exponent α, for all lines, based on theoretical considerations, instead of determining α from the data themselves.

Nomura (1926) seems to have been the first to fit extensive sets of bivariate data to a power function, estimating all parameters from his actual measurements, which consisted of the dimensions of some fresh-water bivalves. Nomura's work was little noticed in the West, however, and the use of a power law to explain relative growth did not become generalized until Huxley (1932) reintroduced it in his book "Principles of Relative Growth", under the name of heterogony (later called allometry).

No multivariate form of the allometry equation is in general use, although Jolicoeur (1963) has proposed and formulated such a generalization. Thompson (1917) introduced his cartesian transformations, which accomplish essentially the end of a multivariate equation, but in a graphical manner, by means of an orthogonal grid superimposed on one of two forms to be compared and then deformed so that it passes through homologous points in

the second form. Although these transformation grids provide a very striking insight into the patterns of growth gradients (being akin to Needham's (1942) developmental fields), they have defied an analytic treatment until Sneath (1967) subjected them to trend-surface analysis. It is interesting to note that Huxley (1932) remarks that he arrived at the allometry equation while attempting to obtain an analytic function to quantify the cartesian transformations.

The second approach, that of a growth function, relating size to age in an analytic or empirical formula, has been taken by many authors (reviewed comprehensively by Brody, 1945, Medawar, 1945 and Bertalanffy, 1960). There is an infinity of empirical functions that can be fitted to growth data, and none of them is very simple or provides much explanatory power, so they need not detain us. As to the analytical functions, there are four now currently in use: the Verhulst-Pearl equation (also called monomolecular-autocatalytic), first employed in population growth studies (Pearl and Reed, 1923); the Gompertz equation (Laird et al., 1965); the Pütter-Bertalanffy equation (von Bertalanffy, 1960); and the Zotina-Zotin equation (Zotina and Zotin, 1972, with bibliography). They will be briefly discussed in the next section, together with some alternatives to them.

2.3 Models for anisometric growth

2.3.1 An empirical growth function. Growth in organisms is, in general, a function of both size and age:

$$\frac{dy}{dt} = G = F(y,t) \qquad 2.3.1.1$$

One could then measure the changes in growth rate at constant age and at constant size and integrate the equation

$$dG = \frac{\partial G}{\partial y} dy + \frac{\partial G}{\partial t} dt \qquad 2.3.1.2$$

Then, performing a second integration, an experimental equation for growth could be obtained which would be of practical use. If the same process were performed with another size parameter, time could be eliminated as a variable from the two resulting equations and in general, a two-variable anisometry relationship would be obtained. A model like this, although practical, lacks explanatory power and generality and cannot, even with modifications, be applied outside of the range of observations from which it was derived. It is this characteristic that prompts the search for more general models.

2.3.2 Analytical models. It is also possible to assume a model in which different constraints act upon the increase in size at a given size and instant of time. Essentially,

this amounts to expressing the growth process in terms of differential equations. The equations are then integrated by analytic or numerical methods, whichever are appropriate. In general, in this approach one must balance a need for realistic approximations that make sense from the viewpoint of the physiology of the organism involved on the one hand, and on the other, the need for reasonably simple relationships that would in fact reflect the complexity of the growth process.

In general, growth equations can be derived from the conditions for growth rate.

We will assume

$$y' = \frac{dy}{dt} = f(y,t) \qquad 2.3.2.1$$

where y is a measure of size and t is time.

If one assumes certain functional relationships between growth rate (y'), y and t, the result is a differential equation which, upon integration, becomes a deterministic equation expressing the dependence of size on time.

Two further inputs can be superimposed on the differential equation: one corresponding to random departures from the deterministic value and the other, to systematic, periodic fluctuations in the growth rate. The first is a high frequency input (noise), having a zero expected value (average); it can be simulated by a random number generator in numerical examples. The second is a lower frequency input, corresponding

to seasonal variations in growth rate. Note that, since the growth is accretionary, it is the growth rate and not the size, that should be modified by these inputs.

The general differential equation for growth then becomes:

$$y' = f(y, t) \{ K \mid \sin(at + b) \mid \} + \varepsilon(t) \qquad 2.3.2.2$$

where a = frequency and b = phase angle

$\varepsilon(t)$ is a random function and its expected value

$E \{ \varepsilon(t) \} = \bar{\varepsilon} = 0$

In this model the growth rate is multiplied by a factor $0 \leq K|\sin(at + b)| \leq K$, so that it is assumed that the periodicity is simple. If more complicated periodicity is present, this factor can be replaced by a Fourier series fitted to observed data, or by a step function whose effect would be to change the growth rate after a certain time threshold is passed.

If either a longer time average or only the cumulative effect of growth are needed, the periodic factor can be dropped; if several observations are available and/or a best fit function is desired, the error term can be dropped and its role taken by the standard deviations of the fitted parameters, estimated from the data; they are then a measure of departure from the deterministic function.

In the table that follows, these two courses have been taken, that is, the different growth equations have been derived from the model of equation 2.3.1.1.

There are several requirements that a growth equation must fulfil: (a) it must be analytical, continuous and differentiable. If it is not, there is not much advantage to be gained by the use of this function; in particular, there would not be a reduction in complication over just having the raw data. The requirement of continuity exists because to any age we should be able to ascribe a size; that of differentiability, because a growth rate should be ascribed to every age. (b) Growth must be incremental, that is, the first derivative of the growth function should be everywhere non-negative. This condition applies particularly to the case of accretionary growth, but in general, it is assumed that wastage and resorption take place by other mechanisms than those that cause growth. (c) The growth rate must approach zero asymptotically as time increases. (d) Maximum size must be finite. (e) Both the growth rate and the size functions must not have discontinuities or singular points in their domains of existence, that is, for time $0 \leq t \leq \infty$; (f) The value of all parameters or properties must be independent of (not fixed by) the form of the equation.

For example, in the table below (Table 2.3.2.1) equations 1-3 are unsuitable as growth equations by three criteria: growth rate is either constant or ever increasing,

maximum size is infinite, and the times of minimum and maximum growth rate are fixed.

Next come two equations which have been used as models of growth in populations and also sometimes in individuals; the Verhulst-Pearl (logistic) (Pielou, 1969) equation and the Gompertz equation (Goel et al., 1971). Both are sigmoidal curves, a desirable characteristic in a growth curve, with an initial period in which growth is roughly proportional to size, followed by approximately linear growth, followed by declining growth, asymptotically approaching the maximum size, finite in both cases. However, both curves have their maximum growth rates at fixed sizes, the Verhulst-Pearl equation at one-half the maximum size and the Gompertz at slightly over one-third the maximum size. So that all commonly used growth equations are inappropriate to their purpose. Equations 6-10 in the table are believed to be new and they all fulfil the four conditions enumerated above. These equations can be solved for y either analytically or numerically and are probably the simplest to fulfil all four requirements. There is possibly an infinite number of functions that could be used as growth equations and only those cases which correspond to simple, physiologically plausible growth conditions, are dealt with.

If what is desired is the relationship between two size variables irrespective of time, the four restrictions listed above need not all be heeded, as these constraints depend on the time.

TABLE 2.3.2.1

Equations for Growth

1). $y' = K_1 \quad dy = K_1 dt \quad y = K_1 t + K_2 \quad$ at $t = 0 \quad y = y_o$

integrating: $y = K_1 t + y_o$ Linear

2). $y' = K_1 t + K_2 \quad d_y = K_1 t dt + K_2 dt$

integrating: $y = K_1 t^2 + K_2 t + y_o$ Quadratic

3). $y' = K_1 y \quad \frac{dy}{y} = K_1 dt \quad \ln y = K_1 t + K_2$

$y = y_o \exp(K_1 t)$ Where $K_2 = y_o$ when $t = 0$

Exponential

4). $y' = y(K_1 - K_2 y) \quad \frac{dy}{y} + \frac{K_2\, dy}{K_1 - K_2 y} = K_1\, dt$

$y = \frac{K_1/K_2}{1 + \exp(-K_1 t)/K_3 K_2}$ let $t \to \infty \; y_f = \frac{K_1}{K_2}$

Logistic or Verhulst-Pearl

$y = \frac{y_f}{1 + A \exp(-Bt)}$

Maximum growth: $y'' = y' (K_1 - 2K_2 y) \quad y_{y'max} = \frac{yf}{2}$

$t_{y'max} = \frac{1}{K_1} \ln (K_3 K_2) = -\frac{1}{B} \ln A$ where $1/K_3 K_2 = A \quad K_1 = B$

Table 2.3.2.1 (continued)

5). $y' = K_1\, y \exp(-K_2 t)$ $\quad \frac{dy}{y} = K_1 \exp(-K_2 t)\, dt$

$\ln y = -\frac{K_1}{K_2} \exp(-K_2 t) + K_3$ $\quad$ let $t \to \infty$, $K_3 = \ln y_f$

$$y = y_f \exp\left\{ -\frac{K_1}{K_2} \exp(-K_2 t) \right\} \quad \text{Gompertz}$$

Maximum growth: $y'' = K_1 \exp(-K_2 t)\ (-K_2 y + y')$;

$t_{y'max} = -\frac{1}{K_2} \ln\left(\frac{K_2}{K_1}\right)$; $\quad y_{y'max} = y_f \exp(-1) \approx 0.36\, y_f$

6). $y' = K_1\, t \exp(-K_2 t)$ $\quad dy = K_1 t \exp(-K_2 t)\, dt$

$y = -\frac{K_1}{K_2} (K_2 t + 1) \exp(-K_2 t) + K_3$ $\quad$ let $t \to \infty$: $\quad K_3 = y_f$

$$y = y_f - \frac{K_1}{K_2^2} (K_2 t + 1) \exp(-K_2 t)$$

Maximum growth: $y'' = K_1 \exp(-K_2 t)\ (-K_2 t + 1)$; $t_{y'max} = \frac{1}{K_2}$

$y_{y'max} = y_f - \frac{2K_1}{K_2^2} \exp(-1) = y_f - \frac{.7358 K_1}{K_2^2}$

7). $y' = K_1\, y \exp(-K_2 t - K_3 y)$ $\quad \frac{\exp(K_3 y)}{y}\, dy = K_1 \exp(-K_2 t)\, dt$

$\ln y + K_3 y + \ldots + \frac{(K_3 y)^n}{n \cdot n!} + \ldots = -\frac{K_1}{K_2} \exp(-K_2 t) + K_4$

$$F(y, K_3) = F(y_f, K_3) - \frac{K_1}{K_2} \exp(-K_2 t)$$

Table 2.3.2.1 (continued)

Where $F(x,a) = \ln x + ax + \frac{a^2 x^2}{2.2!} + \ldots + \frac{(a x)^n}{n.n!} + \ldots$

solving for t : $t = -\frac{1}{K_2} \ln \left[\frac{K_2}{K_1} \left\{ F(y_f, K_3) - F(y, K_3) \right\} \right]$

Maximum growth is then calculated numerically.

8). $y' = K_1 t \exp(-K_2 t^2)$ $\quad dy = K_1 t \exp(-K_2 t^2) dt$

$y = -\frac{K_1}{2K_2} \exp(-K_2 t^2) + K_3$ let $t \to \infty$, then $K_3 = y_f$

and redefining $K_1 = \frac{K_1}{2 K_2 y_f}$

$$y = y_f \left\{ 1 - K_1 \exp(-K_2 t^2) \right\}$$

Maximum growth: $y'' = K_1 (1 - 2K_2 t^2) \exp(-K_2 t^2)$

$t_{y'max} = \frac{1}{\sqrt{2 K_2}}$ $\quad y_{y'max} = y_f \left\{ 1 - K_1 \exp(-0.5) \right\}$

9). $y' = K_1 y \exp(-K_2 t^2)$ $\quad \frac{dy}{y} = K_1 \exp(-K_2 t^2) dt$

$\ln y = K_1 \int \exp(-K_2 t^2) dt + K_3$ $\quad$ if $t \to \infty$, $K_3 = \ln y_f$

$$y = y_f \exp \left\{ K_1 \int \exp(-K_2 t^2) \, dt \right\}$$

Table 2.3.2.1 (continued)

Integrating between limits:

$$\ln \frac{y_\infty}{y_o} = K_1 \int_0^\infty \exp(-K_2 t^2)dt = \frac{K_1}{2}\sqrt{\frac{\pi}{K_2}}$$

$$y_f = y_\infty = y_o \exp\left(\frac{K_1}{2}\sqrt{\frac{\pi}{K_2}}\right)$$

Maximum growth: $y'' = K_1 \exp(-K_2 t^2)\left\{-2K_2 ty + y'\right\}$

$$t - \frac{K_1}{2K_2} \exp(-K_2 t^2) = 0$$

The solution of this equation, which can be obtained numerically, is $t_{y'max}$.

$y_{y'max}$ is obtained by substituting $t_{y'max}$ into equation 9.

10). $y' = K_1 yt \exp(-K_2 t^2)$ $\quad \frac{dy}{y} = K_1 t \exp(-K_2 t^2)\, dt$

$$\ln y = -\frac{K_1}{2K_2} \exp(-K_2 t^2) + K_3. \quad t\to\infty,\ K_3 = \ln y_f$$

and redefining $K_1 = \frac{K_1}{2K_2}$:

$$y = y_f \exp\left\{-K_1 \exp(-K_2 t^2)\right\}$$

Maximum growth: $y'' = K_1 \exp(-K_2 t^2)\left\{y - 2K_2 t^2 y + t_{y'}\right\}$

Table 2.3.2.1 (continued)

$$y - 2K_2 t^2 y + t K_1 y t \exp(-K_2 t^2) = 0 \quad /: \; y \; (\neq 0)$$

$$t^2 \left\{ K_1 \exp(-K_2 t^2) - 2K_2 \right\} + 1 = 0$$

Solving this numerically we obtain $t_{y'max}$

$y_{y'max}$ is obtained by substituting $t_{y'max}$ into equation 10.

11). $y' = K y (t_m - t)$

$\ln y = K t (t_m - 0.5t) + K_1$ if $t=t_m$, $y=y_m$ and

$$K_1 = \ln y_m - \frac{K}{2} t_m^2$$

$$y = y_m \exp\left\{ -\frac{K}{2} (t_m - t)^2 \right\}$$ Zotina-Zotin equation

Maximum growth: $y'' = K y_m \left\{ K(t_m - t)^2 - 1 \right\} \exp\left\{ -\frac{K}{2} (t_m - t)^2 \right\}$

if y" equals zero, then

$K (t_m - t)^2 = 1$

$t_{y'max} = t_m - \frac{1}{\sqrt{K}}$

$y_{y'max} = y_m \exp\left\{ -\frac{K}{2} (t_m - t_m + \frac{1}{\sqrt{K}})^2 \right\} = y_m \exp(0.5) \approx 0.6 y_m$

2.3.3. An equation for organic growth and its use. In the collection of data on the growth of organisms, two main types of study are used (Tanner, 1962): in the longitudinal study an organism is followed through time and its dimensions are recorded at successive intervals; in the cross-sectional study, a set of organisms is measured in each occasion, and the identity of each of them is not ascertained. An advantage of the use of growth equations over that of bivariate equations (in which one dimension is expressed as a function of another) is that both longitudinal and cross-sectional studies can be analyzed by a growth equation, and the interrelations of both types of data can be ascertained.

In the pages that follow, the model of equation 7, in Table 2.3.2.1 is developed, an anisometry function is deduced from it, and a least-squares fit to measured data by the method of steepest descent (Marquardt, 1963) is provided, together with a computer program to carry out the fit.

Similar functions are deducible from the other growth equations in Table 2.3.2.1; equation 7 has been chosen because of its appropriateness to accretionary growth (see below), its generality (it contains terms in t and y) and its resemblance to actual growth curves. No simple interpretation is possible for all the parameters in equation 7, but the differential equation is consistent with a model in which each unit of tissue (normally a cell) is capable of producing a certain

amount of extra tissue in a given length of time, this capability deteriorating through time due both to decreased effectiveness of the control system for growth and the random death of tissue units (cells) which possess then a characteristic half-life. A region is eventually reached at which there is effectively no further growth. In a non-accretionary structure, attrition or resorption will take place, but in an accretionary one, size remains stationary.

It is assumed that the specific growth rate $(\frac{1}{y}\frac{dy}{dt})$ decreases steadily through time, due to two causes: an exponential time damping, as proposed first by Wright (1926); and a further damping of the resulting rate, operative whenever growth itself is effected by diffusion processes. As in the majority of cases growth is mediated by active transport processes, this type of damping does not exist (the damping coefficient β would then equal zero); however, in the growth of molluscan shells and other accretionary structures, diffusion plays an important role in the extracellular transport and deposition of shell material (Digby, 1968; Wilbur and Simkiss, 1968). Under simple conditions of diffusion with constant diffusion coefficient and a first-order chemical reaction of the diffusing substance, the diffusion equation takes the form of a negative exponential slowed down with respect to the case of diffusion without reaction (Crank, 1956, p.121 ff.); accordingly, to an increase in size would correspond a damping

off of the specific growth rate.

Let y be a measure of size (a length, area, volume or weight) in a growing organism, and t, time.

If the growth rate, $y' \left(= \frac{dy}{dt}\right)$ is proportional to size and is damped with both size and time:

$$y' = K y e^{-(\alpha t + \beta y)} \qquad 2.3.3.1$$

Where K is a proportionality constant and α and β are damping coefficients with respect to age and size, respectively.

Upon integration equation 1 becomes:

$$\ln y + \frac{\beta y}{1.1!} + \frac{(\beta y)^2}{2.2!} + \ldots + \frac{(\beta y)^n}{n.n!} + \ldots = -\frac{K}{\alpha} e^{-\alpha t} + C \qquad 2.3.3.2$$

where C is a constant of integration. The infinite series in the left hand side of equation 2.3.3.2 is a single-valued, always convergent function for all positive y, a condition consistent with the nature of the problem.

Call the left hand side expression in equation 2.3.3.2 $F(y,\beta)$.

To determine the value of the constant C, let the final size, y_∞, be the unit of measurement. Thus:

$$F(1,\beta)_{t\to\infty} = -\frac{K}{\alpha} e^{-\alpha t} + C = C \qquad 2.3.3.3$$

So that equation 2.3.3.2 is reduced to:

$$\frac{K}{\alpha} e^{-\alpha t} = F\cdot(1,\beta) - F\ (y,\beta) \qquad 2.3.3.4$$

Equation 2.3.3.4 cannot be solved for y explicitly. However, since it is a single-valued function of both t and y, it is feasible to solve the equation for t and make the calculations with y as the independent variable:

$$t = -\frac{1}{\alpha} \ln\left[\frac{\alpha}{K}\left\{F\ (1,\beta) - F\ (y,\beta)\right\}\right] \qquad 2.3.3.5$$

Alternatively, equation 2.3.3.4 can be solved by numerical methods. Fig. 2.3.3.1 shows several growth curves generated by choosing different values for α, β and K.

Rate of growth. As can be seen upon examination of equation 2.3.3.1, growth rate will start at a finite value for $t = 0$, increase to a maximum value for a certain finite value of t and then decrease towards zero for $t \to \infty$.

To find the time at which growth rate is maximum, equation 2.3.3.1 is differentiated with respect to time:

$$y'' = y'\left\{K \exp(-\alpha t-\beta y) - \alpha - \beta y'\right\} \qquad 2.3.3.6$$

Setting $y'' = 0$ produces the trivial solution $y' = 0$, $y = 0$ and introducing equation 2.3.3.5 in the remaining factor:

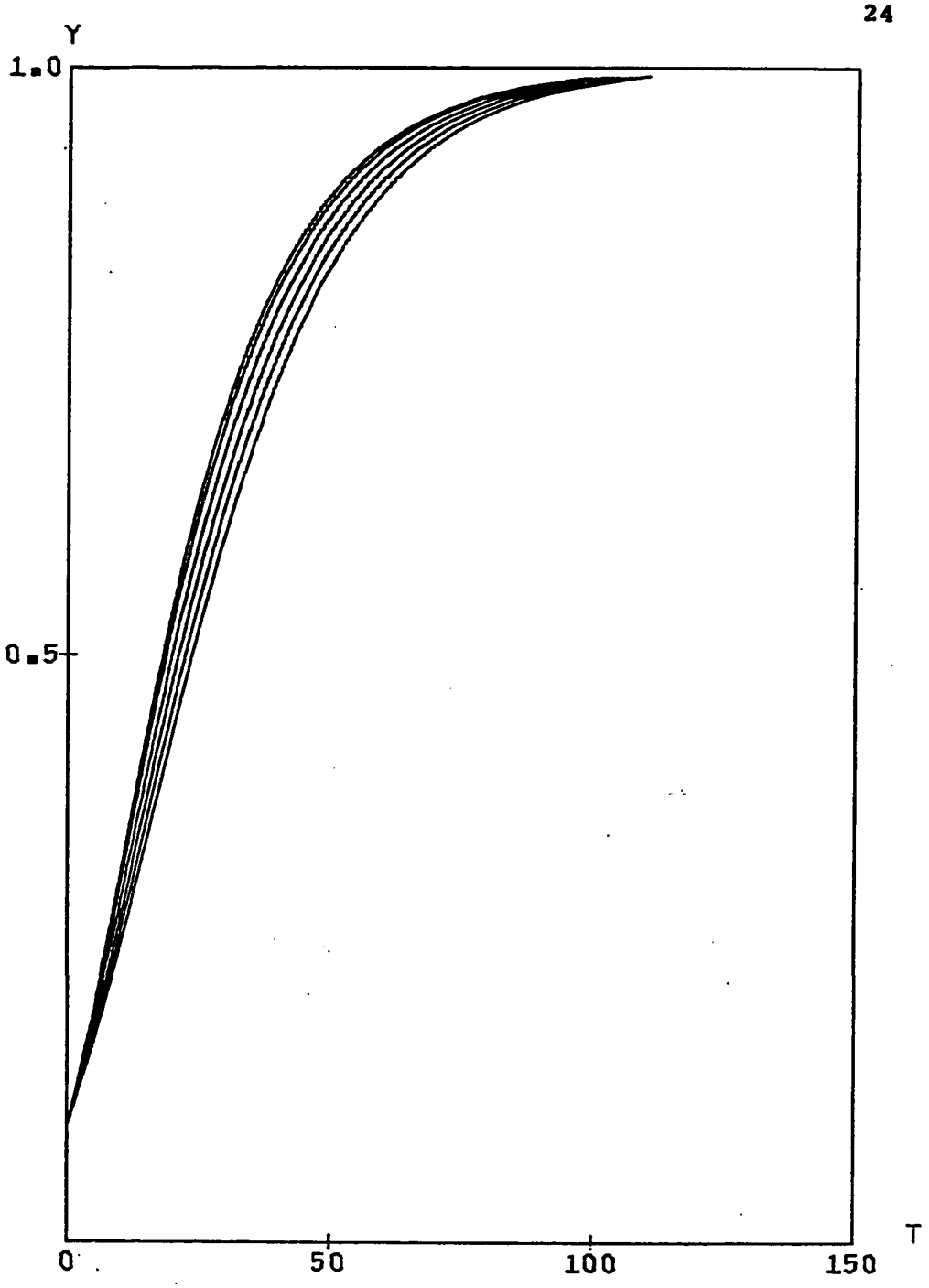

Fig. 2.3.3.1 A family of typical simulated growth curves (size vs. age), derived from equation 2.3.3.4 (double-damped growth equation)

$$\left(1-\beta\right) \exp \ln\left[\frac{\alpha}{K}\left\{F\ (1,\beta) - F\ (y,\beta)\right\} - \beta y\right] - \alpha = 0 \qquad 2.3.3.7$$

dividing 2.3.3.7 by α produces the trivial solution $\alpha = 0$ and:

$$\left\{F\ (1,\beta) - F\ (y,\beta)\right\} \exp\left\{-\beta y \quad (1 - \beta y)\right\} - 1 = 0 \qquad 2.3.3.8$$

Equation 2.3.3.8 is solved numerically for $y_{y'max}$, which, as can be seen by inspection, is a function of β only.

In our region of interest ($0<y\leq 1$, $|\beta|\leq 1$), equation 2.3.3.8 can be approximated with accuracy better than $y \times 10^{-6}$ by:

$$y_{y'max} = A\beta + B\beta^2 + \exp\ (-1) \qquad 2.3.3.9$$

Where $A = -.038024262$ $\qquad B = -.000866241$

The time at which growth rate is maximum is then found by introducing $y_{y'max}$ into equation 2.3.3.5:

$$t_{y'max} = -\frac{1}{\alpha} \ln\left[\frac{\alpha}{K}\left\{F\ (1,\beta) - F\ (y_{y'max},\beta)\right\}\right] \qquad 2.3.3.10$$

and the maximum growth rate itself, y'_{max} from equation 2.3.3.1:

$$y'_{max} = K\ y_{y'max} \exp\ (-\alpha t_{y'max} - \beta y_{y'max}) \qquad 2.3.3.11$$

Estimation of parameters in the growth equation. If longitudinal observations are available, that is, individuals have been followed through their growth, and a set of times t_i, and corresponding size measures y_i, is at hand, the growth equation 2.3.3.4 can be fitted to these data. This is done by the program GROFIT (see Appendix), based on an algorithm due to Marquardt (1963); it employs the method of steepest descent and linearization of the fitted function in the neighbourhood of the solution.

If comparative or cross-sectional data (sets of two or more size measures at different ages) are available, the same procedure permits an estimation of the parameters of equation 2.3.3.13. This is accomplished by program ANSFIT (see Appendix).

The anisometry equation. If y_i and y_j are two dimensionally homogeneous measures of size (lengths, volumes, etc.), their growth equations (from equation 2.3.3.4) are:

$$F(1,\beta_i) - F(y_i,\beta_i) = \frac{K_i}{\alpha_i} \exp(-\alpha_i t) \qquad 2.3.3.12$$

and

$$F(y_j,\beta_j) - F(y_j,\beta_j) = \frac{K_j}{\alpha_j} \exp(-\alpha_j t) \qquad 2.3.3.13$$

$\lim_{t \to \infty} y_j$ is a constant, the maximum dimension attainable by y_j, and can be measured or estimated.

Call it y_{jf}. Eliminating t from equations 2.3.3.12 and 2.3.3.13:

$$F(y_j,\beta_j) = F(y_{jf},\beta_j) - \frac{K_j}{\alpha_j}\left[\frac{\alpha_i}{K_i}\left\{F(1,\beta_i) - F(y_i,\beta_i)\right\}\right]^{\alpha_j/\alpha_i} \qquad 2.3.3.14$$

Solutions for this equation are plotted in Fig. 2.3.3.3. Program GOMORRA (see Appendix) calculates the growth equation 2.3.3.4 and the anisometry equation 2.3.3.14 from its parameters. Fig. 2.3.3.2 shows growth rate curves corresponding to growth curves in Fig. 2.3.3.1.

2.3.4. The allometry equation. The "Huxley-Teissier" allometry equation:

$$y = bx^{\alpha} \qquad 2.3.4.1$$

has been used extensively, ever since Snell (1891) first proposed it. There are several striking facts about this simple, alluring relationship that, in spite of extensive discussions, have always hampered any biological interpretations of the equation:

1). As it stands, the equation is not dimensionally homogeneous, and it is not clear precisely how one would make it so. This might require a completely different meaning of b and α in each instance, in which case the usefulness of the equation would be severely restricted. Huxley (1932) and many other workers (see review in Gould, 1971), have used it to compare lengths, lengths with areas, with volumes, masses, etc.

The equation seems to work well with a variety of data, although cases of poor fit are presumably unreported.

2). The equation is a purely empirical formulation, for which apparently no theoretical or functional explanation has been offered. It just fits most of the data. That's all.

3). The meaning of the two constants is not at all clear and conflicting explanations are offered. Gould (1971) interprets b as a scale factor "that expresses differences in size between comparable animals of the same shape on two or more regressions of constant α.".

4). The exponents are usually, but not always, numbers that are not "simple" at all, defeating the purpose of a mathematical law as used in any other science. Surely no fundamental relationship is uncovered by the fact that $Y = 1.127\ X^{0.731}$.

The complication of the original data is not reduced significantly and the exponent has no obvious functional significance. Growth is a universal phenomenon in the organic world, but its laws are probably not the same in all kinds of organisms. Accretionary growth and in particular, extracellular growth, follow metabolic pathways very different from those controlling most tissue growth (Wilbur and Simkiss, 1968). It would be surprising, then, if the same form of growth equation would be valid in different types of growth.

The two most widely used growth equations at present

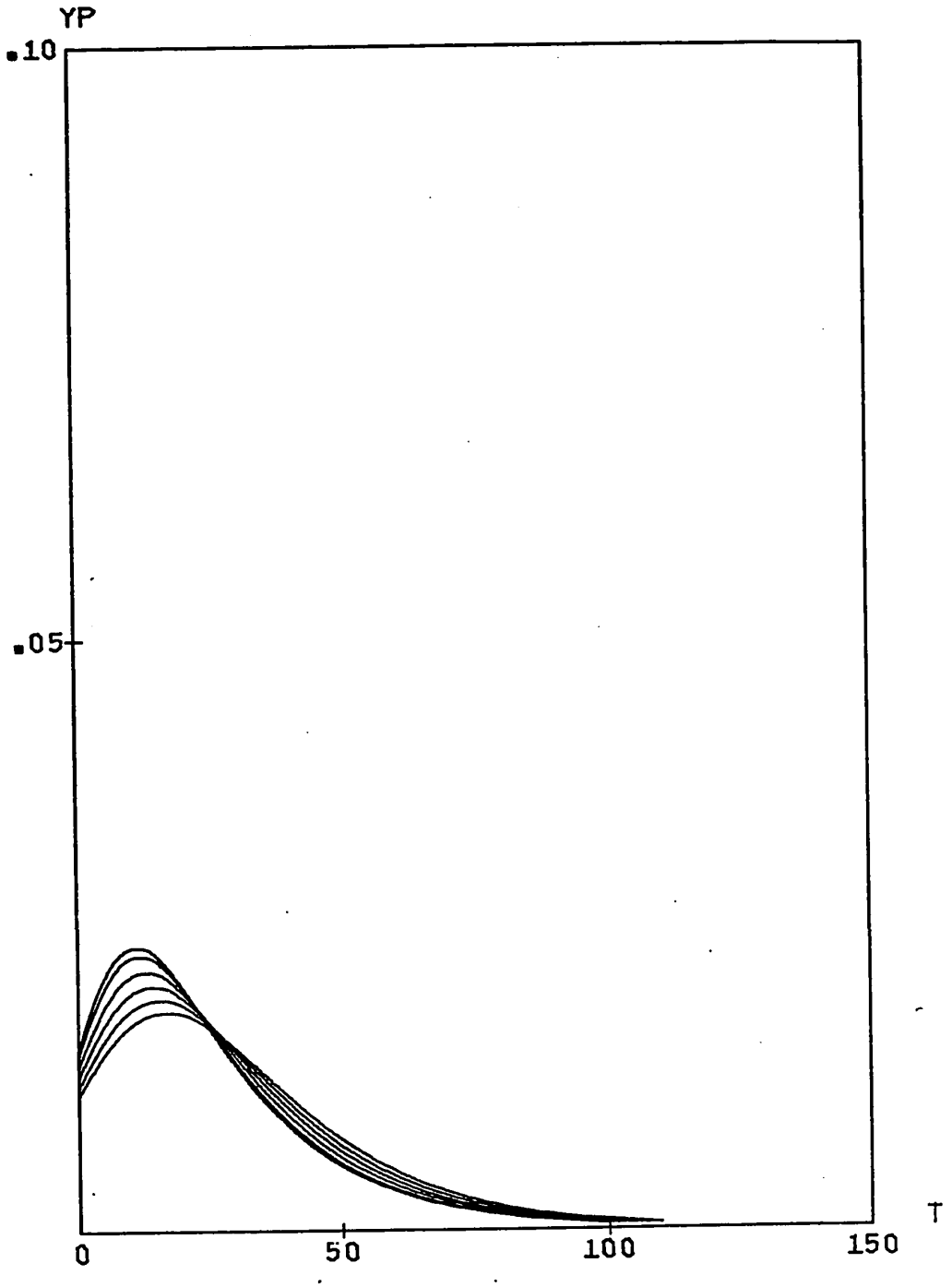

Fig. 2.3.3.2 Growth rate curves (growth rate vs. age) for the curves of Fig. 2.3.3.1

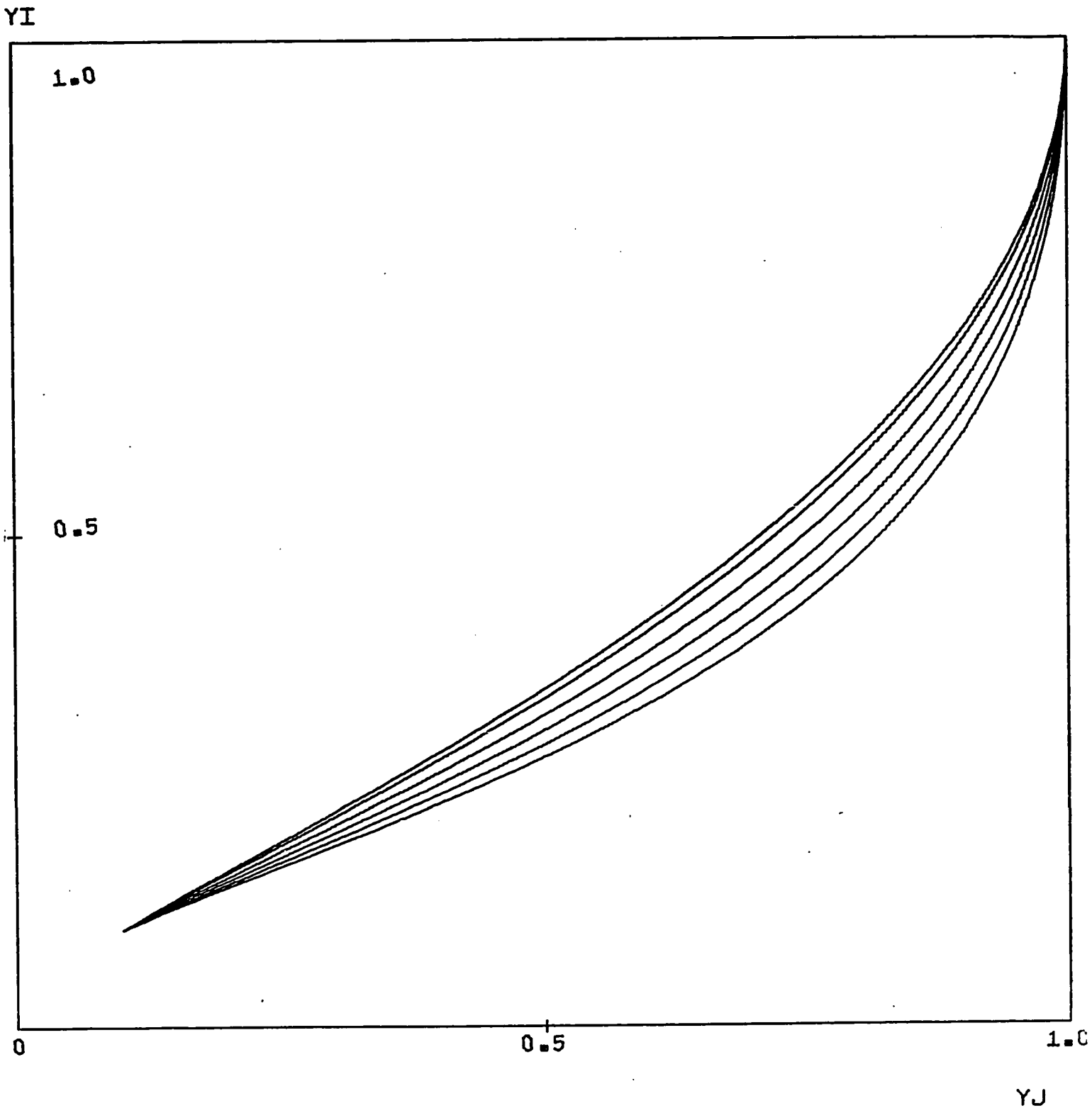

Fig. 2.3.3.3 Bivariate double-log plot of the anisometry function (equation 2.3.3.14) for different values of the ratio x_j/α_i

are the Pütter-Bertalanffy (equation 2.3.4.2) and the Gompertz (equation 5, Table 2.3.3.1). Their relative success can probably be explained by their being founded on sound theoretical assumptions and a choice between one or the other seems to be controlled to a large extent by the availability of longitudinal or cross-sectional growth data. Thus, the Pütter-Bertalanffy equation is used in fisheries almost exclusively (Ricker, 1958); it is especially useful to estimate maximum attainable size from cross-sectional data. On the other hand, the growth of mammals, for which longitudinal samples are the rule, and for which the estimation of growth rates is most important, is analyzed mostly by means of the Gompertz equation (Laird, 1966).

In spite of the growth curves of these diverse animals being of different forms, their relative growth is explained by means of the same allometry equation. This is particularly puzzling for the case where the Pütter-Bertalanffy or Gompertz equations are used, since one of the main reasons for their acceptance is their having parameters to which a meaning can be attached. We have seen above that this is hardly the case with the allometry equation.

What in fact seems to happen is that the allometry equation is just a by-product of two or more other growth processes that are themselves governed by exponential laws. It is these laws which really concern us.

Basal metabolism rates (Kleiber, 1961) and brain

weight (Jerison, 1961) when plotted against body weight in a double log scale produce lines with a slope (α) of approximately 2/3. This is also von Bertalanffy's (1960) first choice for the exponent a in his differential equation for growth:

$$y' = K_1 y^a - K_2 y \qquad 2.3.4.2$$

in which it is assumed that the growth rate is proportional to the difference between the volume and the surface of the animal. Von Bertalanffy went further to divide animals in three types according to the value of this exponent; it is indeed fairly common for the coefficient to have a value around 2/3. In these three cases it seems clear that the exponent α indicates a relationship between growth processes dependent on volume and on surface area.

These cases are, however, the exception. In general, both parameters of the equation defy explanation and differ significantly from simple ratios.

As discussed in section 2.3.3, one of the main reasons to advocate equation 2.3.3.4 as a growth function for accretionary shells is the fact that it incorporates damping factors. The only other commonly used growth equation with a damping factor is the Gompertz equation (number 5 in Table 2.3.2.1), and an anisometry function derived from it is given below. For comparison with Fig. 2.3.3.1, the Gompertz equation has been plotted for different values of the parameter K_2 in

Fig. 2.3.4.1. The parameter $y_f = 1$ for all curves and K_i has been chosen so as to make the initial size (at t=0), 0.1 y_f. Fig. 2.3.4.2 shows growth rates for the same parameter values.

If y_i and y_j are two dimensionally homogeneous size variables, K_i and K_j their size proportionality coefficients and α_i and α_j their damping coefficients, so that their differential equations for growth are of the form

$$\frac{dy}{dt} = K\, y \exp(-\alpha t) \qquad 2.3.4.3$$

then their anisometry equation is:

$$y_j = y_{jo} \exp\left[\frac{K_j}{\alpha_j}\left\{1 - \left(1 - \frac{\alpha_i}{K_i} \ln \frac{y_i}{y_{io}}\right)^{\alpha_j/\alpha_i}\right\}\right] \qquad 2.3.4.4$$

Figs. 2.3.4.3 to 2.3.4.5 show a selection of anisometry curves for different values of the parameters

$$\frac{\alpha_j}{\alpha_i}, \quad \frac{K_j}{\alpha_j}, \quad \text{and} \quad y_{jo}$$

If the damping coefficients α_j and α_i in equation 2.3.4.3 are equal, the equation reduces to

$$y_j = y_{jo} \left(\frac{y_i}{y_{io}}\right)^{K_j\alpha_i/K_i\alpha_j} \qquad 2.3.4.5$$

which is Huxley's familiar allometry equation. Equation 2.3.4.4 is then like equation 2.3.3.14, a generalization of the

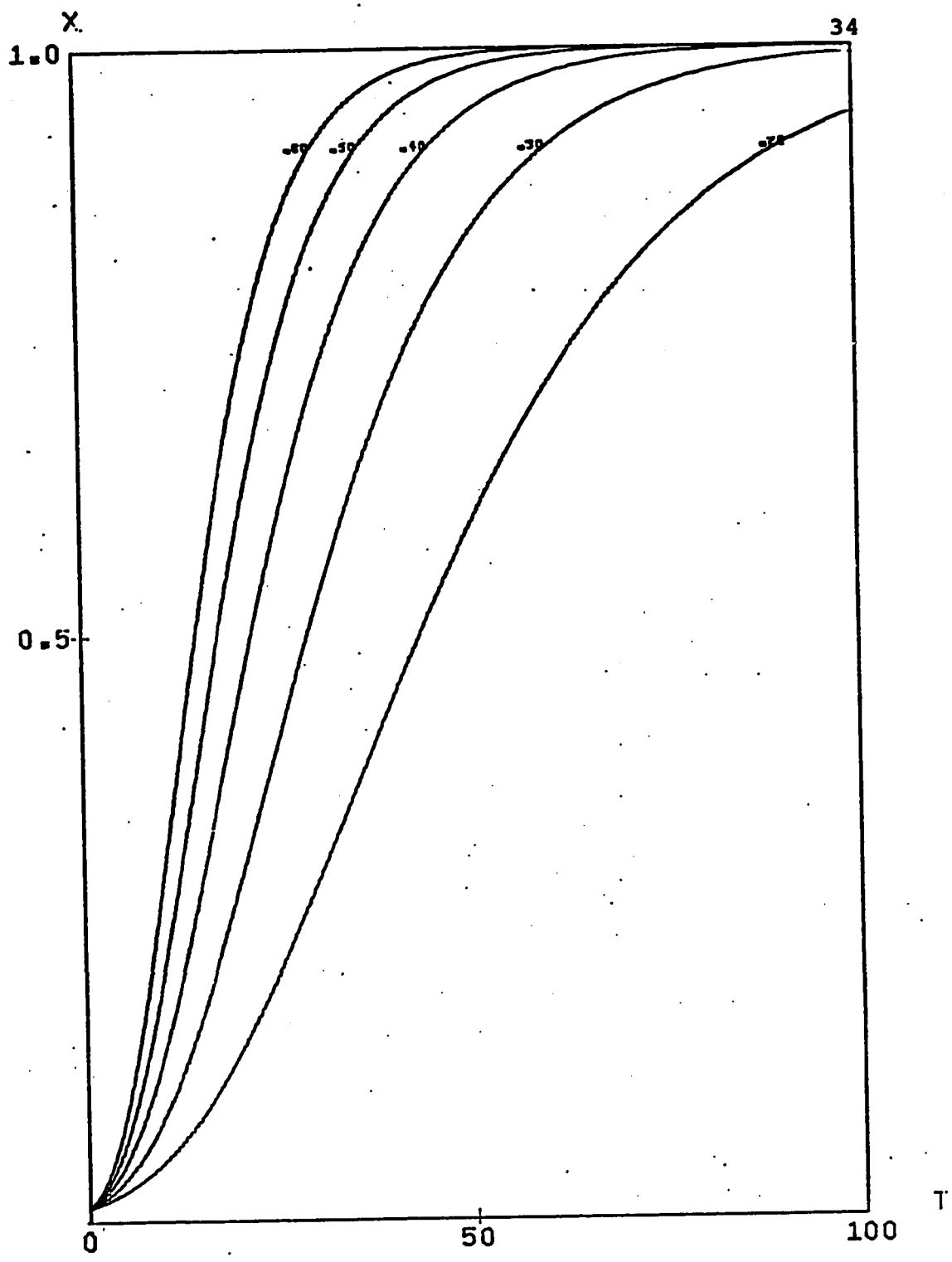

GROWTH CURVES FOR VARIABLE C

Fig. 2.3.4.1 The Gompertz growth function (explanation in text)

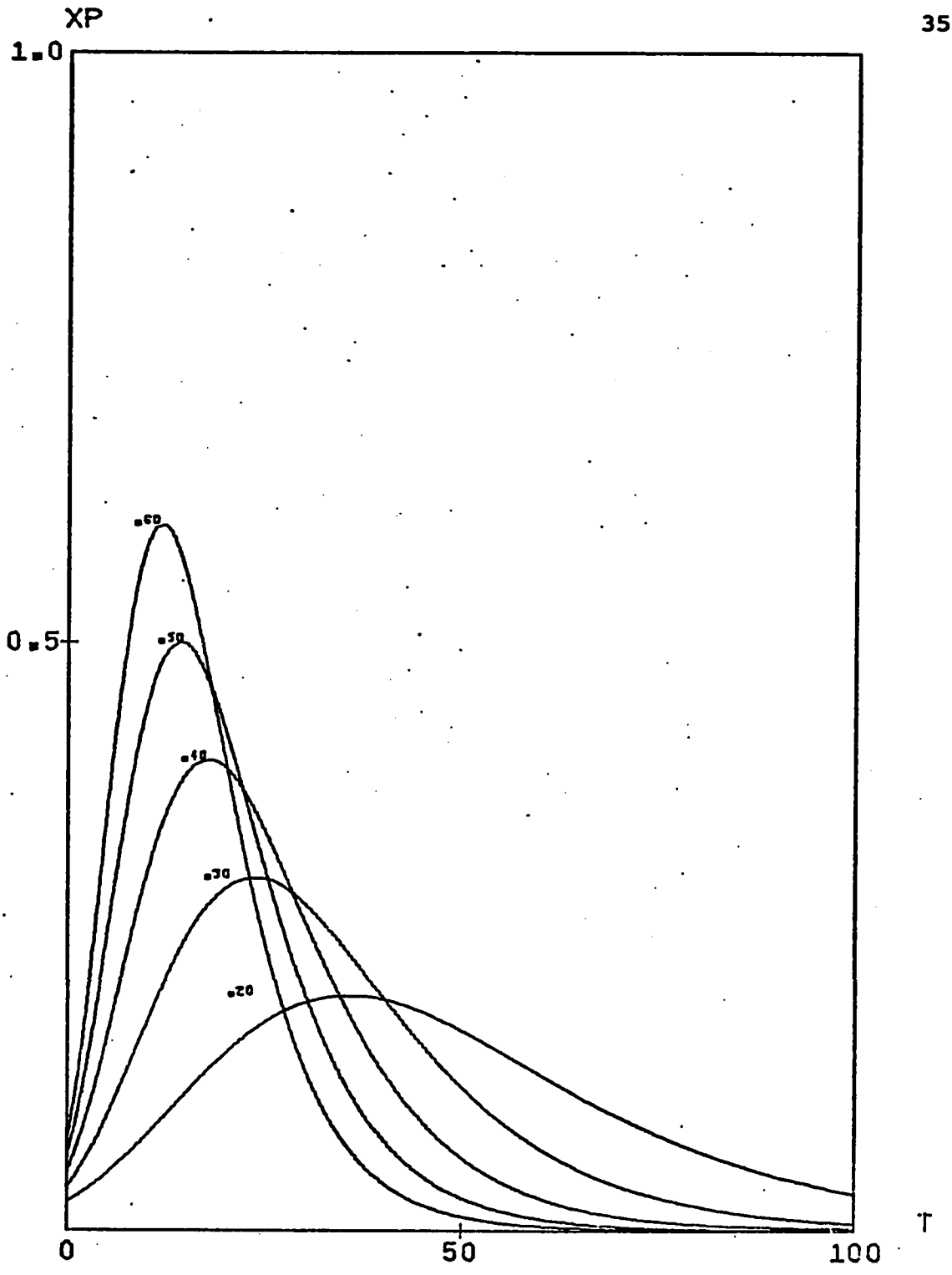

GROWTH RATES FOR VARIABLE C

Fig. 2.3.4.2 Gompertz growth function:growth rates (see text)

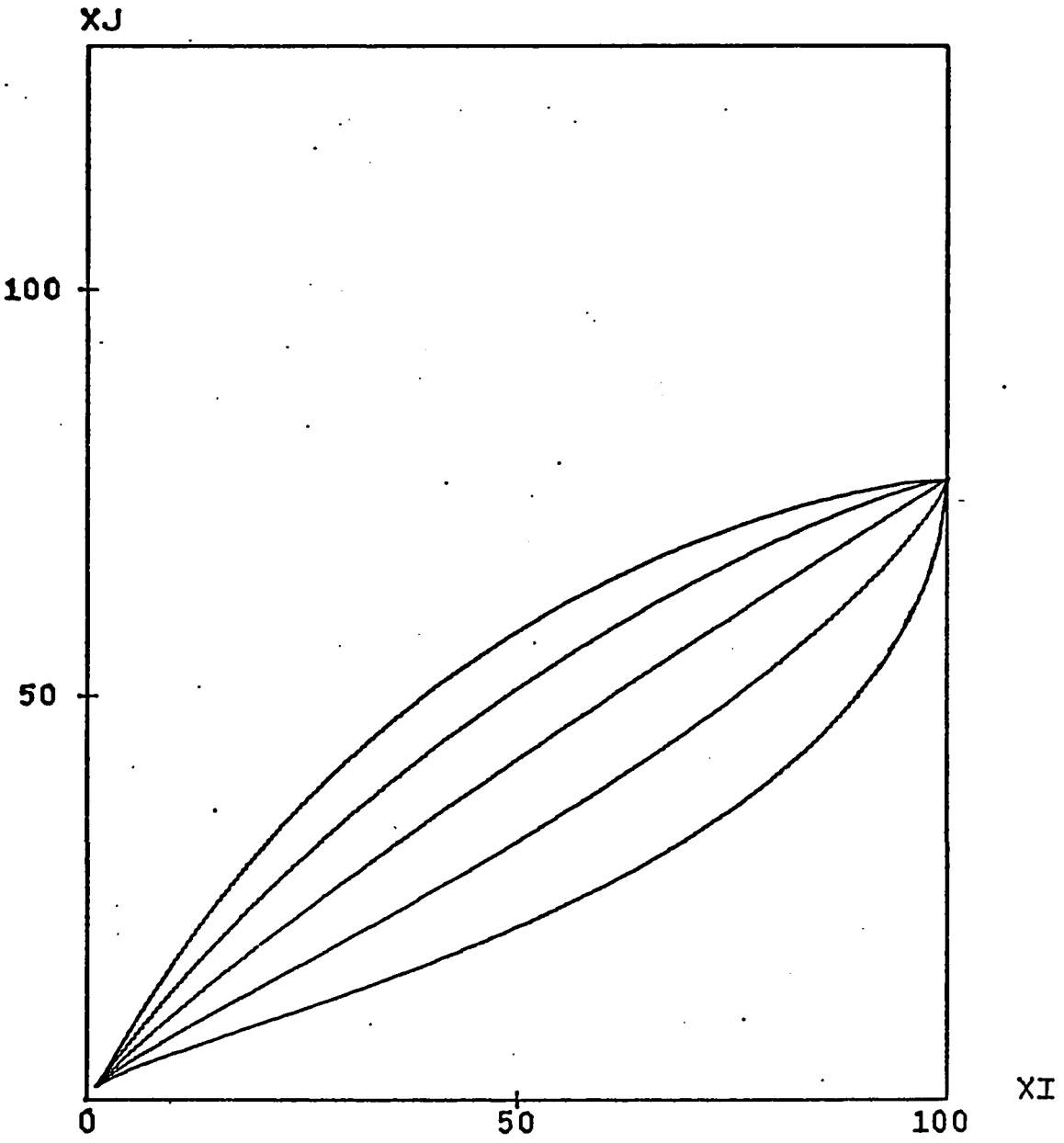

GENERALIZED ALLOMETRY FUNCTION

CJAJ = 4.0 XJ(0) =1.4 AJAI VARIABLE

Fig. 2.3.4.3 Bivariate plot of Gompertz allometry function (see text)

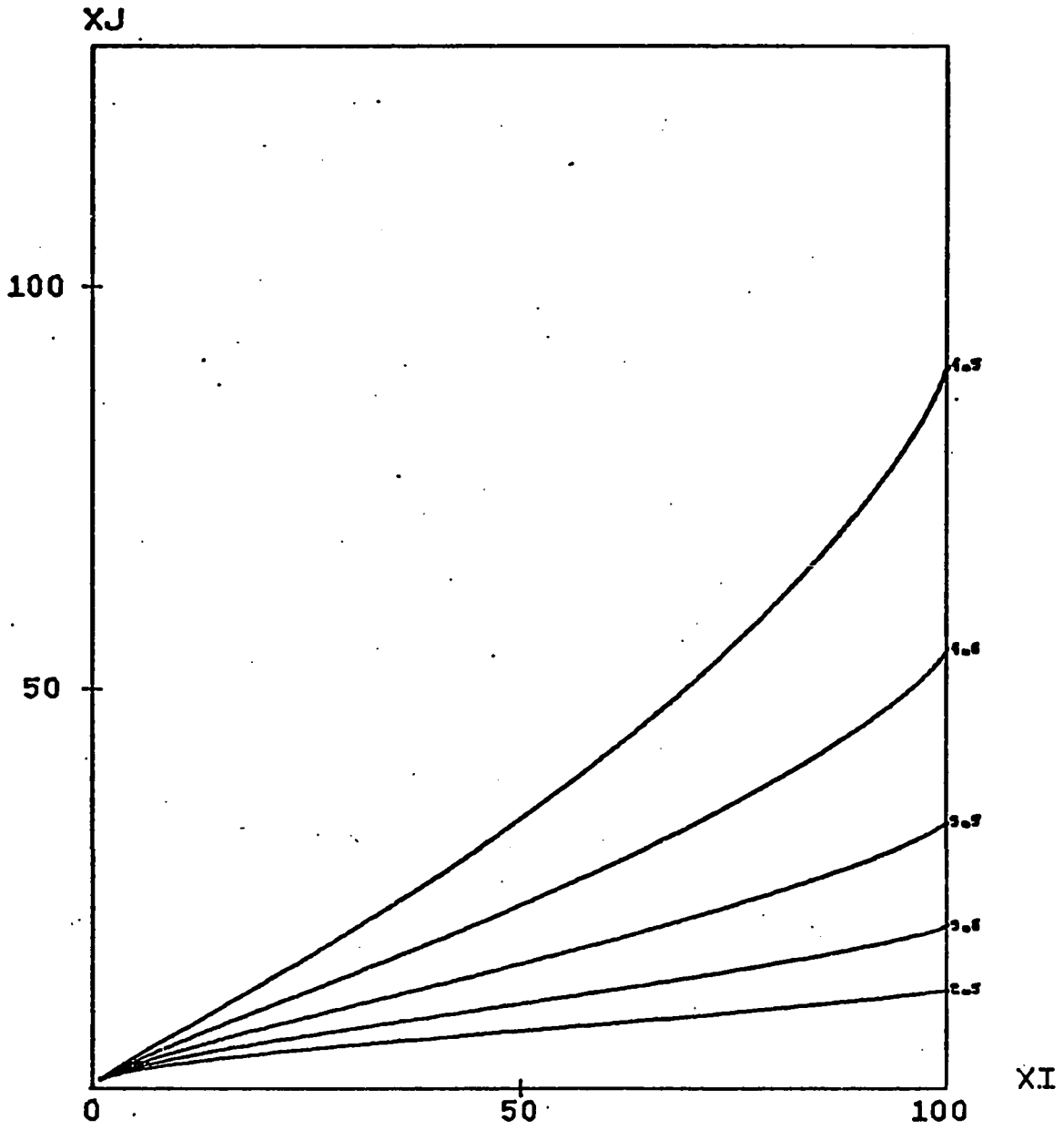

GENERALIZED ALLOMETRY FUNCTION

AJAI = .8 XJ(0) =1.0 CJAJ VARIABLE

Fig. 2.3.4.4 Bivariate plot of Gompertz allometry function (see text)

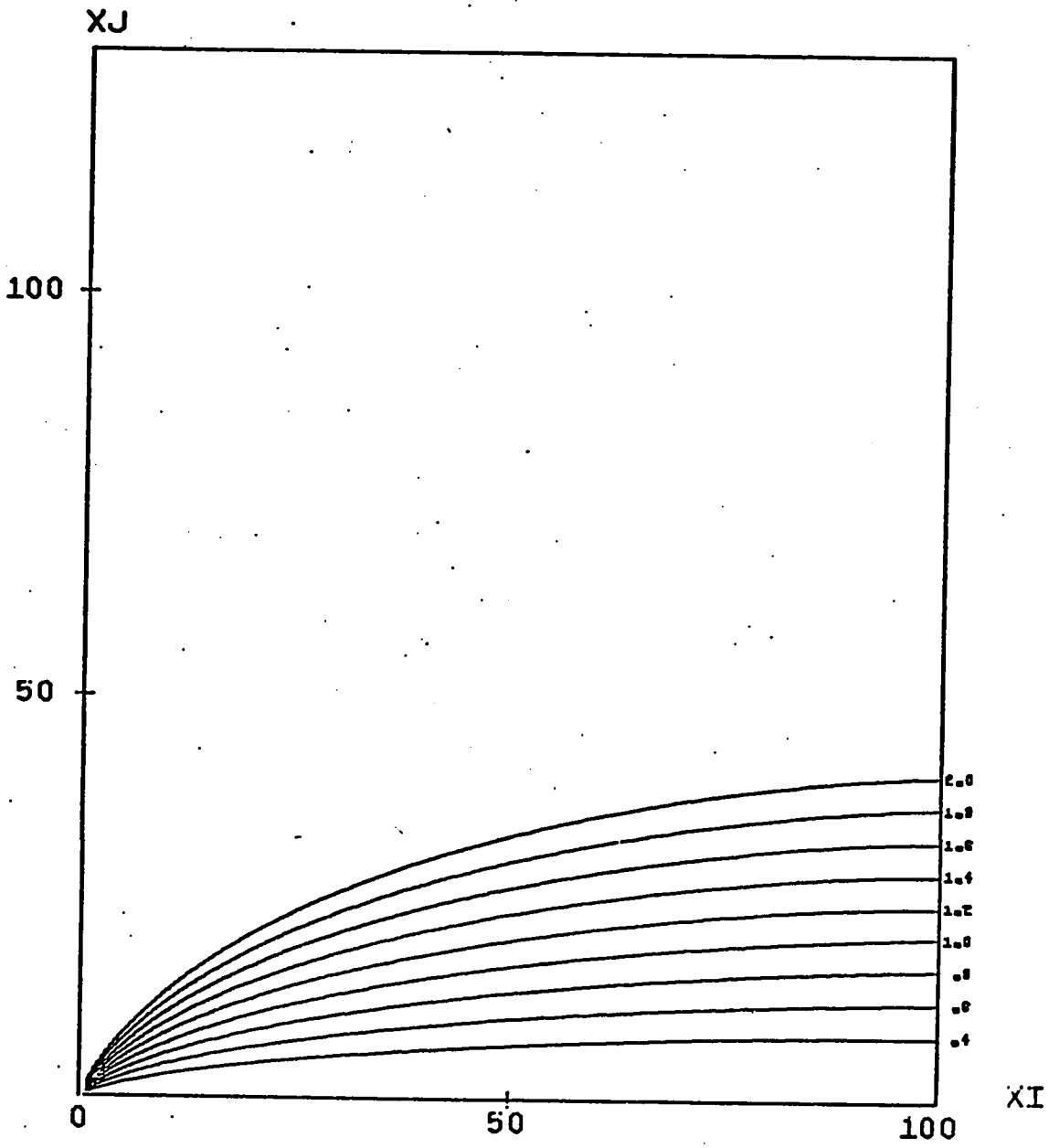

GENERALIZED ALLOMETRY FUNCTION

AJAI = 1.4 CJAJ = 3.0 XJ(0) VARIABLE

Fig. 2.3.4.5 Bivariate plot of Gompertz allometry function (see text)

allometry equation, and it is here termed an anisometry equation. Its parameters can be estimated by means of Marquardt's (1963) algorithm (section 2.3.3).

2.3.5 Other models. Deterministic equations for the growth function are not the only alternative available if a quantitative analysis of growth is desired. Two other alternatives described in the literature will be briefly discussed: a vector model of continuous transformation (Walnut, 1967) and a piecewise linear time series in which growth parameters are estimated by exponential smoothing at discrete intervals (Hirschfeld, 1970).

Walnut (1967) considered the apositional growth of bone and associated to a series of discrete, identifiable points on the bone surface, a characteristic velocity. When each of these points is traced through an ontogenetic series, the sets of homologous points obtained (Walnut's "equivalent" points) can be expressed as vector functions of the initial positions of the points, and of time.

If $\mathbf{r}$ is the position of each point and t is time, the velocity vector $\mathbf{v} = \mathbf{v}(\mathbf{r},t)$.

If an analytic function for $\mathbf{v}$ exists and a judicious choice of points is made, this velocity vector can always map into a regular growth function. If, as will more commonly be

the case, v does not have an analytic function, numerical or graphical methods can be used; in either case, Walnut's growth vector fields are totally equivalent to Thompson's (1942) cartesian transformations. It is difficult to see in what situation, apart from Walnut's example of tracer feeding, the use of the growth vector field will be preferable to the standard techniques mentioned above.

Hirschfeld (1970), also using longitudinal growth data, treated them as a time series. Assuming this series to be incremental (that is, with no strong seasonal components; he used Human craniofacial data) and linear over small time increments, he then proceeded to estimate and predict the value of the function by means of an exponential smoothing technique. Unlike the deterministic methods, Hirschfeld's method can be made to fit the data as accurately as desired, by taking time intervals small enough. It will probably be of better use when predicting growth, particularly since the technique of exponential smoothing seems more appropriate to growth data than either moving averages or linear regression estimates. This technique, however, makes no significant reduction in the complexity of the data.

CHAPTER 3

A DESCRIPTIVE MODEL FOR ACCRETIONARY SHELLS

3.1 The representation of morphology

In the context discussed here, morphology is taken to comprise: size, geometry (including shape and texture) and topology (interrelations of parts). The method of representation described in this chapter is concerned mostly with size and shape.

The total amount of morphological data that can be obtained from a single fossil specimen is effectively infinite, so that ways must be devised to reduce it to an amount that has as little redundance as possible, and at the same time is sufficient to characterize adequately the morphology for the user's purposes.

Based upon experience in ammonoid shells of relatively simple morphology, it seems that no useful summarization of a morphology can be limited to a small collection of measurements (say, 4 or 5), but that we shall need to represent the morphology as a vector of several components, in many cases including data on the morphological changes through ontogeny.

The description of a particular morphology, especially that of a growing organism, can be achieved in any number of ways. It would be convenient if one could provide

a summarization of the measured phenetic characters in the simplest possible way. There are several avenues of approach open here, which will be discussed with reference to the molluscan shell:

a). in a deterministic, theoretical framework, one can develop a model of the sequence of events leading to growth and development (morphogenesis) and test this model against observations made on actual specimens. To the extent that the model is not disproved by the observations, one can say that the model explains the observations in a simple way ("accounts" for their variations). As several different models might fit the observations equally well (as far as we can tell or test), one can decide between them on the basis of the simplicity of either (i) the mechanisms involved (in the case of molluscan shell growth these are primarily biochemical and mechanical), or (ii) the resulting mathematical expression. Point (i) is primarily an experimental question and is related, on the one hand, to the biochemical control and release of several extracellular peptides, proteins and ionic substances into the extrapallial fluid, and on the other, to the mechanics of the growing edge of the mantle (muscles, pallial attachment, turgidity). Point (ii) will be taken to mean that a mathematical expression is simpler than another if it has less parameters.

The line of approach sketched above under (a) has

been taken by Turing (1952), who dealt primarily with the chemical variables; using only hypothetical situations and making several other simplifying assumptions, he arrived at sets of linear differential equations for several morphogenetic processes. In most cases, however, there will be too many unknowns for the equations to be solvable, and solutions might be attempted by, for example, Monte Carlo methods.

b). In an empirical, stochastic framework, one can record the observations and decide between different models using best fit as a criterion. Since, given enough parameters, an expression can fit the observations as exactly as one wishes, the criterion of simplicity (lowest number of parameters for a given quality of fit) must also enter in these models.

The morphology of a coiled accretionary shell can be conveniently divided into three main components: the coiling geometry of the shell, its ornamentation and its internal structures. The coiling geometry is determined by the course of the coiling (or directing) spiral and by the cross-sectional shape (generating curve of Thompson, 1942). Raup (1966, 1967) has modelled the morphology of coiled shells in a system of cylindrical coordinates in which a closed curve (the generating curve) generates the shell tube by revolving around a coiling axis at a regularly increasing distance as its size increases (the expansion rate), all the while sliding

parallel to the coiling axis at a fixed rate (the translation rate). Any given combination of these four parameters will produce a different shell, and the spectrum of possible shell morphologies has been analyzed by Raup (op. cit.) for the actual occurrence of coiled shells that correspond to different regions of the resulting four-dimensional morphological space.

Some different morphogenetic modes for ribbing in molluscs will be briefly discussed in Chapter 4, but the present model will restrict itself to the coiling geometry. In addition, the complication and major features of the ammonoid suture line will be submitted to a separate analysis.

3.2. The coiling spiral

All previous models for the molluscan shell (Moseley, 1838; Naumann, 1840a, 1840b; Thompson, 1942; Lison, 1949; Fukutomi, 1953; Stasek, 1963; Raup, 1966, 1967) used the directing spiral as a basis for describing the shell, and all, with the exception of Naumann, assumed this spiral to be logarithmic. Burnaby (1966), assuming an allometric relationship between the peripheral length of the ammonoid midventer spiral and the radius vector, proposed a generalization of the logarithmic spiral. Neither Naumann's nor Burnaby's efforts to depart from a logarithmic spiral model have had followers, the main reason being that, while it is known that even so-called regular "planispiral" ectocochliate cephalopods

depart significantly from the equiangular spiral in their coiling, the simplification provided by the equation of this curve overcomes the need for a more precise description. Moreover, there is the widespread belief that, since the logarithmic spiral is homothetic to any part of itself, a spiral shell would maintain its functional significance constant, regardless of its increase in size. Thus, Thompson (1942) states: "In the growth of a shell, we can conceive no simpler law than this [the spiral], namely, that it shall widen and lengthen in the same unvarying proportions: and this simplest of laws is that which Nature tends to follow". But precisely the opposite is true. We would be surprised to find that any organism retained its shape during growth.

The rule is rather that, since mechanical conditions are a function of size, we <u>expect</u> a change in proportions during a scaling-up of an organism or a mechanical structure. This is Galileo's "principle of similitude" and is one of the main explanations of allometric (or, in general, anisometric) growth. This is a point that Gould (1966, 1967) among others, has made abundantly clear in ontogenetic development and also in phylogenetic series. What is then, in need of explanation, is the number of mollusks that do retain a constancy of shape.

The most definitive critique of the justification for the logarithmic spiral model was provided by Lison (1949; see also Carter, 1967), who argued that Thompson's force vector,

directed to the pole of the spiral, had no physical justification, particularly since the pole is not even accessible to the majority of mollusks, or claws, teeth or horns that grow in a similar manner. Lison (1949, p.44-45) says about this force: "The main stumbling block of the theory is the force supposed to be exerted in the direction of the pole. What is its nature?" (translation). In the end, however, Lison accepts the logarithmic spiral as a directing curve for the bivalve shell, but bases his decision on Huxley's (1932) explanation of the origin of spirals in accretionary structures as being a necessity whenever there was a uniform gradient of skeletal secretion along the growing edge. This viewpoint will also be taken here, but with the reservation that, since this gradient can change (see Chapter 4), so can the shape of the coiling spiral, as in fact it does. The change in the spiral is particularly important in the ammonoids, where it is, as a rule, a character of taxonomic importance (Arkell et al., 1957, p.L292).

If not visible, the center of the spiral can be determined by the method of Vašíček (1967), provided it does not depart much from the logarithmic spiral.

The spiral can be recorded simply by measuring sets of radii r_i and their subtended angles, θ_i. It is convenient to measure the spiral from the outside towards the pole. If the radii are converted to logarithms, a test for linearity of the function

$$\ln r = f(\theta) \qquad 3.2.1$$

will indicate departure from the logarithmic spiral. No difficulty has been encountered with this method.

Sometimes it is more convenient to make use of

$$\frac{dr}{d\theta} = r \cot \psi \qquad 3.2.2$$

measuring r and ψ, the spiral angle (Fig. 3.2.1), at regular intervals of θ, the subtended angle. If the values of $\frac{dr}{d\theta}$ obtained are plotted against the θ values, then

$$r = \int r \cot \psi \, d\theta = g(\theta)d\theta \qquad 3.2.3$$

This relation proves useful when an analytic function suggests itself for $\frac{dr}{d\theta}$. Since this function is used for descriptive purposes only, its exact nature does not matter, as long as it is an analytic function.

3.3. Cross-sectional shape

3.3.1. Conventional descriptions of the whorl cross-section and some alternatives. The majority of authors have traditionally employed a purely descriptive terminology for the description of the cross-sectional shape of ammonoids and other mollusks. Terms such as subquadrate, fastigate, etc.

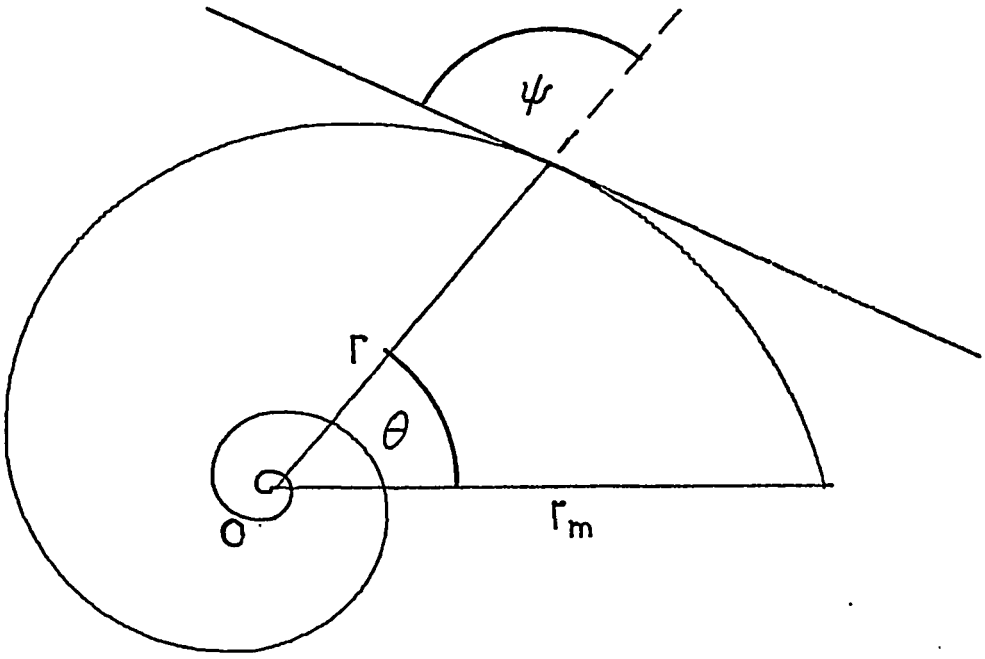

Fig. 3.2.1 The ammonoid spiral, showing measurements.
r = radius vector. θ = angle subtended by r.
ψ = spiral angle. r_m = apertural radius.

are commonly in use. The only quantitative measure of cross-sectional morphology in current use is the height:width ratio (H/W). As shown in Fig. 3.3.1.1, this can be a very misleading measure, since in all probability, at least the points of maximum width are not homologous, neither throughout ontogeny nor from one taxon to another. H/W is also a very poor discriminator of shape; as can be seen in Fig. 3.3.1.1, it is possible to have both similar shapes with different H/W ratio and very different cross-sections with the same H/W. Since the descriptive terms mentioned above are in common use (Arkell et al., 1957) and the cross-sectional shape is a character useful in taxonomy, it appears that a more accurate, quantitative description would be desirable. If an ammonoid is oriented in its inferred living position and viewed aperturally, in a cartesian set of coordinates the cross-section is a bilaterally symmetric, double-valued curve. Any attempt to fit to it the regular polynomials used in curve-fitting would lead to high-degree curves, usually quite unmanageable.

The lower part of the cross-section (below the point of maximum width) resembles quite strongly a parabola, and even better, a catenary. Fig. 3.3.1.2 shows an ammonoid cross-section with a parabola and a catenary fitted to it. If we recall that the catenary of equal resistance is a parabola, the significance of this resemblance for the statics of the cross-section is enhanced. The catenary is a curve of static

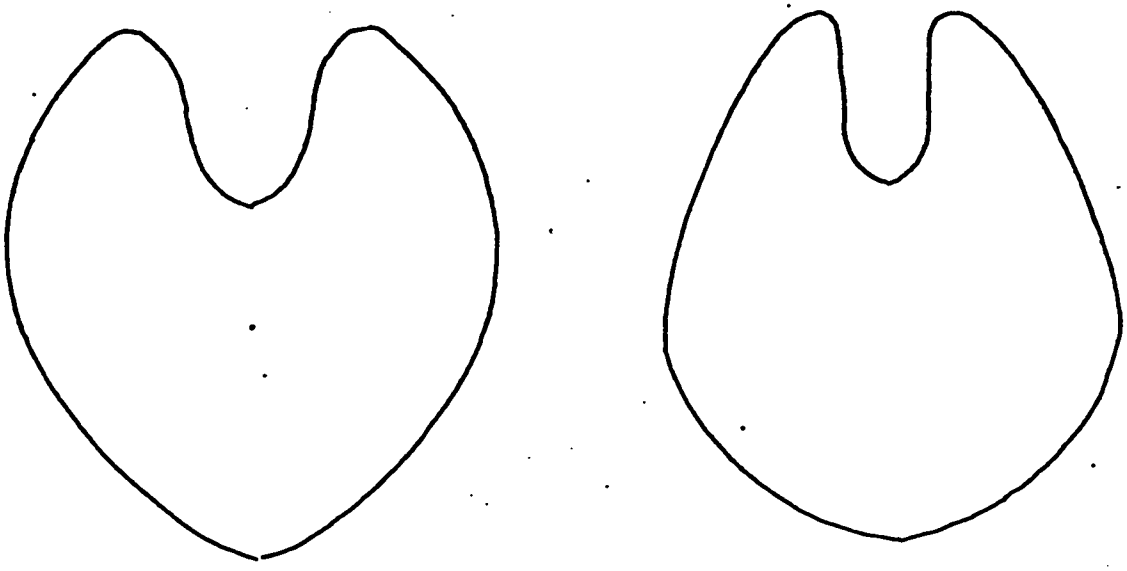

Fig. 3.3.1.1. Two hypothetical cross-sections with the same height:width ratio but different overall shape

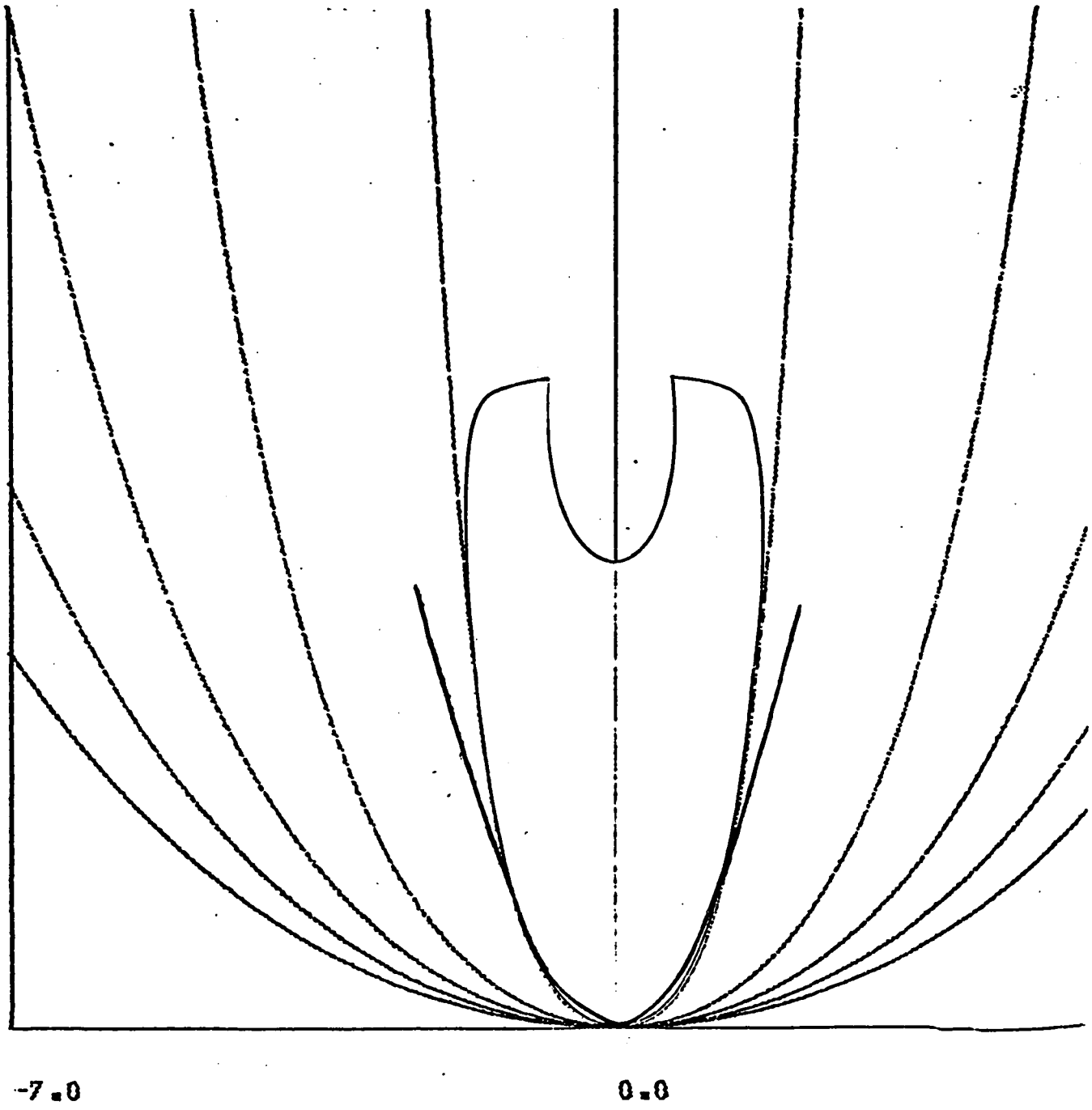

Fig. 3.3.1.2. An ammonite cross-section (Sonninia sp.) with a parabola and a catenary fitted to its lower half. Dotted lines: catenaries (several of a family). Thick line: parabola. Thin line: ammonite cross-section.

equilibrium and has the interesting property of having the lowest centre of gravity of all isoperimetric curves, making it optimal from the viewpoint of minimizing the expenditure of shell. This observation prompted the static model presented in Chapter 4.

It appears then that all the descriptive methods for the cross-sectional shape commonly in use are inexact and that a more flexible method that could describe these shapes in a more complete way would be desirable.

3.3.2 Characterization of the cross-section by harmonic analysis. Instead of choosing a fixed origin for the description of the shell, as is customary (Thompson, 1942; Lison, 1949; Stasek, 1963), choose the growing edge of the shell, an instantaneous section, approximately coincident with the usual whorl section; within it, take the midventer point as a pole and the axis of symmetry as a polar axis. A point on the section is determined by its coordinates, ρ, the radius vector from the pole to the point, and ϕ, the angle subtended by the radius vector. Thus, ρ exists and is continuous in the interval $-\frac{\pi}{2} \leq \phi \leq \frac{\pi}{2}$ (Fig. 3.3.2.1).

If ρ sweeps the cross-section from $-\frac{\pi}{2}$ to $\frac{\pi}{2}$, it will take values dependent on the value of ϕ: $\rho = f(\phi)$.

Repeating this function along the ϕ axis by reflection on the lines $(2K - 1)\frac{\pi}{2} = \phi$ we obtain a cyclic periodic function of period π. This function can now be expressed as

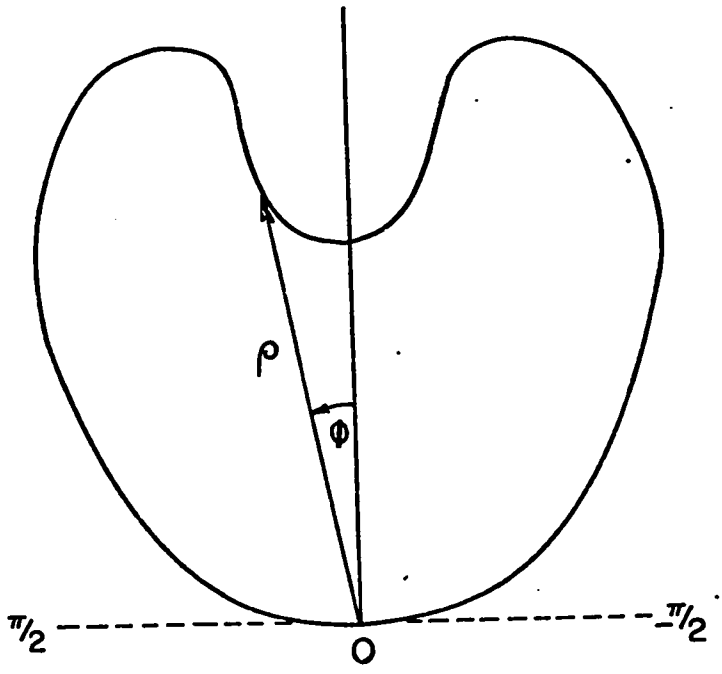

Fig. 3.3.2.1. Ectocochliate cephalopod whorl cross-section in polar coordinates, to illustrate measurements taken. Polar axis is vertical. ρ = radius vector, ϕ = subtended angle.

a Fourier series (Fig. 3.3.2.2.),

$$\rho = a_{o/2} + \sum_{i=1}^{\infty} (a_i \cos i\phi + b_i \sin i\phi) \qquad 3.3.2.1$$

If the section is bilaterally symmetrical, $f(-\phi) = f(\phi)$ and the odd-function terms (sine) vanish. The coefficients a_i in 3.3.2.1 are calculated according to:

$$a_k = \frac{1}{\pi} \int_{-\pi}^{\pi} f(\phi) \cos k\phi \, d\phi \qquad 3.3.2.2$$

The calculations were done by means of a computer program by Preston and Harbaugh (1965).

Procedure: The ammonites are sectioned, with a thin blade diamond saw, through a plane perpendicular to the plane of symmetry and passing as close to the protoconch as feasible. On one half of the specimen or a peel taken from it, measurements are taken, by means of a special protractor with a graduated movable arm, of both angle and radial distance every 5°, from the midventer of each successive whorl; the distance between successive midventer points is also measured. A harmonic analysis is conducted for the radii vectors. The result of the harmonic analysis is a set of coefficients a_i. Fig. 3.3.2.2 shows an ammonite cross-section and its line spectrum.

In a number of trials it was found that 4 or 5 terms in the series are enough to account for more than 95% of the

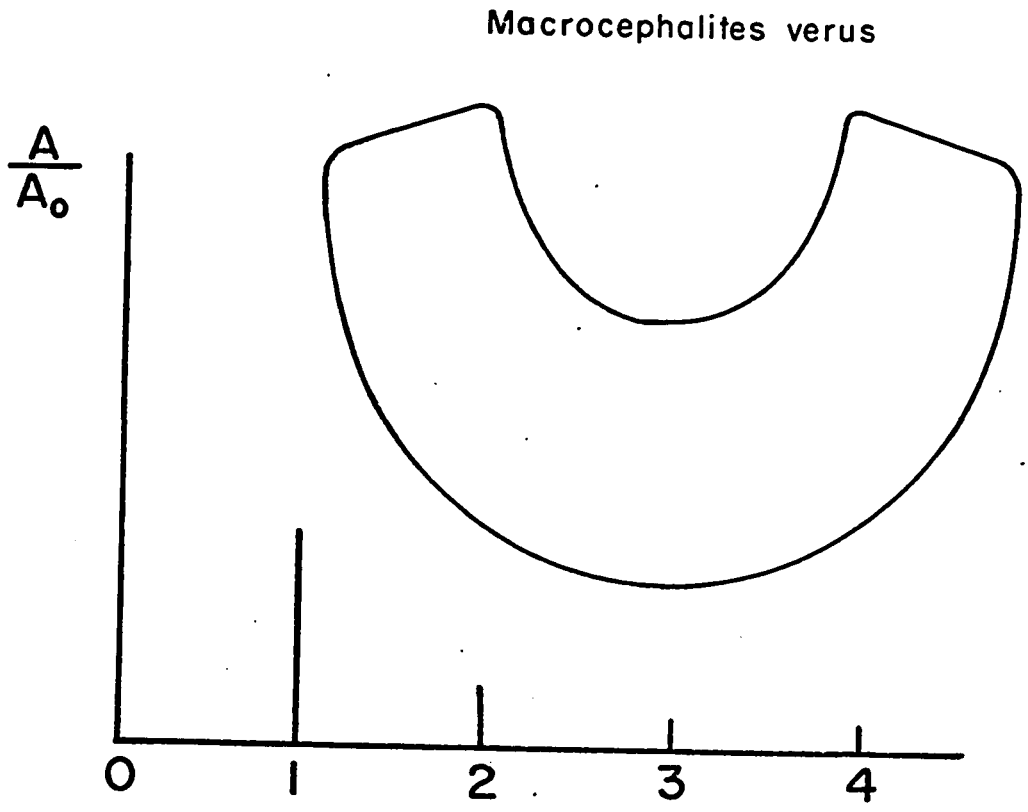

Fig. 3.3.2.2. An ammonoid cross-section and its line spectrum. The four harmonics shown account for 96% of the total variance. Compare with Figs. 3.3.2.3. to 3.3.2.6.

total variation (expressed as sums of squares). To decide whether a new term added to the series would improve the fit significantly, the variance ratio (F test) was used.

A further aspect of this study includes the production of a set of instructions to generate different types of shells, which Chamberlain (1969) has done geometrically.

Figs. 3.3.2.3 to 3.3.2.6 show synthetic cross-sections produced by giving arbitrary values to the parameters a_i; these cross-sections can be used for visual comparison with actual cross-sections (instead of doing the harmonic analysis) or to produce synthetic shells.

This method of characterization of cross-sectional shape has the advantage of being able to describe the shape as accurately as desired; half as many harmonics as data points can be extracted. The fact that 4 or 5 harmonics suffice in the majority of cases is a point in favor of the method. More complicated shapes, however, will require more harmonics to obtain the same quality of fit.

3.4. Derived parameters

It is convenient to be able to obtain the same parameters normally used to describe the cross-section from the Fourier series that represents the cross-section, so that this system of description in effect incorporates the old one.

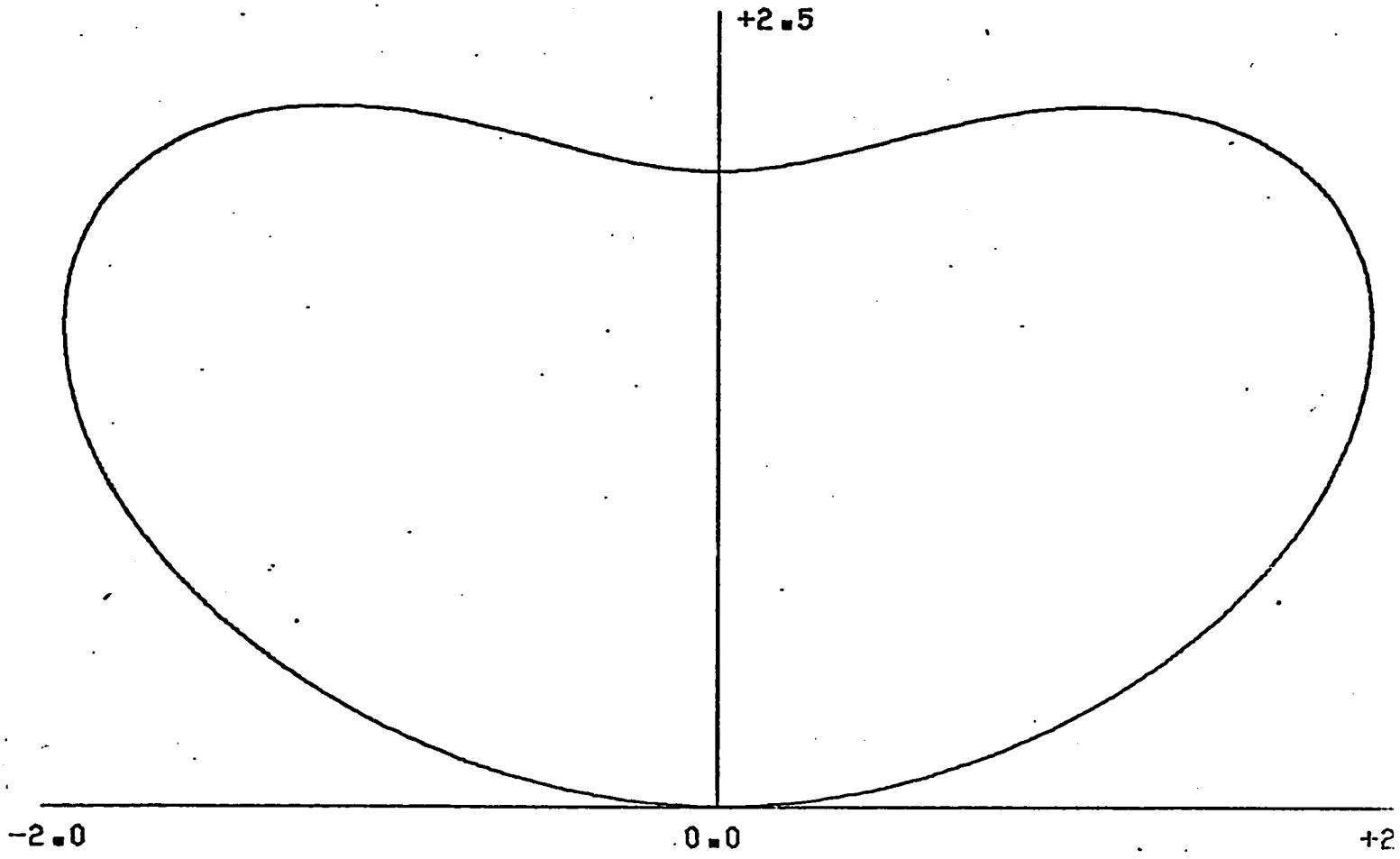

AMMONOID CROSS SECTION GENERATED BY 5-TERM FOURIER SERIES

A(0)= 1.00 A(1)= 1.20 A(2)= .80 A(3)= -.80 A(4)= -.20

Fig. 3.3.2.3. Synthetic ammonoid cross-section

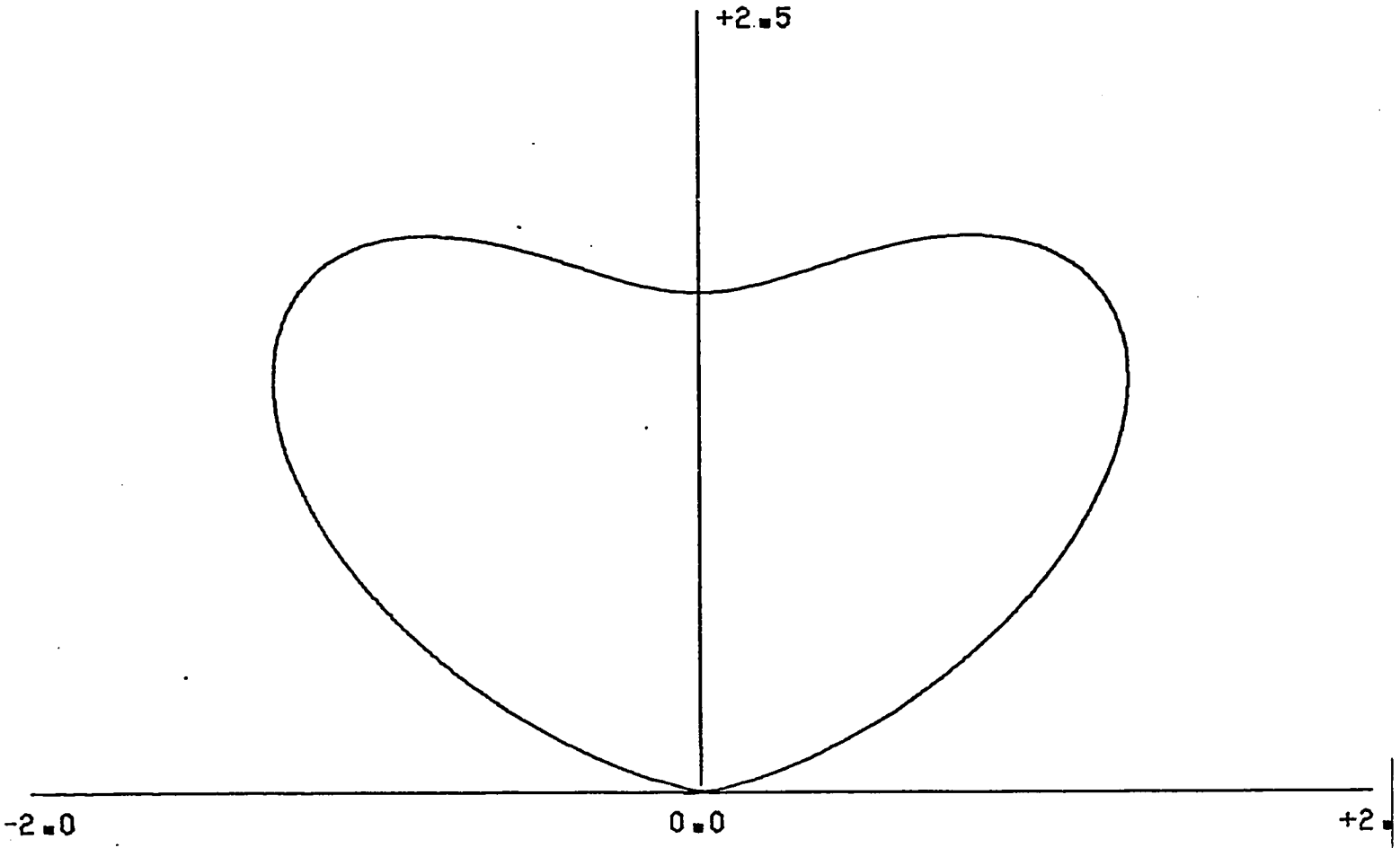

AMMONOID CROSS SECTION GENERATED BY 5-TERM FOURIER SERIES

A(0)= 1.00 A(1)= .60 A(2)= .20 A(3)= .60 A(4)= -.80

Fig. 3.3.2.4. Synthetic ammonoid cross-section (suite)

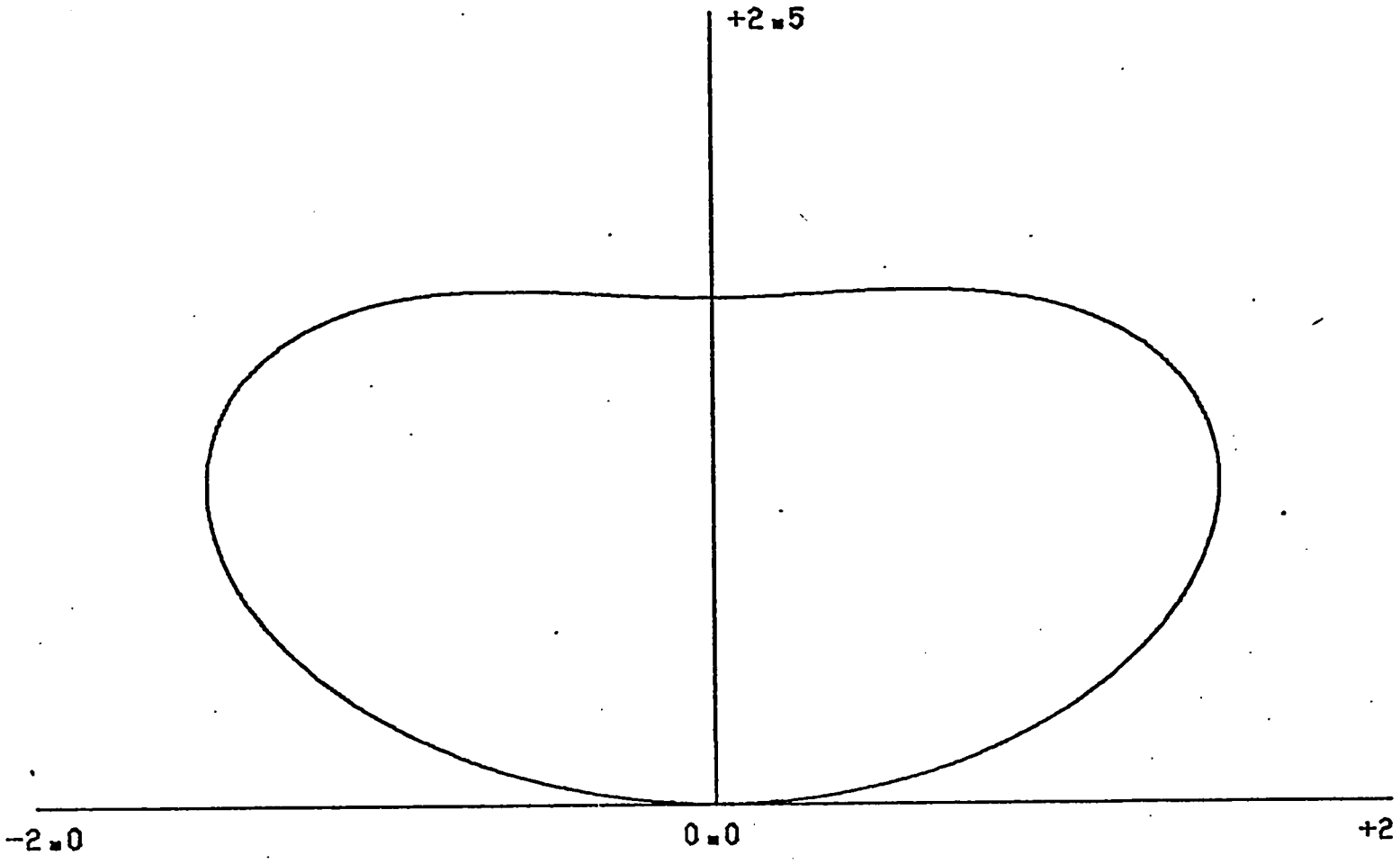

AMMONOID CROSS SECTION GENERATED BY 5-TERM FOURIER SERIES

A(0)= 1.00 A(1)= .40 A(2)= 1.20 A(3)=-1.20 A(4)= .20

Fig. 3.3.2.5 Synthetic ammonoid cross-section (suite)

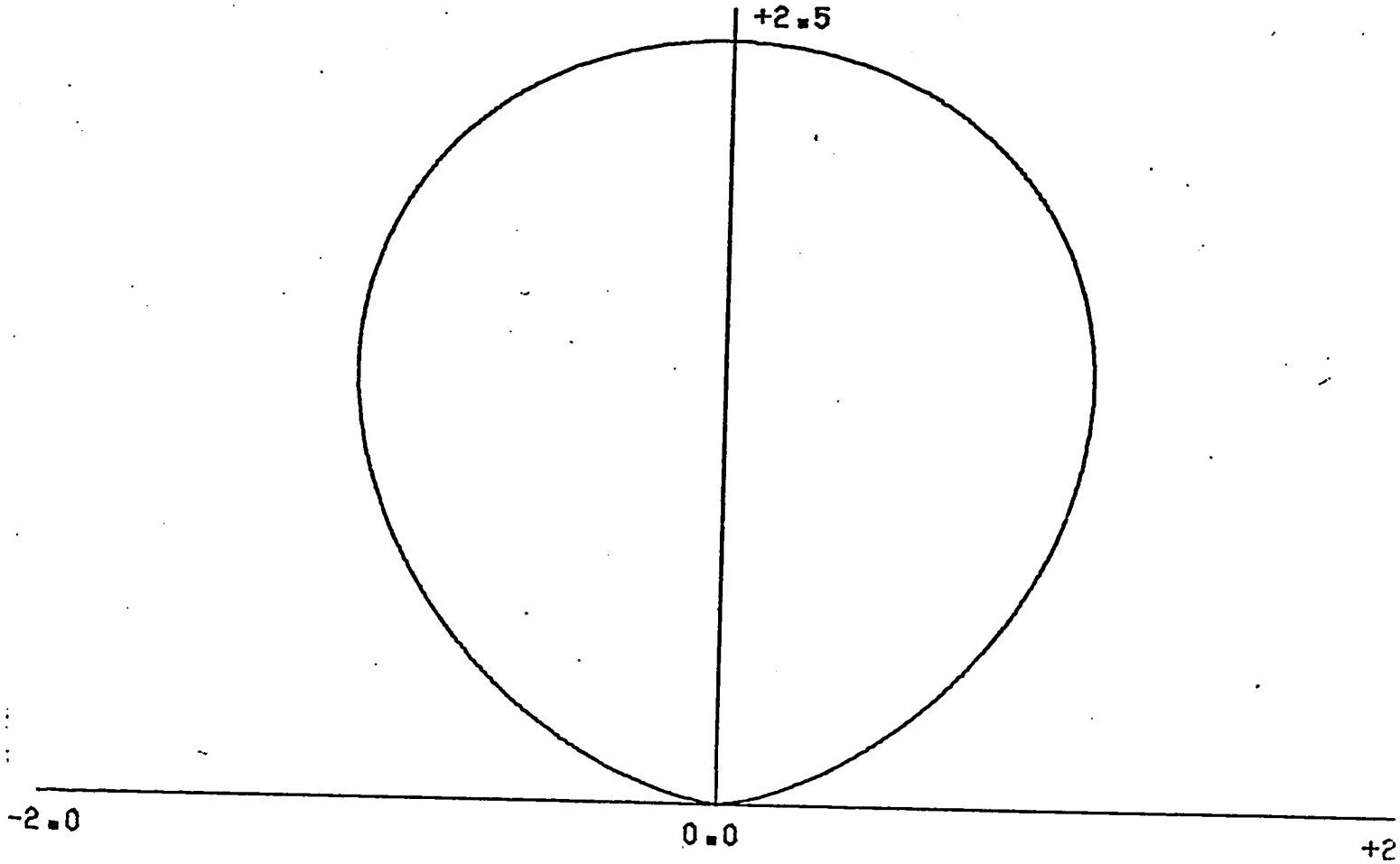

AMMONOID CROSS SECTION GENERATED BY 5-TERM FOURIER SERIES

A(0)= 1.00 A(1)= .60 A(2)= .80 A(3)= .20 A(4)= -.20

Fig. 3.3.2.6. Synthetic cross-section of a tubular uncoiled ammonoid, with no whorl overlap

All other traditional measurements and indices used in ammonites can be obtained from these data:

Whorl height

$$H = \rho \cos \phi = (\cos \phi \sum a_i \cos i \phi)_{max.} \qquad 3.4.1$$

Whorl width

$$W = 2 \rho \sin \phi = (2\sin \phi \sum a_i \cos i \phi)_{max.} \qquad 3.4.2$$

Cross-sectional area

$$A = \frac{1}{2} \int_{-\pi/2}^{\pi/2} \rho^2 d \phi \qquad 3.4.3$$

or:

$$A = \frac{\pi}{4} (2a_o^2 + a_1^2 + a_2^2 + a_3^2 + a_4^2) + 2(a_o a_1 + 1/3\ a_1 a_2 - 1/3\ a_o a_3 + 3/5\ a_2 a_3 - 1/15\ a_1 a_4 + 3/7\ a_3 a_4) \qquad 3.4.4$$

Peripheral length of cross-section

$$L = \int_{-\pi/2}^{\pi/2} \sqrt{(-\sum i a_i \sin i\phi)^2 + (\sum a_i \cos i\phi)^2}\ d\phi \qquad 3.4.5$$

All of these values can be computed from the original angular and radial measurements in the process of conducting the harmonic analysis of the data.

Volume - is computed by integration of the cross-sectional area through the coiling spiral, be it logarithmic or not, as the integration is numerical.

$$V = 2\int_0^{\theta}\left\{\int_{-\pi/2}^{-\phi\rho\cos\phi max} f(\theta,\phi)\, d\phi - \int_{-\phi\rho\cos\phi max}^{0} f(\theta,\phi)\, d\phi\right\} d\theta \qquad 3.4.6$$

Where

$$f(\theta,\phi) = \rho\sin\phi\cos\phi\sqrt{(\rho^2+r^2-2\rho r\cos\phi)\, d\theta^2 + \frac{(2r-2\rho\cos\phi)^2 dr^2}{\rho^2+r^2-2\rho r\cos\phi}} \qquad 3.4.7$$

Umbilical diameter

$$U_\theta = f(\theta) + f(\theta-\pi) - \left\{\rho\cos\phi_{max\theta} + \rho\cos\phi_{max\theta-\pi}\right\} \qquad 3.4.8$$

Where $r = f(\theta)$ is the equation of the midventer spiral

3.5 The morphology of the ammonoid suture line

The fluted septa of ammonoids, although used extensively by several authors for taxonomic purposes, have never been described quantitatively. Since most of the complication of the septum is present at its intersection with the shell, the suture line, and also to avoid boundary problems, we will look at the two-dimensional picture only. Following the ontogenetic development of the suture line, the primary suture

(from Schindewolf, 1965, fig. 265) shown in Fig. 3.5.1 (Pleurocephalites sp.) was subjected to harmonic analysis using the same techniques mentioned above. In this case it was necessary to carry the analysis to 8 terms in the series to account for more than 95% of the total sum of squares. A line spectrum is shown in Fig. 3.5.1. This is illuminating: it shows at $f = 2\pi/8$ the so-called "quinquelobate" type of this suture line (this is a misnomer, since there are only 8 lobes in the total suture, or 4 in the half suture shown in Fig. 3.5.1). It can also be seen from this spectrum that $f = 2\pi/6$ is the single most important frequency (this is Schindewolf's "quadrilobate" pattern which is masked in the primary suture by the higher frequency harmonic).

In Schindewolf's phylogenetic scheme, the "quinquelobate" pattern evolved from the "quadrilobate" one and accordingly these traits are given great taxonomic importance.

During further growth of the shell, the suture line grows preferentially in the periumbilical area (Fig. 3.5.3), and the complexity introduced by growth make it impossible to do a harmonic analysis: even after a 15-term smoothing by the running averages technique, the line remains multiple-valued.

To describe such a suture, data are recorded by taking the lowest ordinate for a given abscissa, an unequivocal procedure, and then the analysis proceeds as before.

As ontogeny proceeds, more and more elements are added

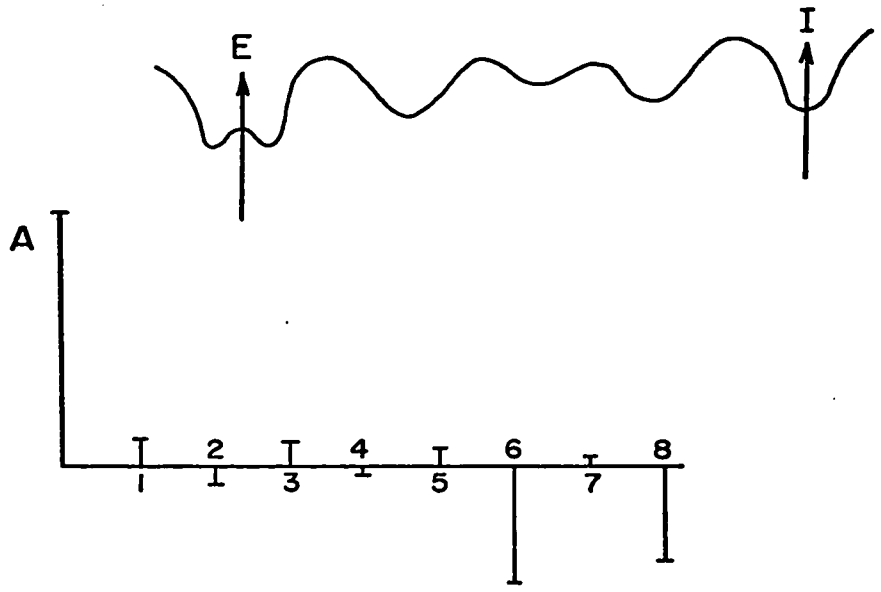

Pleurocephalites sp.

Fig. 3.5.1 and 3.5.2. An ammonoid primary suture line and its linear spectrum. The sixth and eighth harmonics account for 75% of the variance.

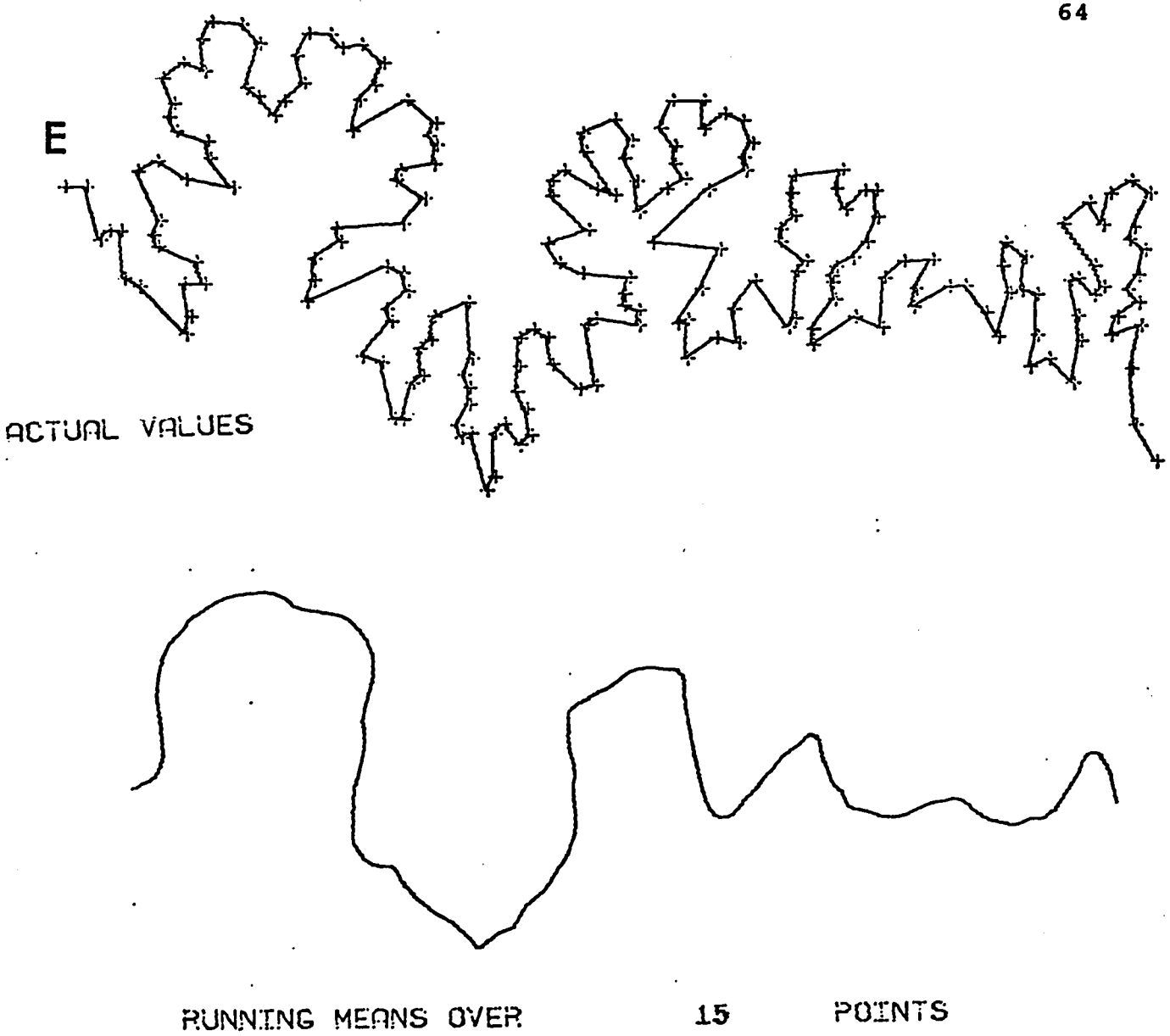

Fig. 3.5.3. An ammonoid suture line, digitized at major changes of direction, and a 15-term running average smoothing of it, showing still some significant complication and a flattened periumbilical region. Compare with Fig. 3.5.4

to the suture line, which soon becomes quite a complicated structure, as illustrated in Fig. 3.5.4 (from Palframan, 1968). The complication of a linear structure can be conveniently expressed by the ratio of arc length (along the line) over straight-line distance between the line ends. However, when this was done with suture lines, the length was found to be strongly dependent on the size of the unit of measurement (dots, Fig. 3.5.5.), as Richardson (1961) found to be the case for coastlines. It seems that this type of curve could be measured to have any total length desired, by using a unit of measurement small enough. Length in this case must be defined to be of a particular order, that is, defined only for a given unit of measurement.

An important consequence of this property is that these curves, not having an integrable length at any point, are not continuously differentiable in any region and therefore cannot have an equation. Steinhaus (1954) demonstrates that the usual concept of length is meaningless when applied to this type of curve, which he calls "non-rectifiable". In the case of natural linear structures, like river banks, coastlines, suture-lines or diffusion boundaries, non-rectifiability is due to their being, in a statistical sense, self-similar (Mandelbrot, 1967); each portion of the line shows, when blown up, the same degree of frilling as the complete line. Of the suture line, this is true at least as far as we can measure it, since it is

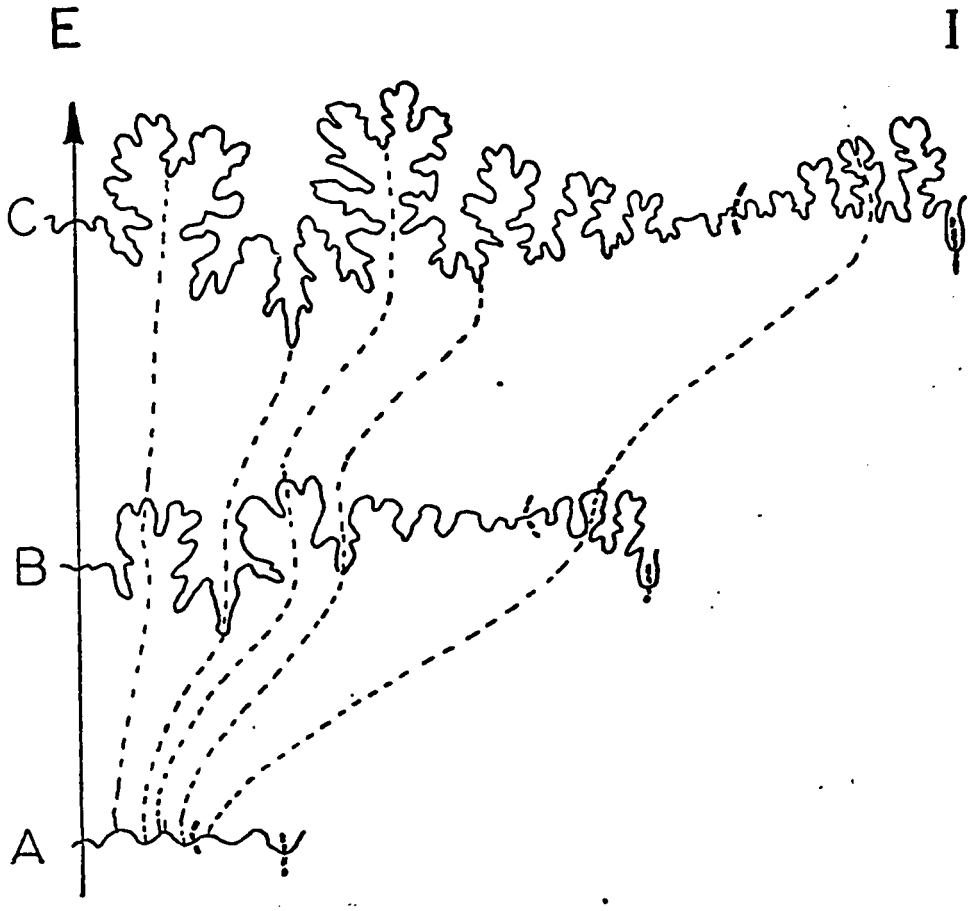

Fig. 3.5.4. Ontogeny of an ammonoid suture line (from Palframan, 1968), showing how most growth takes place in the periumbilical area. E: external lobe. I: internal lobe. A,B,C: successive (not continuous) ontogenetic stages.

probably not justifiable to use a unit of measurement much smaller than 0.5 mm, due to the accuracy of reproduction involved.

In contrast with non-rectifiable curves, rectifiable curves follow the behaviour illustrated by the measurements taken on a sinusoid, plotted as the line shown in Fig. 3.5.5: as the size of the unit of measurement is decreased, the length increases steadily, but instead of doing so without bounds, it approaches asymptotically a finite value, which we call the arc length of the curve.

As can be seen from Fig. 3.5.5 there is a linear relationship between the logarithms of unit of measurement and of total length for a non-rectifiable curve. That is:

$$\ln nd = \ln \Sigma d = a \ln d + b \qquad \text{with } a < 0 \qquad 3.5.1$$

$$\text{or} \qquad \Sigma d = s = Kd^{a} \qquad 3.5.2$$

$$\text{and also} \qquad n = Kd^{a-1} \qquad 3.5.3$$

where: d is the unit of measurement, n the number of times d is contained in the length of the line being measured, s the arc length of this line, a and b (= log K) the slope and ordinate intercept of the line plotting log d vs. log Σd.

If a=0 or if it tends asymptotically to zero, the curve is rectifiable. Otherwise, it is, as Mandelbrot (1967) has pointed out, of fractional dimension and non-rectifiable.

A convenient measure of complication is:

$$C = |a| \qquad 3.5.4$$

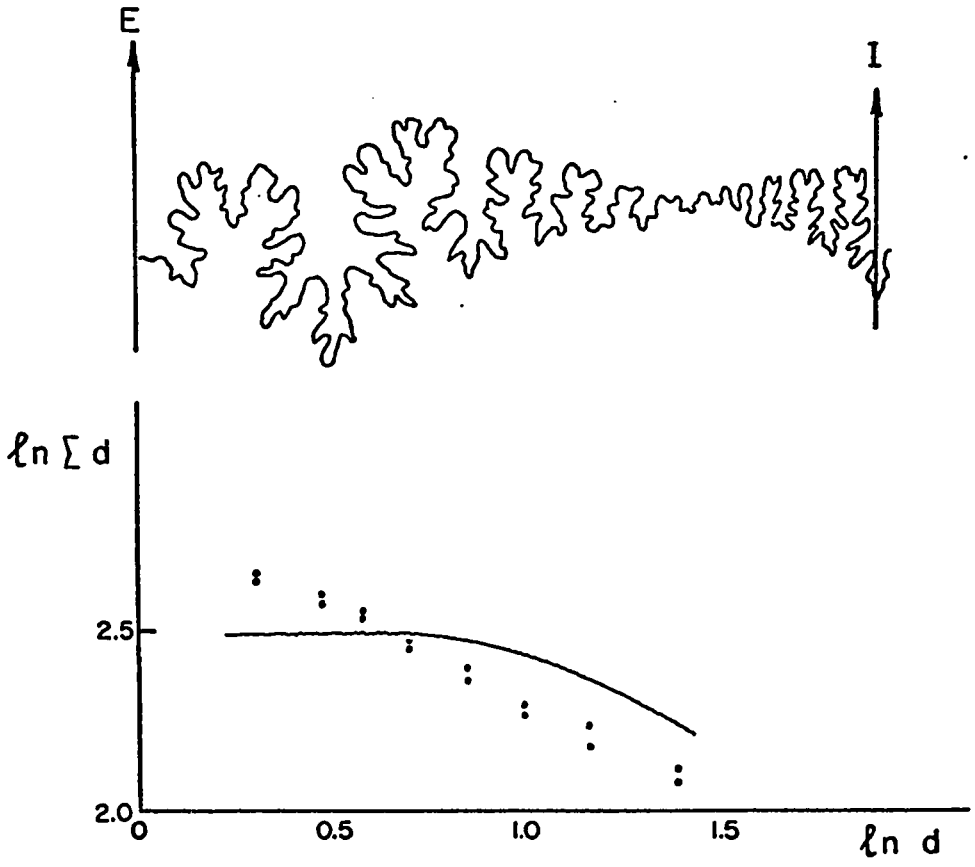

Fig. 3.5.5. An ammonoid suture line (Creniceras renggeri [Oppel]) and a logarithmic plot of its length vs. the unit of measurement (in mm.), showing that there is no fixed length for a structure of this type (dots). The length plot of a rectifiable curve (a sinusoid) is shown as a continuous line for comparison.

Its range is $0 \leq C \leq 1$ and it is linked to the dimension D of the line (in Mandelbrot's sense of fractional dimension) by $a=D-1$.

The values obtained for C in a sample of several ammonoids range from 0.15 to 0.82. The one illustrated in Fig. 3.5.5 has C=0.51. It appears that C is a useful, objective measure of complication.

Procedure. The values shown on Fig. 3.5.5 were obtained by walking a pair of dividers on the suture line, and counting the number of steps, for several openings of the divider's arms. In the case of several intersections, the one closest along the line was counted. If the unit of measurement is small enough, forward and backward measurements give the same results; otherwise they are averaged.

An alternative procedure, and one that lends itself to machine-reading of the data, is that proposed by Steinhaus (1954), based on a probabilistic measure of length: if a template with a set of equidistant parallel line is superimposed on the suture, an estimate of length is obtained from the number of intersections between the suture and the set of lines.

The suture line is scanned at regular intervals δx. The total number of intersections N is recorded; suture line is now rotated by an angle $\gamma = 2\pi/k$ and scanned again, k times. A probabilistic estimate of the arc length of the curve is:

$$L = N \pi \delta x / 2k \qquad 3.5.5$$

(Steinhaus, 1954), where L is length, δx the unit of measurement. At the same time, the lowermost intersection at each abscissa, recorded when the suture was oriented in horizontal position is obtained. From this single-valued function, a harmonic analysis is performed.

In conclusion, the morphology of the ammonoid suture live has been partitioned into three main components: (a) a sinusoidal primary pattern, whose prime example is the primary suture, (b) a pattern of ontogenetic transformation by anisometric growth of the suture, and (c) complication, a degree of indentation of the linear structure, for which an index is provided. Component (b) is left untreated here, as it can be readily dealt with by the standard allometric techniques.

CHAPTER 4

A MORPHOGENETIC MODEL FOR THE MOLLUSCAN SHELL

4.1 Shell growth in mollusks: a review

4.1.1 Structure and composition of the molluscan shell.

The detailed microscopic and submicroscopic morphology of the molluscan shell is fairly variable and complex and has been the object of numerous studies; comprehensive works on the subject include those of Bøggild (1930), Grégoire (1962), Mutvei (1964) and MacClintock (1967). The composition of the shell has been recently reviewed by Dodd (1967); Degens and Spencer (1967) and Wilbur and Simkiss (1968) discuss the composition of the organic matrix. Some factors pertinent to the morphogenetic model presented here will be briefly discussed below, with particular reference to the postulated existence of a set of sequential morphogenetic instructions, according to which the shell is built.

The molluscan shell is a two-phase composite material, in which an organic proteinaceous (conchiolin) mesh (the matrix) surrounds and penetrates into a crystalline array of aragonite and/or calcite (rarely vaterite). Like other composite materials, the shell combines the hardness of the crystalline phase with the elasticity of the matrix. Breakage is reduced due to the matrix impeding the propagation of cracks by

interrupting them and absorbing the strain. As a material, the shell probably resembles ferrocement best.

The shell is made up of several layers: an uncalcified outside layer, the periostracum, and two or more calcareous layers, the structure of which differs in different mollusks. Two types of structure are, however, universally present: prismatic, with short prisms arranged approximately normal to the shell surface; and lamellar, with thin lamellae in parallel arrangement, separated by conchiolin sheets. In addition, several other types of structure may be present: spherulitic, apparently homologous to the prismatic structure, but with smaller crystals arranged in spherical arrangements (spherulites), in different orientation within each spherulite; granular (homogeneous), with a compact arrangement of small crystals in irregular orientations; and crossed lamellar, with parallel-twinned lamellae oriented parallel to the shell surface. The crossed lamellar structure, present only in the mollusks is, however, absent in cephalopods (Mutvei, 1964).

The amount of organic matrix varies widely in the different molluscan taxa, from a minimum of 0.01% in some gastropods to a maximum of 5% in Nautilus; it is of course much higher in the internal shell of Sepia and squids.

The arrangement and distribution of the conchiolin matrix is also characteristic of each type of shell structure, although irregular concentrations of conchiolin are present in

all types of structure (Mutvei, 1964), decalcification of shell layers has also revealed a regular matrix pattern for each layer. In particular, the trabecular sheet pattern of the lamellar layer has proved to be characteristic in its morphology for the Bivalvia, Gastropoda and Cephalopoda (Grégoire, 1962).

The mineralogy of the shell is relatively simple: depending on the ionic radius, hexagonal and rhombic crystalline networks are possible for the carbonates of divalent cations, with the upper boundary of ionic radius for the hexagonal form being 1.00 Å. As the ionic radius of Ca^{+2} is 0.99 Å, calcite, the hexagonal form, is the stable polymorph, but the rhombic metastable form, aragonite, is almost equally likely to form (Wilbur and Simkiss, 1968) given especially the other controls present during carbonate precipitation (other ionic substances, epitaxy, impurities). The primitive mineralogical composition of the mollusk shell is, however, aragonitic; it is also the only form found in cephalopods (with the exception of aptychi, the opercular structures of some ammonites) and in most gastropods. Many bivalves have developed the ability to secrete calcite in the prismatic layer or in the lamellar layer (calcitostracum).

Turning now to the chemical composition of the shell, the mineral phase is primarily calcium carbonate, with minor amounts of other cations (Vinogradov, 1953). The

abundance of some of these cations, especially Mg^{+2} and Sr^{+2} is controlled by the mineral composition of the shell, and the environmental temperature and salinity (Dodd, 1967); it is probable, however, that an ability to discriminate against foreign cations evolved in several groups of molluscs (Hallam and Price, 1966, 1968). Such an ability, which would be especially valuable in thin-shelled mollusks due to the consequent improvement in the mechanical properties of the shell, must be mediated by changes in the composition of the organic matrix.

The conchiolin matrix is variable in composition (Degens and Parker, 1967, provide an adequate summary), being made primarily of proteins, with polypeptides and polysaccharides (including, in some cases, chitin) playing a secondary role. The matrix composition of each layer is different (Wilbur and Simkiss, 1968), which is understandable since each layer is secreted by a different portion of the mantle epithelium (see below), but also, there are differences in composition within parts of the periostracum; this may be caused by the influence of an alkalinity gradient with the external medium. The differences in amino acid composition of the organic matrices of different shell layers are of taxonomic importance, but their significance is far from clear, and are the object of much current research.

4.1.2 Shell secretion. The different layers of the mollusk shell are secreted in a cavity located between the mantle and shell, filled with a fluid (the extrapallial fluid) mostly secreted by an outer layer of mantle epithelium, but also partly owing its origin to diffusion of ionic substances from the external medium through the periostracum (Wilbur, 1964; Mutvei, 1964; Digby, 1968). The main source of calcium is the blood, which is supersaturated with calcium carbonate; calcium diffuses through the epithelium to the pallial cavity. Its precipitation, however, is inhibited by the presence of PO_4^{-3} in the blood. It appears, then, that three conditions are necessary for shell formation to take place: the existence of an organic matrix, the presence of an extrapallial fluid supersaturated with respect to calcium carbonate, and the removal of some inhibitory ions from the extrapallial fluid (Wilbur and Simkiss, 1968).

Mutvei (1964) presents evidence for the different shell layers being formed by the same epithelial cells but in different phases of their existence. The same evidence, however, can be interpreted differently, the type of layer formed depending on the thickness of shell between it and the external medium (Digby, 1968). One thing is clear: new epithelial cells are generated exclusively in the outer mantle fold, at the shell edge.

The mechanism of shell secretion is far from clear;

the processes that mediate the formation of the matrix and the precipitation of the calcium carbonate are obscure and the chemicals involved and their mode of action unknown. The processes postulated, then, are mostly at the stage of generalities and are presented below as such.

Briefly, there are two current theories of shell formation: the template theory and the electrochemical theory.

The template theory (Wilbur, 1964) postulates, first, the formation of matrix from the polypeptides present in the extrapallial liquid by a selective linking of these polypeptide chains, and second, the precipitation, by a process of epitaxis, of calcium carbonate on the conchiolin matrix, which, acting as a template, controls the composition and structure of the crystalline phase. That the synthesis of the matrix proteins in the extrapallial fluid is a selective process is evidenced by the vastly different amino acid composition of fluid and matrix (Wilbur and Simkiss, 1968).

The electrochemical theory (Digby, 1968), attributes the precipitation of calcium carbonate to the alkalinity of the inner face of the periostracum, which is also electropositive. The alkalinity gradient and potential are presumed to be caused by diffusion of salt water through the periostracum, due to mantle suction, the periostracum being a semiconducting membrane. In this theory, a prismatic layer will be formed as long as the shell thickness permits the sucking of water

between crystallites. Afterwards, shell precipitation takes place entirely from the extrapallial fluid and a lamellar layer results. The organic matrix would thus play no role in the precipitation of the shell, and would be a by-product of shell formation.

Both theories are entirely consistent with the episodic nature of molluscan shell growth and it is difficult at present to obtain information or devise an experiment that would disprove either. One characteristic, though, both theories have in common: that shell deposition is mediated by diffusion or diffusion-like phenomena. Once shell deposition is initiated at one point, this deposition impulse travels along the growing edge of the shell, either by propagation of epitaxial crystal formation (template theory) or by consecutive change of the electrochemical potential and of alkalinity along the newly formed periostracum (electrochemical theory). This property is made use of in the mechanism proposed below (section 4.2) to account for the shell morphology resulting from a diffusion model of shell growth.

4.2. Accretionary growth and shell expansion

4.2.1 Steps in a model for shell secretion.

Accretionary growth in mollusks is episodic, that is, it takes place at discrete intervals, when the mantle margin is protruded over the shell edge, extrapallial fluid is secreted and

precipitation of organic matrix and calcium carbonate proceeds. Between intervals, no growth at all can take place. The episodic nature of this type of growth makes it possible to simulate it by means of a series of sequential instructions. The essential features of molluscan accretionary growth can be reproduced with a fair degree of accuracy by the morphology resulting from such a sequential set of instructions. A model that simulates the growth of the molluscan shell can be specified by the following five steps:

i) the mantle edge rests in static equilibrium, supported by the shell edge and pushed against it by the turgor of the mantle connective tissue; it protrudes over the edge of the shell and in so doing, creates a pallial cavity along the shell margin.

ii) In this cavity, filled with extrapallial fluid, diffusion of a substance that induces shell accretion is initiated at one or more points. The substance responsible for the initiation of shell deposition, called a morphogen (Turing, 1952) diffuses along the shell edge. Due to the episodic, discontinuous mode of growth under discussion, there is no need to consider equilibrium situations, and Turing's (1952) system of two morphogens can be reduced to only one. The patterns of interest are obtained by the interruption of the diffusion process at some finite time after its initiation, that is, under non-equilibrium conditions. This requirement

is compatible with theories of shell formation and could correspond, for example, to the removal of the crystallization inhibitory ions from the extrapallial fluid (Wilbur and Simkiss, 1968, p.236).

iii) After the morphogen has diffused a certain variable period of time, accretion begins. The amount of shell accreted is proportional to the amount of morphogen present at a given point along the mantle edge, and the morphogen is consumed by a chemical reaction also proportionately to its concentration (first-order reaction). This is a non-equilibrium process, since no differential growth will result if diffusion is allowed to continue indefinitely.

iv) The mantle is retracted; during this step, multiplication of the mantle epithelial cells takes place.

v) The process recurs back to (i).

Each of these five steps admits several variants, the different combinations of which can produce all the morphological variation present in molluscan shells.

4.2.2 Some morphological consequences of the model.

In what follows, alternatives for the five morphogenetic steps proposed in section 4.2.1 will be examined and the most important will be translated into the forms resulting from them.

i) The static equilibrium resulting from the

conditions outlined in this step determines the shape of the cross-section and will be dealt with in a separate section (see below).

ii) For the concentration of the morphogen along the mantle edge, the fundamental equation (Crank, 1956) is given by Fick's one-dimensional second law of diffusion in a two-component system, with a linear sink (first-order reaction):

$$\frac{\partial u}{\partial t} = \frac{\partial}{\partial s}\left[D_u \frac{\partial u}{\partial s}\right] - ku \qquad 4.2.2.1$$

where u = concentration of morphogen

t = time

s = distance along the mantle edge from morphogen source

D_u = diffusion coefficient at concentration u

k = constant, characteristic for the reaction, where the rate of morphogen removal is ku

This equation has no analytical solution unless D_u is a fairly simple function of the concentration. The following alternatives are of interest:

a. The diffusion coefficient. If we assume low morphogen concentrations then D_u = constant.

In this case, equation 4.2.2.1 reduces to:

$$\frac{\partial u}{\partial t} = D \frac{\partial^2 u}{\partial s^2} - ku \qquad 4.2.2.2$$

which has the analytical solution

$$u = k \int_0^t u_1 \exp(-kt')\, dt' + u_1 \exp(-kt) \qquad 4.2.2.3$$

where u_1 is a solution of

$$\frac{\partial u}{\partial t} = D \frac{\partial^2 u}{\partial t^2} \qquad 4.2.2.4$$

and equals

$$u_1 = \frac{u_0 \exp(-s^2/4Dt)}{2\sqrt{\pi Dt}} \qquad 4.2.2.5$$

where u is the amount of morphogen secreted at time t=0 from the source s=0 and which is allowed to diffuse away from the source.

b. Number and position of sources. A single point-source in median position, of course, is the simplest case, but other interesting cases include: three sources, with two of them arranged symmetrically on either side of a central one; this condition would generate an outline similar to an ammonoid opening (see below). Or, an asymmetrical source, that is, at least two sources differing in amount of flux; a helical spiral

would be the result in this case.

c. Boundaries of secreting area. If the secreting area is considered to be a ring, the solution takes a periodic form, as a summation of an infinite series with exponential terms (Turing, 1952,p.49). As a first approximation, however, and considering only the non-equilibrium case, that is, diffusion taking place over a small, finite length of time, equation 4.2.2.3 can still be used as a solution, with the proviso that solutions must be calculated only for $-\frac{s_m}{2} \leqslant s \leqslant \frac{s_m}{2}$, where s_m is the total length of the secreting ring. The final effect of adding the terms of the series solution is to produce the same morphogen concentration distribution as would be produced by allowing diffusion to take place over a longer period of time, that is, adding more terms to the series solution flattens out the morphogen concentration-distance curve, but its shape remains basically the same.

The second case of interest in regard to boundaries is the presence of impermeable boundaries. In this case, the boundary acts as a reflecting layer and the solution for any given point is obtained by the superposition of two solutions: that calculated directly from equation 4.2.2.3 and a virtual solution obtained by extending the length s beyond the reflecting boundary at $s_m/2$ and calculating the value at U_{s_m-s} . Again, this is an approximation of an infinite series solution and is valid only for short periods of time. As an example,

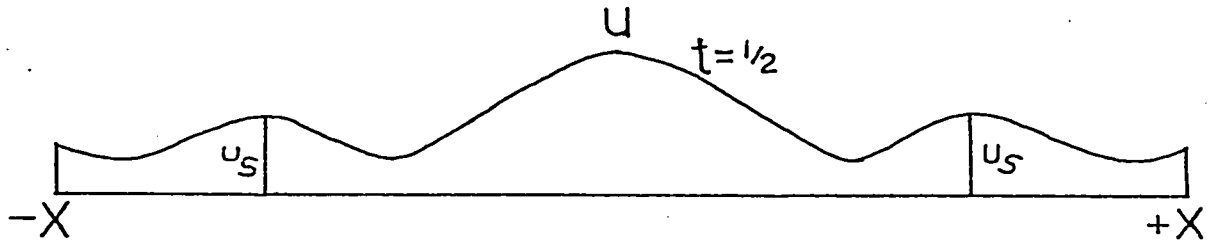

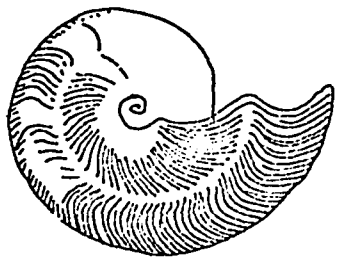

Fig. 4.2.2.1 Nonequilibrium solution of diffusion equation with 3 sources and a reflecting boundary, obtained by adding three partial solutions.
u = morphogen concentration
t = time
The aperture of an ammonoid, Harpoceras sp. is shown for comparison.

Fig. 4.2.2.1 shows a solution obtained for the case: three sources, one at s=0 and one each at s=±2/3 (with initial concentration $u_s=u_{0/2}$) with a reflecting boundary at s=±1. The graphical solution (for Dt=1/2) was obtained by adding the solutions of equation 4.2.2.3 for each source and adding to them the values reflected at the impermeable boundary. The shape of an ammonite aperture and growth lines (Harpoceras sp.) are shown for comparison.

d. Initial and boundary conditions for integrating of the diffusion equation. If the rate of production (flux) of morphogen is such as to maintain a constant concentration at the source, as in the case of equilibrium with an external source medium, then the initial and boundary conditions are:

$$u = 0 \qquad t = 0$$

$$u = u_0 \qquad t > 0$$

Other interesting condition is that arising from an initial, instantaneous amount of morphogen being secreted and then allowed to diffuse with no further secretion. This condition amounts to the total flux being constant for each accretion episode:

$$M = \int_{-1}^{+1} uds = C_2 \qquad 4.2.2.6$$

If the final ratio of concentrations at the source and at the distal end of the secreting edge (reflecting boundary) is

$$\frac{u_0}{u_1} = \frac{u_0}{u_{-1}} = C_3 \qquad 4.2.2.7$$

This is reflected in the shell in the ratio between the lengths of the midventer line and of the umbilical seam. If this ratio is constant, the shell is self-similar and it follows a logarithmic spiral. The higher this ratio, the smaller the angle of the logarithmic spiral and the higher the rate of expansion of the shell.

The concentration at the distal end is zero:

$$u_1 = u_{-1} = 0$$

This is the case of most brachiopods and some bivalves, like Gryphaea.

The concentration of morphogen is constant along the mantle margin:

$$\frac{\partial u}{\partial s} = 0$$

This situation can arise through two different conditions: a very high diffusion rate (see below) or a long time allowed for diffusion to take place, thus leading to an equilibrium concentration gradient. Notice that this condition is incompatible with the first listed condition, that is, in a given discrete secretion episode, for a constant morphogen concentration to exist, secretion must have stopped for some time while diffusion is still taking place.

This condition leads to tubes and, if expansion accompanies accretionary growth, to orthoconic shells.

e. Diffusivity. Over a range of low concentrations and in ionic substances, the diffusion coefficient is constant or almost so. In molecular substances and at all but the lowest concentrations it is strongly dependent on concentration, showing an inverse relationship to it.

From molecular kinetics considerations, the diffusion coefficient is also inversely proportional to molecular weight. The substances we are dealing with (morphogens) are presumably protein precursors and thus have a high molecular weight, so that diffusion coefficients are probably an important factor in the model (see below under "homeomorphy and iterative evolution").

It is also possible that the chemical composition of the morphogen be altered during ontogeny, thus accounting for changes in the geometry of the shell. This is especially possible for apertural modifications in the ammonoid shell (lappets and rostra). These effects can also be produced by behavioral changes (see below).

iii) Time interval during which diffusion takes place. The periods of shell accretion vary widely in mollusks, depending upon the seasons of the year, the weather, tidal cycles, the ecologic conditions (subaerial exposure, wave energy, food availability, etc.) and the physiologic state of the

animal (Rhoads and Pannella, 1970; Dodd, 1969; Evans, 1972). In general, though, one can state that accretion intervals have a frequency of the order of a few hours (Pannella and MacClintock, 1968, have observed apparently daily growth rings in a variety of mollusks, including some ammonoids).

If the periods of mantle protrusion (during which morphogen diffusion and subsequent calcification take place) could be modulated, this would account for changes in the morphology of the growing edge, and as a consequence, of the whole shell, if the modulation is maintained for a long enough period of time.

Figure 4.2.2.2 (after Crank) shows non-equilibrium concentration profiles for different time intervals. The effect of shortening the time allowed for diffusion is similar to that of lowering the value of the diffusion coefficient.

iv) The periods when the mantle is retracted usually alternate cyclically with the periods of shell accretion. Growth of the mantle edge epithelium is assumed in this model to take place by cell division and during this stage. Naturally, the perimeter of the mantle edge has to increase if there is to be expansion of the shell. Otherwise, the shell would be an accretionary tube. Observations of wounds that apparently damaged the mantle (Fig. 4.2.2.3) and also of longitudinal ribbing (strigations) show that most of the mantle growth in ammonoids takes place by addition of new cells away from the

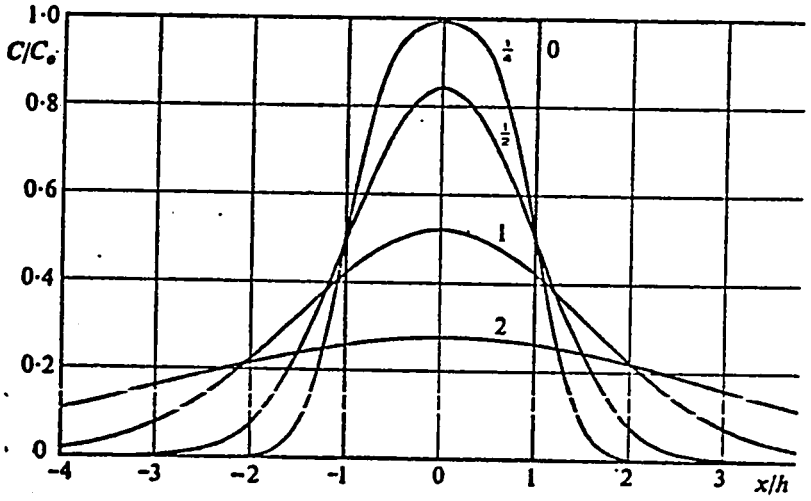

Fig. 4.2.2.2 Typical non-equilibrium concentration-time curves (after Crank, 1956).

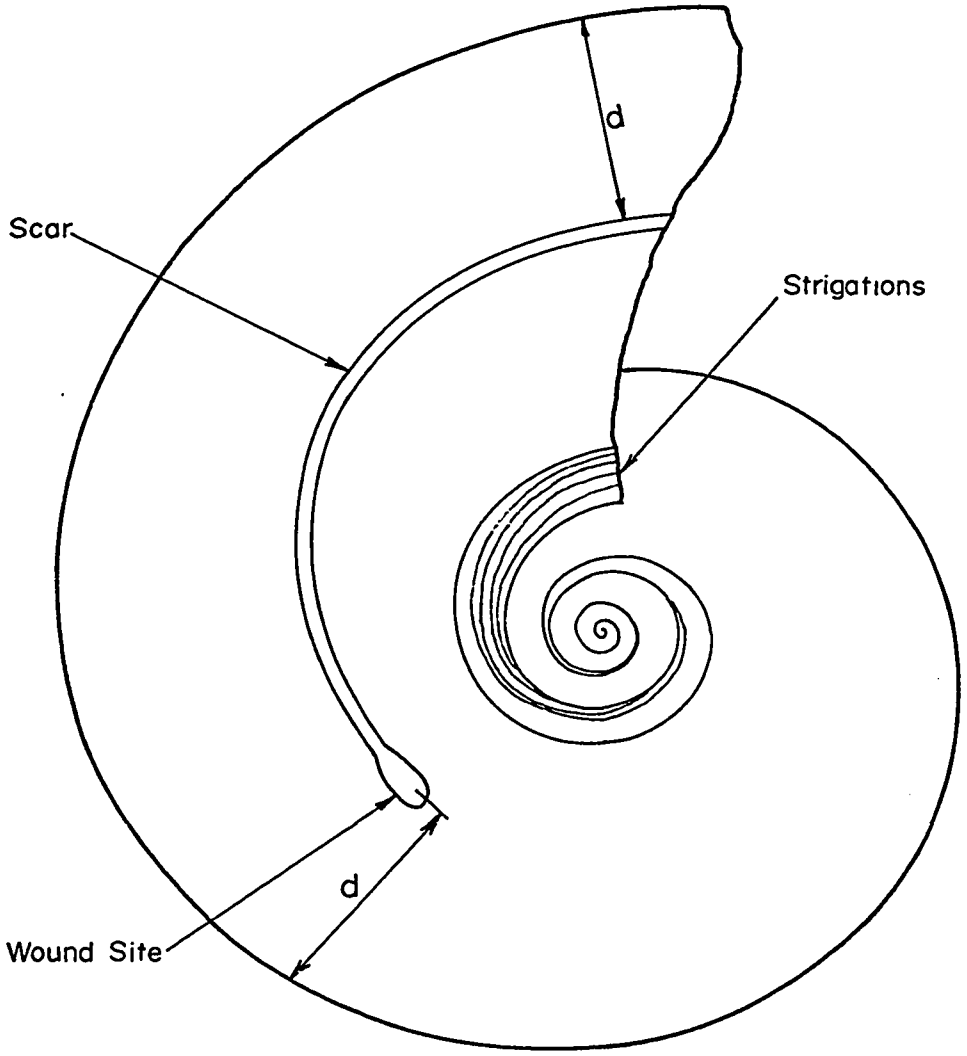

Fig. 4.2.2.3 Composite sketch of ammonite shell showing a wound that injured the mantle and the scar that trails it. Longitudinal markings (striqations) appear from the umbilical region. Both lines of evidence show growth to occur primarily in the umbilical region.

umbilical seam. Under the mechanical conditions discussed in section 4.3 this means that in general, through ontogeny, the cross-section will become more and more protracted (Fig. 4.2.2.4). This effect is probably enhanced by the fact that the analysis in section 4.3 neglects surface forces, which are certainly important at larval and early post-larval growth stages, and account then for the universally present globose shape of the earliest growth stages in ammonoids. Since the rigid framework of the shell provides a template upon which successive layers of calcium carbonate are deposited, its initial shape becomes an inherited form which is only slowly modified as the mantle grows in size.

The model assumes then that new cells are added to a region centered on the umbilical shoulder (Fig. 4.2.2.5 shows homologous points on the cross-section and a hypothetical frequency distribution of new mantle epithelial cells). It is worth noticing that this model of mantle growth in ammonoids is consistent also with Schindewolf's observations of the septal growth (in the form of elongation of the septal suture) taking place mostly in the umbilical seam region. This can be clearly seen in Fig. 3.5.3 showing a smoothed adult suture line that gives the impression of having been stretched in the umbilical region and Fig. 3.5.4, showing the course of ontogenetic development of a suture line, with most of the growth restricted to the periumbilical region.

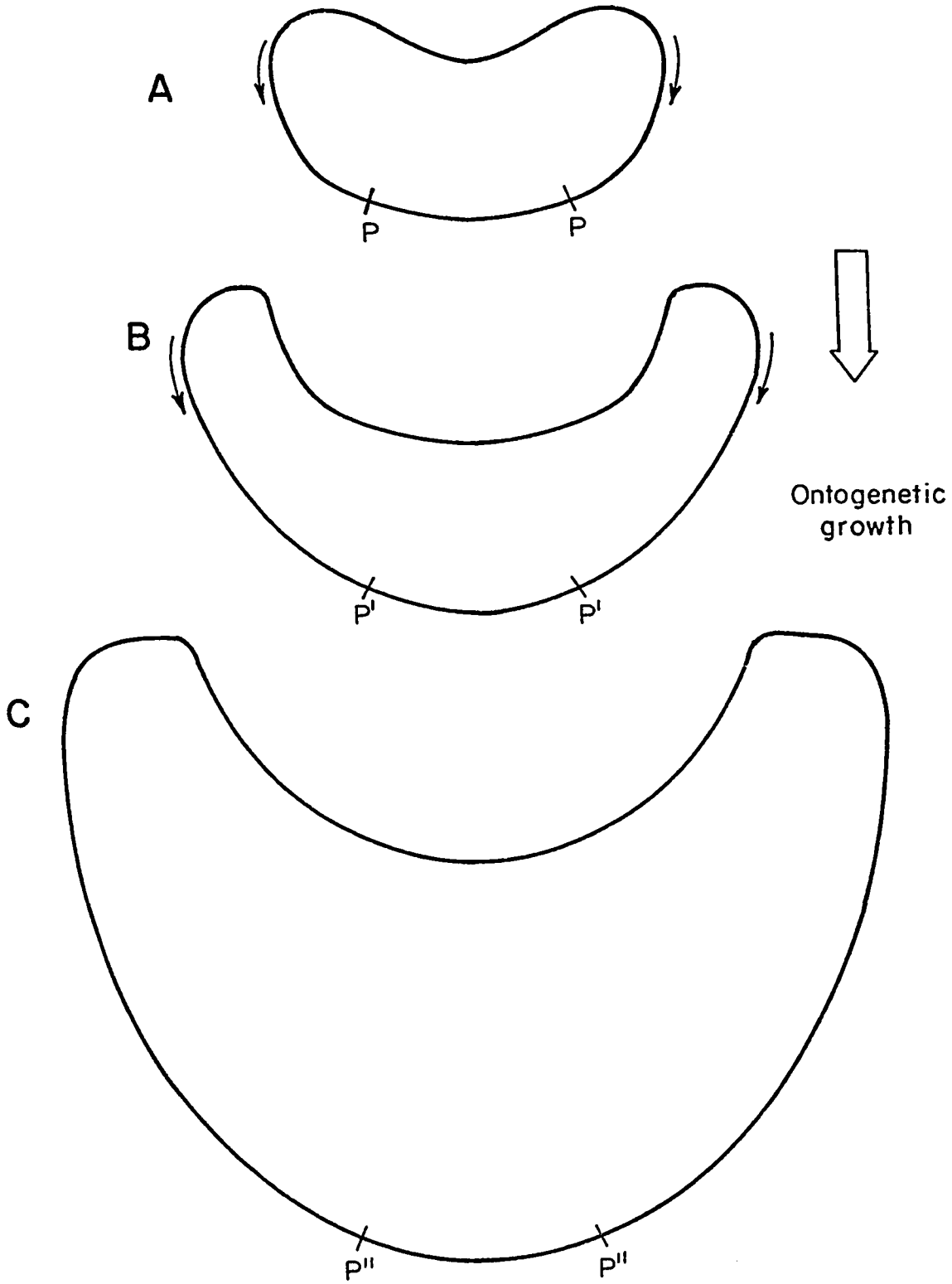

Fig. 4.2.2.4 Sketch of the change in cross-sectional shape accompanying growth in the ammonoid shell. PP, P'P' and P"P" are pairs of homologous points that migrate ventrad relative to the rest of the shell. A,B,C: successive growth stages.

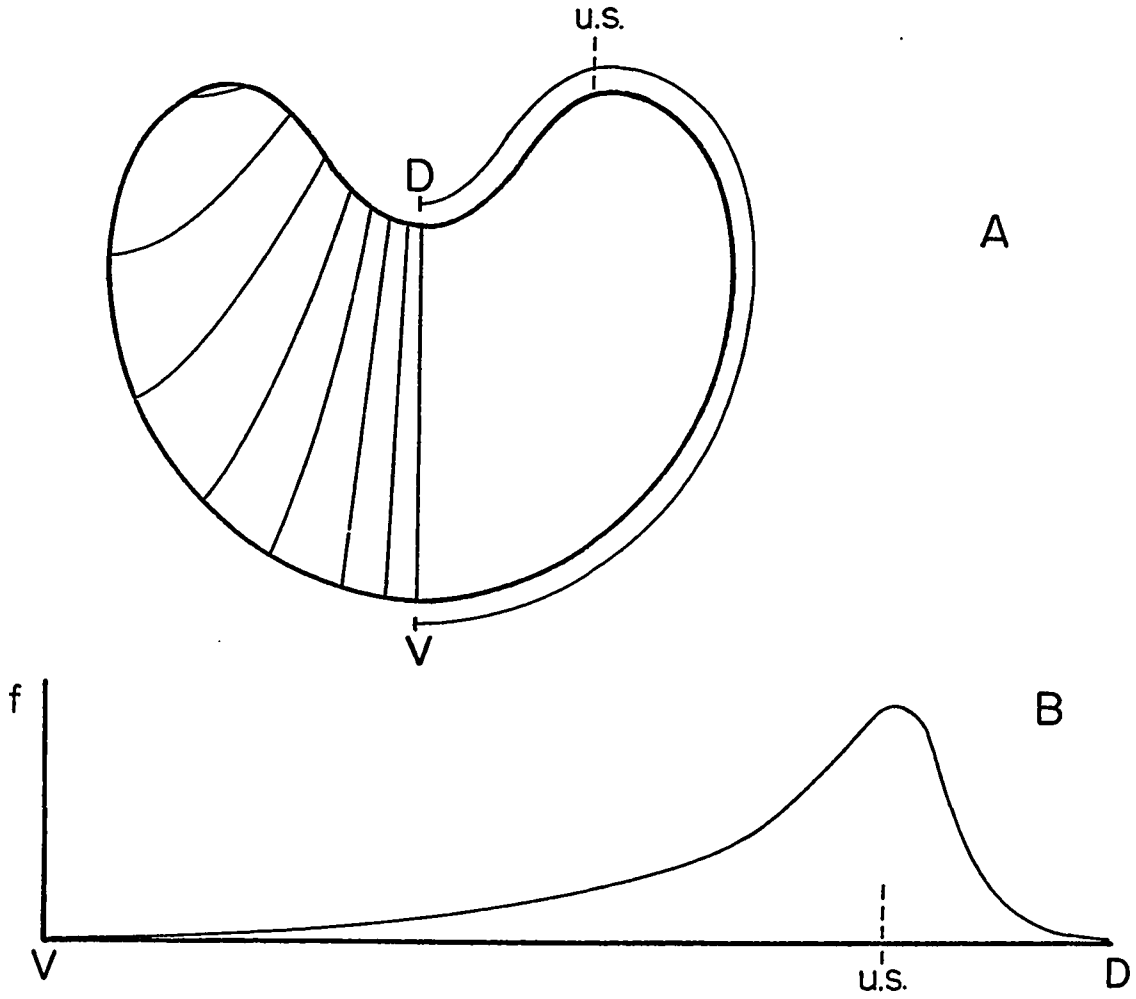

Fig. 4.2.2.5 A: Ammonoid cross-sections with isogrades of equal mantle cell proliferation, as postulated by the model of section 4.2.2.

B: Frequency distribution of cell proliferation along the mantle edge (hypothetical).

D: dorsal region; V: ventral region
U.S.: umbilical shoulder

4.2.3 Homologous points in the mantle. The presence of longitudinal striations (strigations) and of longitudinal wound scars in ammonoid shells has two main implications:

i) that they mark homologous points in the mantle, otherwise impossible to identify;

ii) that at least part of the shell secretion is very local, showing that the model that assumes diffusion of a morphogen in the extrapallial fluid followed by calcification is incomplete.

Point i) enables one to trace, by means of Thompson's (1942) deformation grids or other similar transformation techniques, the development of the cross-sectional shape. This has made in part possible the formulation of the model for growth of the mantle edge.

Point ii) makes it plausible that the explanation of most longitudinal markings in molluscan shells is that they are produced by substances with very low diffusion rates. Thus, practically all colour markings are longitudinal, a fact consistent with the high molecular weights of most of these pigments. The same explanation is offered for strigations, which are then seen as very different in character from regular ribbing. This is consistent with observations of the finer structure of strigations, which unlike regular (radial) ribs are not undations of the shell but are usually concave in cross-section and raised at the rims, and thickened overall, with

accretion lines normal to the direction of the strigation.

Apart from strigation and wounds, the only other homologous points in the shell correspond to the directive rib of Lison (1949), which in ammonoids corresponds to the midventer line.

A similar explanation to that of longitudinal strigations has been offered by Waddington and Coe (1971) for the deposition of pigment in the shell of some marine gastropods (Conidae). Diffusion rates are here in between the ones for radial and those for longitudinal ribbing. If one assumes that there are threshold values for the concentration of the pigment morphogen above and below which deposition does not take place, a V-shaped pattern pointing apicad results. A similar model but with relatively higher diffusion rates accounts for bifurcating ribs in ammonoids, in which at least one of the furcated ribs must be transgressive over the growth lines.

4.2.4 Homeomorphy and iterative evolution. The morphogenetic model can also account for two frequent occurrences in the evolution of the ammonoids: homeomorphy and iteration.

i) Homeomorphy (Buckman, 1895) can arise in two main ways: (a) by a coincidental repetition of the same set of morphogenetic instructions (presumably this is possible only in the case of simple morphologies), or (b) due to two

different sets of instructions having the same total (or final) effect. This second mechanism is of course the more interesting one, as it allows two groups of quite different ancestry to give rise to similar morphologies, and to the same successions or morphologies (for example, Juvavites - Macrocephalites, Parajuvavites - Xenocephalites.).

ii) Iterative evolution. The existence of iterative evolution as a common occurrence in ammonoids points out to two sets of factors: (a) external factors, that is, the periodic recurrence of similar environmental conditions that make the evolution of certain morphologies possible or necessary, and (b) internal factors, a set of mechanical and biochemical instructions and constraints, relatively simple, that permit the evolution of those morphologies virtually whenever they are necessary.

The set of factors (a) is, quite probably, related to the episodic recurrent history of the mesozoic seas, which was reflected especially in the fluctuating levels and especially, areas of the continental shelves and epicontinental seas where the ammonoids, like most present day cephalopods, in all probability bred.

As to the factors in (b), the mere fact that homeomorphy, a rather uncommon occurrence in most animal groups, is so widespread in mollusks, points out in favour of a model like

the one presented here, in which most of the constraints on the morphology and on its modifications (ontogenetic or evolutionary) are determined directly by the mechanical and chemical properties of th e tissues and organic compounds involved and not through the mediation of complex biological processes; if a particular morphology need not be genetically coded for in its entirety, this is, on the one hand, simpler and more economic of genetic material, and on the other, it makes its repetition or the reversal of evolutionary lineages much more possible.

4.3. Cross-sectional shape of the ammonoid shell

The forces acting on most biological structures at the moment of their formation are many and complex, and therefore usually impossible to estimate. A consequence of their complexity is that the resulting form is itself complex.

When the forms resulting from a morphogenetic process are simple, on the other hand, we may suppose that the forces acting upon these forms were also simple. Fig. 3.3.1.2 shows a cross-section of Sonninia sp. superimposed on a family of catenaries. The fit and general shape of the two curves are quite remarkable (especially if we consider that the curve has only one parameter), and it was observed that this fit was better the larger the ammonite. This suggests that weight is a determinant force in shaping the ammonoid cross-section, since a catenary is the curve of static equilibrium of a linear, flexible, inextensible arc deformed by its own weight. A catenary, however, is a monotonically increasing curve, and would not fit a double-valued curve like the ammonoid cross-section beyond the latter's point of maximum width.

The conditions for static equilibrium of the ammonoid cross-section during shell secretion can be stated as follows:

Consider the mantle edge in the ammonoid's normal growing position, as shown in Fig. 4.3.1. An element ds of the mantle edge is subjected to the following forces: H and T = tangential forces acting at the extremities of ds (H constant),

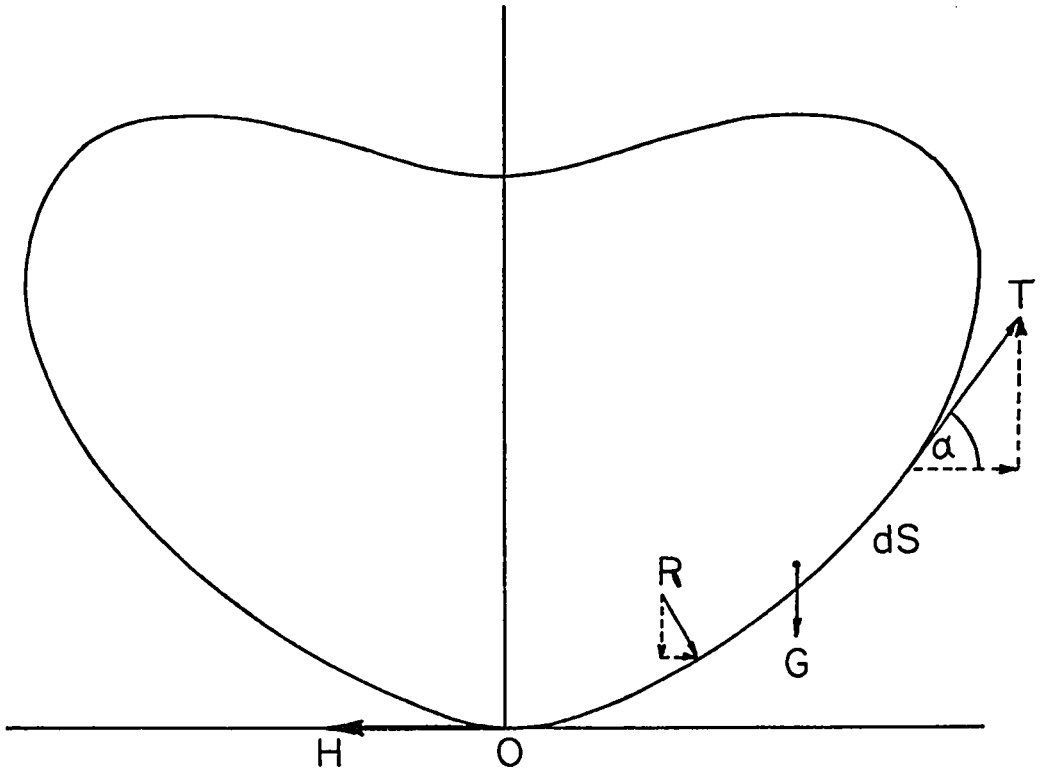

Fig. 4.3.1 The cross-section of an ectocochliate cephalopod shell, showing the forces acting on the mantle edge. H, T = tangential forces. R = radial force. ds = element of arc in mantle rim. G = weight of ds. α = angle of T with the horizontal.

$G = \gamma s$ = weight of the arc ds, where γ = linear weight of the mantle (a constant) and s = length along the mantle edge

α = angle of T with the x-axis

R = radial force, representing the turgidity of the mantle, which is everted over the growing edge of the shell. In general $R = f(s)$.

The condition for static equilibrium states that the vector sums of horizontal and vertical force components should be separately null, that is:

$$H = T \cos \alpha + R \cos (\pi/2-\alpha) \qquad 4.3.1$$

$$\gamma s = T \sin \alpha - R \sin (\pi/2-\alpha) \qquad 4.3.2$$

Rearranging and dividing 4.3.2 by 4.3.1:

$$\tan \alpha = \frac{dy}{dx} = y' = \frac{\gamma s \sqrt{y'^2+1} + R}{H \sqrt{y'^2+1} - Ry'} \qquad 4.3.3$$

Two main cases will be considered for the solution of this differential equation:

a). R = constant

This condition leads to:

$$y'' = \frac{d^2y}{dx^2} = \frac{C (1+y'^2)}{\sqrt{1+y'^2} + Dy'} \qquad 4.3.4$$

with initial conditions: $y'_0=0$ $y_0=0$ where $C=\gamma/H$ and $D=R/H$. Equation 4.3.4 has no analytic solution. Numerical solutions

using a predictor-corrector method (Bevington, 1969) for different values of C and D are shown in Figs. 4.3.2 and 4.3.3. Many more morphologies are possible, and these are meant only as examples.

b). $R = A + B\,s$

In this case, equation 4.3.3 takes the form

$$y'' = \frac{(1+y'^2)\ (E\sqrt{1+y'^2}+C)^2}{C\sqrt{1+y'^2}+E(1-y'^2)-2DCy'} \qquad 4.3.5$$

where $C = \gamma/H$

$D = A/H$

and $E = B/H$

Numerical solutions for D=1, and variable C and E are shown in Figs. 4.3.4 and 4.3.5.

The basic morphology of the ammonoid cross-section is successfully simulated by these equations; it seems reasonable then to conclude that the conditions of static equilibrium for the mantle edge at the moment of shell secretion are closely approximated by those listed above. Other, local forces must be in effect at parts of the mantle edge to account for other aspects of the cross-sectional shape.

Several other conditions are possible for the solution of equation 4.3.3, apart from the simple ones listed under (a) and (b) above. Our choice is, however, limited by the fact that no direct measurements of the forces under discussion

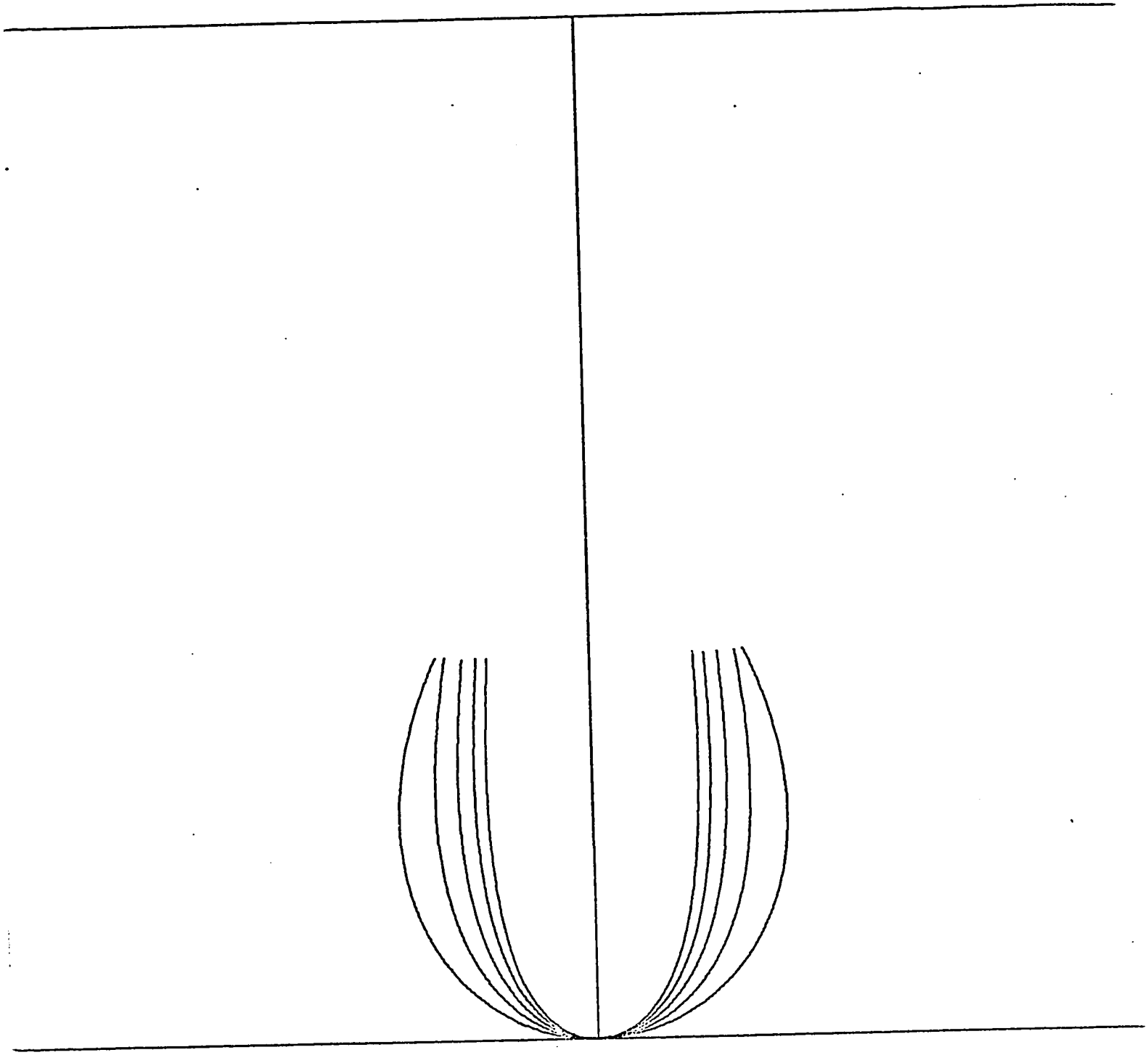

Fig. 4.3.2 A family of cross-sections for different values of C obtained by numerical solution of equation 4.3.4

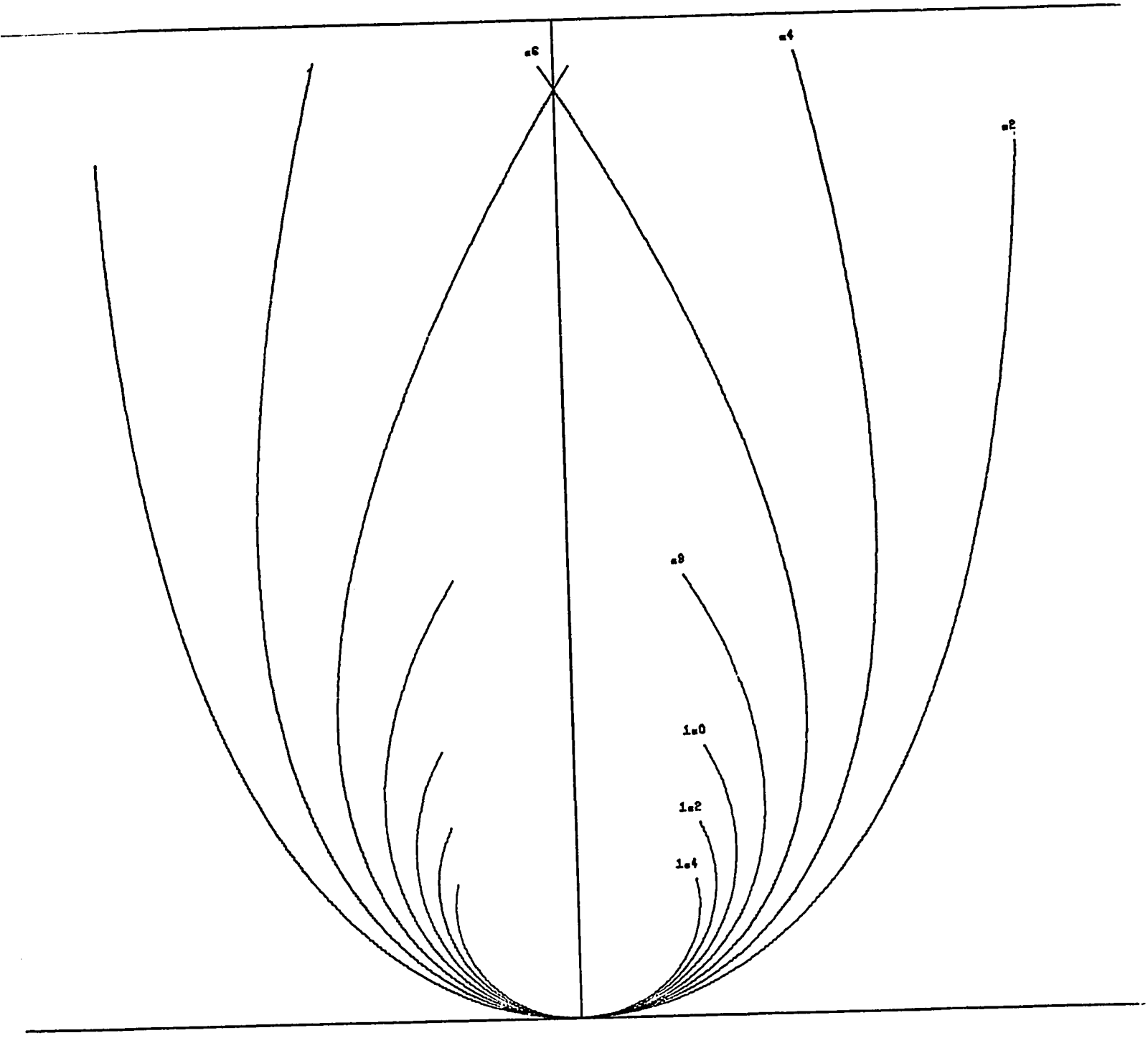

SECTIONS FOR C = .80

Fig. 4.3.3 A family of solutions of equation 4.3.4 for variable D

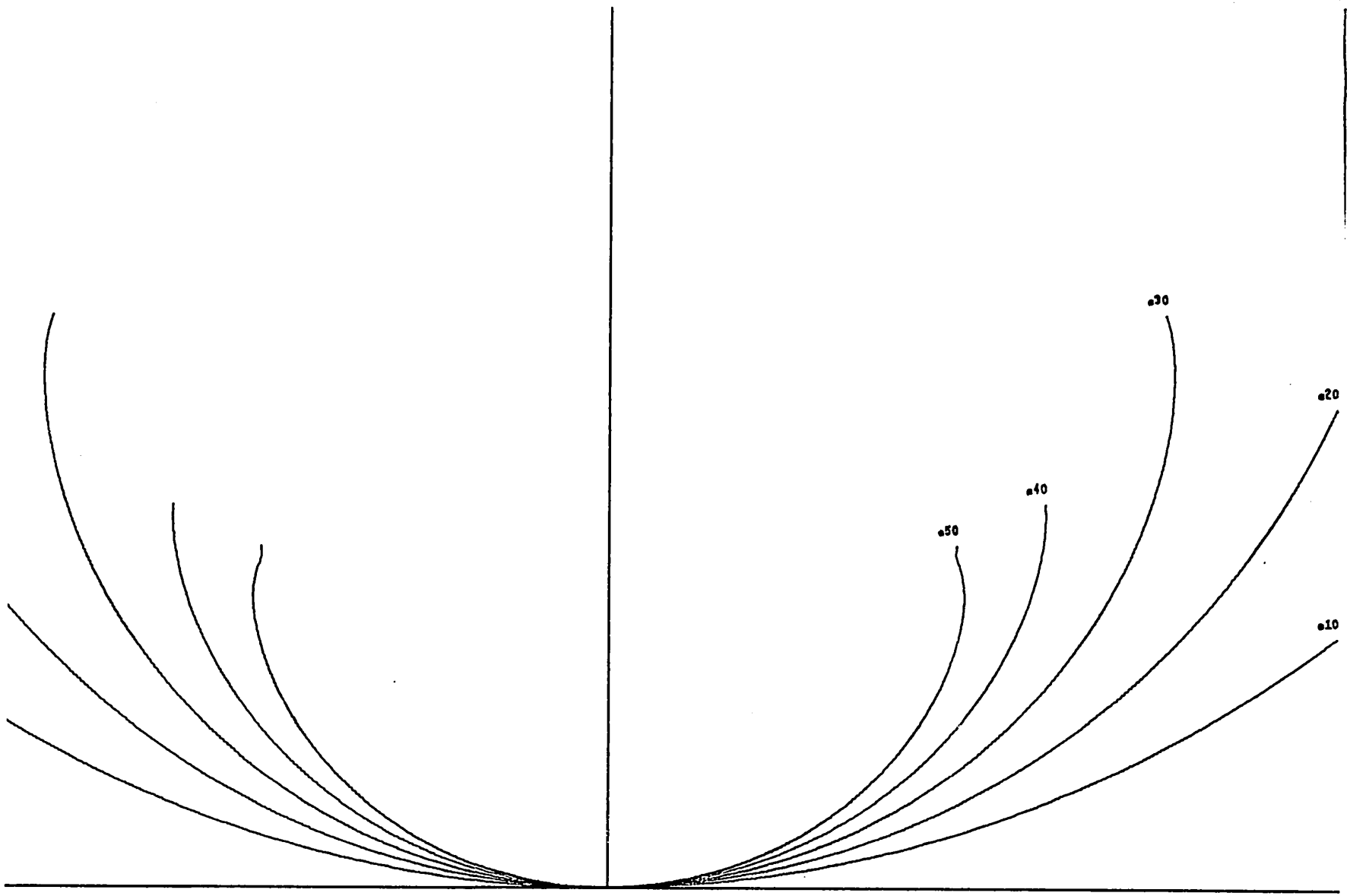

SECTIONS FOR C = .10

Fig. 4.3.4 A family of solutions of equation 4.3.5

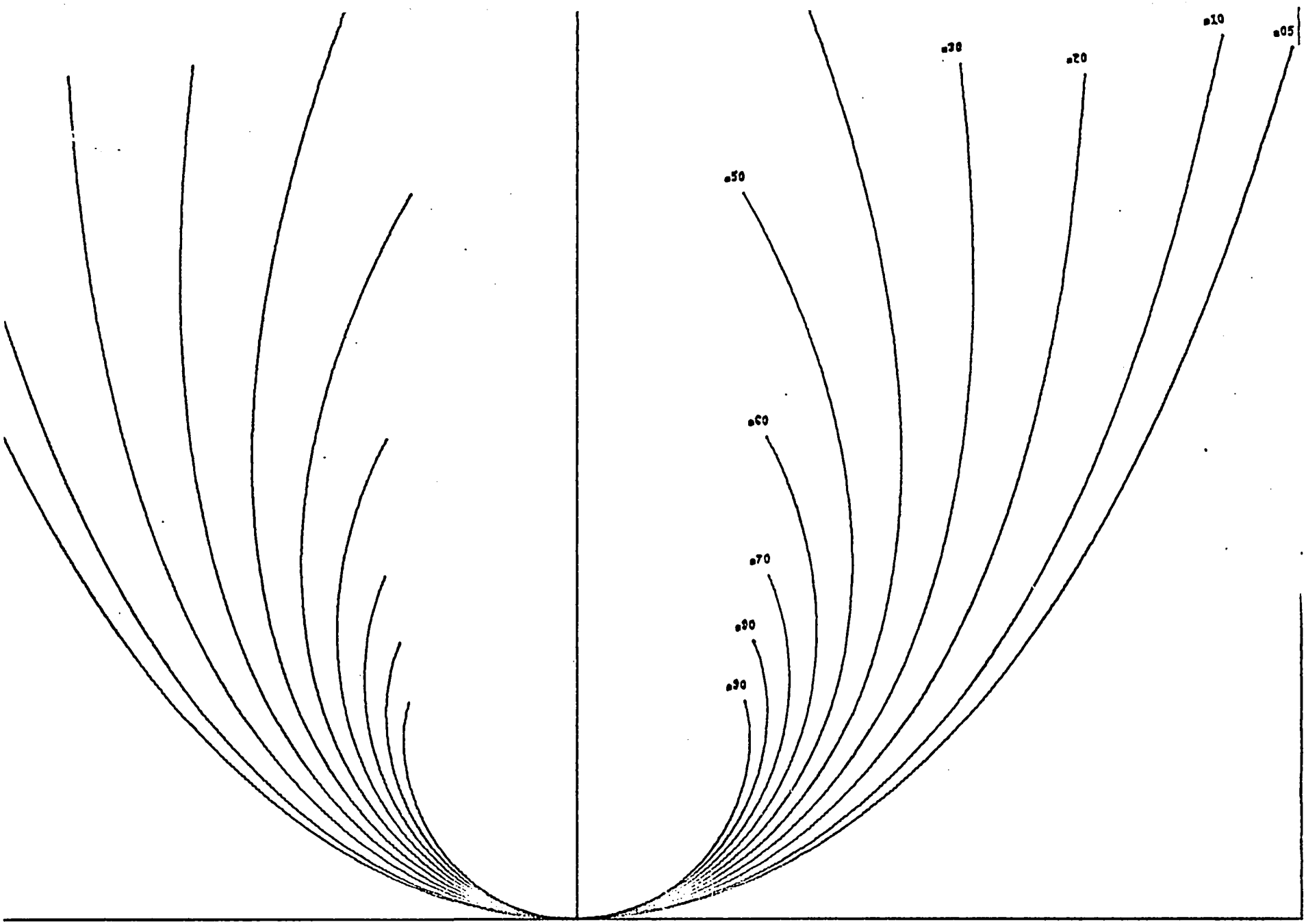

Fig. 4.3.5 A family of solutions of equation 4.3.5

SECTIONS FOR C = .50

are available. The best we can hope for is a visual comparison of the forms obtained with those of actual ammonoids.

One further consequence of this model is that the more muscular an ammonoid was, presumably the larger the value of R was, making its cross-section rounder and accordingly, less streamlined. On the other hand, if the aim was to produce a more streamlined cross-section, this could be done only at the expense of a loss in propulsive power, consequent to a decrease in the turgor of the mantle.

CHAPTER 5

CONCLUSIONS

It was originally expected that the models developed in this study would be tested against actual ammonoid morphologies. This, however, proved to be impossible due to, on the one hand, the absence of the pertinent data, and on the other, to the existence of non-unique solutions for the morphology resulting from a given set of conditions. As pointed out in sections 4.2 and 4.3, this last result may actually have played a role in the evolution of ammonoids and provide an explanation for the phenomenon of iterative evolution.

In the case of the descriptive models proposed in Chapter 3, however, the restrictions pointed out above do not apply, and the models have been successfully tested.

The positive results of this study can be outlined as follows:

1). A new theoretical model for organic growth has been proposed, together with procedures to fit the resulting equations to both longitudinal and cross-sectional data, as well as to anisometric growth. This model considers growth as a deterministic function of size and age, being affected by damping factors for both of these variables; it is considered that this new growth model is particularly appro-

priate to the growth of the molluscan shell and of other accretionary structures in whose growth diffusion plays an important role, but other types of growth might also fit this growth function well.

2). Most growth equations in common use are inappropriate to their objective, some of their consequences for growth being wholly determined by the form of the equation.

3). The allometry equation is a special case of a set of more general anisometry equations, produced when damping factors in growth are the same for both variates. The "power law" relation of variates in allometry is probably a result of the combination of two exponential processes.

4). Growth in different kinds of organisms need not follow the same laws. In particular, extracellular accretionary growth in which morphogenetic substances propagate by diffusion must have different laws than those governing cellular growth.

5). A new descriptive model for the molluscan shell is developed. Based on the harmonic analysis of the cross-section, it allows the separation of form into size and shape. This model is limited in its completeness only by the extent to which one wants to limit the proliferation of harmonics.

6). The complex ammonoid suture line is a non-rectifiable curve of fractional dimension. Its complication

and that of other comparable linear structures can be measured by means of a new index of complication, and comparisons between sutures can be made by the same index.

7). The suture line can be separated into two main components: one due to a regular fluctuating pattern inherited from the early stages of development (which, however, is distorted during growth due to allometry) and the second, a superimposed process that introduces complication.

8). The multiplication of mantle epithelial cells responsible for shell secretion in mollusks, took place primarily in the periumbilical region in the involute ammonoids.

9). The morphology of the ammonoid coiled spiral tube can be derived from a simple set of instructions governing the accretion of the shell at the mantle edge, which is governed by diffusion or diffusion-like phenomena. A consequence of this is that the morphology of the shell must be reflected in the shape of its growth lines.

10). The ectocochliate cephalopod cross-section can be reproduced by considering it as a line in static equilibrium, subjected to the deforming forces of its own weight and the turgidity of the mantle.

11). The phenomena of homeomorphy and iterative evolution have a common explanation, derived from the ability of ammonoids to produce similar morphologies starting from a different set of chemical and mechanical constraints.

REFERENCES

AGER, D.V. and E.A. RIGGS, 1964. The internal anatomy, shell growth and asymmetry of a devonian spiriferid. J. Paleont., 38, 749-760.

ARKELL, W.J., 1956. Jurassic geology of the world. Oliver and Boyd (Edinburgh and London), p.xv+804, 46pl.

ARKELL, W.J., B. KUMMEL and C.W. WRIGHT, 1957. Mesozoic Ammonoidea. In R.C. Moore, editor: Treatise on Invertebrate Paleontology, part L, Mollusca 4, p.L80-L465. Univ. Kansas Press, Lawrence.

BEVINGTON, P.R., 1969. Data reduction and error analysis for the physical sciences. 336p., McGraw Hill, N.Y.

BØGGILD, O.B., 1930. The shell structure of the molluscs. Mém. Acad. Roy. Sci. Lettres Danemark, Sec. Sci., Sér. 9, tome 2, no. 2: 235-326, pl. 1-15.

BONNER, J.T., 1968. Size change in development and evolution. J. Paleont., 42, no. 5, pt. II.

BRODY, S., 1945. Bioenergetics and growth. Reinhold, N.Y.

BUCKMAN, S.S., 1895. The Bajocian of the Mid-Cotteswolds. Q. Jour. Geol. Soc. London, 51, 388-563.

BURNABY, T.P., 1966. Allometric growth of ammonoid shells: a generalization of the logarithmic spiral. Nature, 209, 904-906.

CARTER, R.M., 1967. On Lison's model of bivalve shell form, and its biological interpretation. Proc. Malac. Soc. Lond., 37, 265-278.

CHAMBERLAIN, J.C. Jr., 1969. Technique of scale modelling of cephalopod shells. Palaeontology, 12, 48-55.

CHAMBERLAIN, J.C. Jr., 1971. Hydromechanics of the ectocochliate cephalopod shell. Abstracts Geol. Soc. Amer. Annual Meeting, Washington, D.C.

CLARK, W.E.L. and P. MEDAWAR, Eds., 1945. Essays on growth and form. Oxford, Clarendon Press.

COCK, A.G., 1966. Genetical aspects of metrical growth and form in animals. Quart . Rev. Biol., 41, 131-190.

CRANK, J., 1956. The mathematics of diffusion. Oxford, Clarendon Press. 347p.

DEGENS, E.T. and R.H. PARKER, 1967. Paleobiochemistry of molluscan shell proteins. Comp. Biochem. Physiol., 20, 553-579.

DIGBY, P.S.B., 1968. The mechanism of calcification in the molluscan shell. Symp. Zool. Soc. Lond., No. 22, 93-107.

DODD, J.R., 1967. Magnesium and strontium in calcareous skeletons: a review. Jour. Paleon., 41, 1313-1329.

DODD, J.R., 1969. Effect of light on rate of growth of bivalves. Nature, 224, 617-618.

DUBOIS, E., 1897. Ueber die Abhangigkeit des Hirngewichtes von der Körpergrösse bei den Säugetieren. Arch. Anthropol., 25, 1-28.

DUBOIS, E., 1922. Phylogenetic and ontogenetic increase of the volume of the brain in vertebrata. Proc. Koninklijke Akad. Wetensch. Amsterdam, 25.

EDELSTEIN, B.B., 1971. Cell specific diffusion model of morphogenesis. J. Theor. Biol., 30, 515-532.

EHRLICH, R. and B. WEINBERG, 1970. An exact method for characterization of grain shape. Jour. Sed. Petrol., 40, 1, 205-212.

EVANS, J.W., 1972. Tidal growth increments in the cockle Clinocardium nuttalli. Science, 176, 416-417.

FUKUTOMI, T., 1953. A general equation indicating the regular forms of mollusca shells, and its application to geology, especially in paleontology (1). Hokkaido Univ., Geophys. Bull., 3, 63-82.

GOEL, N.S., S.C. MAITRA and E.W. MONTROLL, 1971. On the Volterra and other nonlinear models of interacting populations. Rev. Modern Physics Monographs. Academic Press, n.y., viii+146p.

GOULD, S.J., 1966. Allometry and size in ontogeny and phylogeny. Biol. Rev., 41, 587-640.

GOULD, S.J., 1971. Geometric similarity in allometric growth: a contribution to the problem of scaling in the evolution of size. Amer. Naturalist, 105, 113-136.

GRÉGOIRE, C., 1962. On submicroscopic structure of the Nautilus shell. Bull. Inst. Roy. Sci. Nat. Belg., 38, 49, Bruxelles.

HALLAM, A. and N.B. PRICE, 1966. Sr contents of Recent and fossil aragonitic cephalopod shells. Nature, 212, 25-27.

HALLAM, A. and N.B. PRICE, 1968. Further notes on the Sr contents of unaltered fossil cephalopod shells. Geol. Mag., 105, 52-55.

HIRSCHFELD, W.J., 1970. Time series and exponential smoothing methods applied to the analysis and prediction of growth. Growth, 34, 129-143.

HÖLDER, H., 1960. Zur Frage des Wachstumsendes bei Ammoniten: Paläont. Zeitschr., 34, 61-68.

HUXLEY, J.S., 1932. Problems of Relative Growth. Methuen, London, xix 276p.

JOLICOEUR, P., 1963. The multivariate generalization of the allometry equation. Biometrics, 19, 497-499.

KLEIBER, M., 1961. The fire of life. Wiley, N.Y. 454p.

KUMMEL, B. and R.M. LLOYD, 1955. Experiments on relative streamlining of coiled cephalopod shells. Jour. Paleon., 29, 159-170.

LAIRD, A.K., 1966. Postnatal growth of birds and mammals. Growth, 30, 349-363.

LAIRD, A.K., S.A. TYLER and A.D. BARTON, 1965. Dynamics of normal growth. Growth, 29, 233-248.

LAPICQUE, L., 1907. Le poids encéphalique en fonction du poids corporel entre individus d'une même espèce. Bull. mém. Soc. anthropol. Paris, 8, 313-345.

LISON, L., 1949. Recherches sur la forme et la mecanique de développement des coquilles de Lamellibranches. Mém. Inst. Roy. des Sci. Nat. de Belgique. 2e serie, no. 34, 1-87.

LU, K.H., 1965. Harmonic analysis of the human face. Biometrics, 21, 491-505.

MacCLINTOCK, C., 1967. Shell structure of Patelloid and Bellerophontoid Gastropods (Mollusca). Peabody Mus. Nat. Hist., Yale Univ., Bull. 22.

McCAMMON, H.M., 1969. The food of articulate brachiopods. Jour. Paleon., 43, 976-985.

MANDELBROT, B., 1967. How long is the coast of Britain? Statistical self-similarity and fractional dimension. Science, 156, 636-638.

MARQUARDT, D.W., 1963. An algorithm for least-squares estimation of non-linear parameters. J. Soc. Ind. Appl. Math., 11, 2, 431-41.

MEDAWAR, P.B., 1945. Size, shape and age. In Essays on growth and form. W.E.L. Clark and P.B. Medawar, eds. Oxford, 157-187.

MOSELEY, H., 1838. On the geometrical forms of turbinated and discoid shells. Roy. Soc. Lond. Phil. Trans. for 1838, p.351-370.

MUTVEI, H., 1964. On the shells of Nautilus and Spirula with notes on the shell secretion in non-cephalopod molluscs. Arkiv. Mineral. Geol., Band 16, 221-78.

NAUMANN, C.F., 1840a. Beitrag zur Conchyliometrie. Ann. der Phys., Bd. 50, 5, 223-36.

NAUMANN, C.F., 1840b. Über die spiralen der ammoniten: op. cit., Bd. 51, 5, 245-59.

NAUMANN, C.F., 1845. Über die wahre Spiralen der Ammoniten: op cit., Bd. 64, 5, 538-43.

NEEDHAM, A.E., 1950. The form-transformation of the abdomen of the female pea-crab. Proc. Roy. Soc. Lond., B, 137, 115-136.

NEEDHAM, A.E., 1964. The growth process in animals. Van Nostrand, Princeton, N.J. 522p.

NOMURA, E., 1926. An application of $a=kb^x$ in expressing the growth relation in the freshwater bivalve Sphaerium heterodon Pils. Sci. Rep. Tohoku Imp. Univ. [4], 2, 57-62.

PALFRAMAN, D.F.B., 1968. A method of representing ammonoid suture lines. Jour. Paleon., 42, 4, 1082-4.

PANNELLA, G. and MacCLINTOCK, C., 1968. Biological and environmental rhythms reflected in molluscan shell growth. In Paleobiological aspects of growth and development, a symposium. Paleont. Soc. Mem. 2 (Jour. Paleont., 42, 5, supp.), 64-80.

PEARL, R. and L.J. REED, 1923. On the mathematical theory of population growth. Metron, 3, 6-19.

PFAFF, E., 1911. Über Form und bau der Ammonitensepten und ihre Beziehungen zur Suturlinie. 4. Jahr. Neidersächs. geol. Vereins Hannover, 207-223, pl. XI.

PIELOU, E.C., 1969. An introduction to mathematical ecology. Wiley-Interscience, N.Y. 286p.

PRESTON, F.W. and J.W. HARBAUGH, 1965. Special Distrib. Pub. 24, Kansas Geol. Survey.

RAUP, D.M., 1966. Geometrical analysis of shell coiling: general problems. Jour. Paleon., 40, 1178-90.

RAUP, D.M., 1967. Geometric analysis of shell coiling: coiling in ammonoids. Jour. Paleon., 41, 43-65.

RAUP, D.M., 1973. Depth inferences from vertically imbedded cephalopods. Lethaia, in press.

REYMENT, R.A., 1958. Some factors in the distribution of fossil cephalopods. Acta Univ. Stockholm. Stockholm Contrib. Geology, 5, 2, 19-39.

REYMENT, R.A., 1970. Vertically imbedded cephalopod shells. Some factors in the distribution of fossil cephalopods, 2. Palaeogeography, Paleoclimatol., Palaeoecol., 7, 103-111.

RHOADS, D.C. and G. PANNELLA, 1970. The use of molluscan shell growth patterns in ecology and paleoecology. Lethaia, 3, 143-161.

RICHARDS, O.W. and A.J. KAVANAGH, 1945. The analysis of growing form. In W.E. le Gros Clark and P.B. Medawar, eds., Essays on Growth and Form. Oxford Univ. Press, London, p.188-230.

RICHARDSON, L.F., 1961. The statistics of deadly quarrels. An addendum. General Systems, 6, 139-187.

RICKER, W.E., 1958. Handbook of computations for biological statistics of fish populations. Bull. Fish. Res. Bd. Canada, no. 119, 1-300.

RUDWICK, M.J.S., 1964. The inference of function from structure in fossils. Brit. J. Philos. Sci., 15 (57), 27-40.

SCHINDEWOLF, O.H., 1965. Studien aur Stammesgeschichte der Ammoniten. Abh. Akad. Wissensch. u. Lit., Math.-Naturwiss klasse, Jahrg., no. 3, 137-238.

SALFELD, H., 1913. Über Artbildung bei Ammoniten. Zeitschr. Deutsch. Geol. Gessell., Monatsber., Bd. 65, 437-40.

SNEATH, P.H.A., 1967. Trend-surface analysis of transformation grids. J. Zool., Lond., 151, 65-122.

SNELL, O., 1891. Das Gewicht des Gehirnes und des Hirnmantels der Säugetiere in Beziehung zu deren geistigen Fähigkeiten. Sitzungsberichte Ges. Morphol. Physiol. München, 7, 90-4.

SOKAL, R.R. and P.H.A. SNEATH, 1963. Principles of Numerical Taxonomy. Freeman, San Francisco. 359p.

SPRENT, P., 1967. Estimation of mean growth curves for groups of organisms. J. Theor. Biol., 17, 159-173.

STASEK, C.R., 1963. Geometrical form and gnomonic growth in bivalved mollusca. Jour. Morph., 112, 213-231.

STEINHAUS, H., 1954. Length, shape and area. Colloquium Math. 3, 1, 1-13.

STENZEL, H.B., 1963. Living Nautilus. In Treatise on invertebrate paleontology, R.C. Moore, ed. Geol. Soc. Amer. and Univ. Kansas Press. Part K, p.59-93.

TANNER, J.M., 1962. Growth at adolescence. 2nd ed. Blackwell, Oxford.

TEISSIER, G., 1960. Relative growth. In The Physiology of Crustacea. M. Talbot and H. Waterman, eds., Vol. 1, Academic Press, N.Y., p.537-560.

THOMPSON, D'A.W., 1917. On growth and form. 1st Edition. Cambridge Univ. Press.

THOMPSON, D'A.W., 1942. On growth and form. Cambridge Univ. Press. 1116p.

THOMPSON, T.E. and J.L. ONCLEY, 1961. A method for calculating differential diffusion coefficients in two component systems: application to glycine-water and bovine mercaptalbumin-buffer systems. J. Am. Chem. Soc., 83, 2425-2432.

TRUEMAN, A.E., 1941. The ammonite body chamber, with special reference to th e buoyancy and mode of life of the living ammonite. Qu. Jour., Geol. Soc. London, 96, 339-383.

TURING, A.M., 1952. The chemical basis of morphogenesis. Phil. Trans. Royal Soc. London, B, 237, 37-72.

TYRRELL, H.J.V., 1961. Diffusion and heat flow in liquids. Butterworths, London. 329p.

VAŠÍČEK, Z., 1967. A contribution to the solution of the ammonite spiral. Sborník vědeck praci Vysoké školy báňskě v Ostravě, Ročnik 13, no. 1, 107-113.

VINOGRADOV, A.P., 1953. The elemental chemical composition of marine organisms. Sears Foundation for Marine Research, Mon. 1, Yale Univ.

VON BERTALANFFY, L., 1960. In:fundamental aspects of normal and malignant growth. W.W. Nowinski, ed. Elsevier, Amsterdam.

WALNUT, T.H., 1967. A mathematical analysis of the changes in the size and shape of bones during growth. Growth, 31, 217-230.

WEAVER, W., 1955. Science and people. Science, 122, 1255-1259.

WESTERMANN, G.E.G., 1971. Form, structure and function of shell and siphuncle in coiled Mesozoic ammonoids. Life Sci. Contr., R. Ont. Mus., 78, 1-39, Toronto.

WILBUR, K.M., 1964. Shell formation and regeneration. In Physiology of Mollusca. K.M. Wilbur and C.M. Yonge, eds., Academic Press, N.Y., Ch. 8, xiii+473p.

WILBUR, K.M. and K. SIMKISS, 1968. Calcified shells. In Comprehensive Biochemistry. M. Florkin and E.H. Stotz, eds. Volume 26A, p.229-295. Elsevier, Amsterdam.

WRIGHT, S., 1926. Book review. J. Amer. Statist. Soc., 21, 493-97.

ZOTIN, A.I. and ZOTINA, R.S., 1967. Thermodynamic aspects of developmental biology. J. Theoret. Biol., 17, 57-75.

ZOTINA, R.S. and ZOTIN, A.I., 1972. Towards a phenomenological theory of growth. J. Theoret. Biol., 35, 213-225.

ZUCKERMAN, S., ed., 1950. A discussion on the measurement of growth and form. Proc. Royal Soc. London, B, 137, 433-523.

APPENDIX I

COMPUTER PROGRAMS TO FIT GROWTH AND ANISOMETRY EQUATIONS (EQUATIONS 2.3.3.4 AND 2.3.3.14)

I-A) Calculation of derivatives for parameter fit

Given $t = -\frac{1}{\alpha} \ln\left[\frac{\alpha}{K}\left\{F(1,\beta) - F(y,\beta)\right\}\right]$ A.1

Calculate $\frac{\partial y}{\partial \alpha}$, $\frac{\partial y}{\partial \beta}$, $\frac{\partial y}{\partial K}$ in:

$$F(y,\beta) = F(1,\beta) - \frac{K}{\alpha}\exp(-\alpha t) \quad \text{A.2}$$

$$\frac{\partial F(y,\beta)}{\partial \alpha} = -K\left\{-\alpha^{-1} t \exp(-\alpha t) - \alpha^{-2}\exp(1-\alpha t)\right\} \quad \text{A.3}$$

$$\left(\frac{1}{y} + \beta + \ldots + \frac{\beta^n y^{n-1}}{n!} + \ldots\right)\frac{\partial y}{\partial \alpha} = \frac{K}{\alpha}\exp(-\alpha t)\left\{t + \frac{1}{\alpha}\right\} \quad \text{A.4}$$

$$\frac{\partial y}{\partial \alpha} = \frac{\frac{K}{\alpha}(t+\frac{1}{\alpha})\exp(-\alpha t)}{F'\alpha K\,(y,\beta)} \quad \text{A.5}$$

$$\frac{\partial F\,(y,\beta)}{\partial \beta} = \frac{\partial F\,(1,\beta)}{\partial \beta} \quad \text{A.6}$$

$$\left(\frac{1}{y} + \beta + \ldots + \frac{\beta^n y^{n-1}}{n!} + \ldots\right)\frac{\partial y}{\partial \beta} + y \ldots + \frac{(\beta y)^{n-1} y}{n!} + \ldots$$

$$= 1 + \ldots + \frac{\beta^{n-1}}{n!} + \ldots \quad \text{A.7}$$

$$\frac{\partial y}{\partial \beta} = \frac{1-y + \frac{\beta(1-y^2)}{2!} + \ldots + \frac{\beta^{n-1}(1-y^n)}{n!} + \cdots}{F'_{\alpha K}(y,\beta)} = \frac{F'(y,\beta)}{F'_{\alpha K}(y,\beta)} \qquad \text{A.8}$$

$$\frac{\partial F(y,\beta)}{\partial K} = \frac{-\exp(-\alpha t)}{\alpha} \qquad \text{A.9}$$

$$\frac{\partial y}{\partial K} = \frac{-\exp(-\alpha t)}{\alpha F'_{\alpha K}(y,\beta)} \qquad \text{A.10}$$

I-B) Parameter values

α, β, K, y_o, y_{jo}, $_{jf}$

Program GRØFIT finds (by the method of steepest descent) the parameters α, β and K, given a set of $t_{(i)}$, $y_{(i)}$ values; y_o is calculated then from:

$$F(y_o,\beta) = F(1,\beta) - \frac{K}{\alpha} \qquad \text{B.1}$$

Program ANSFIT calculates $\frac{K_i}{\alpha_i}$, $\frac{K_j}{\alpha_j}$, $\frac{\alpha_j}{\alpha_i}$, β_i, β_j and y_{jf} to fit the equation

$$F(y_j,\beta_j) = F(y_{jf},\beta_j) - \frac{K_j}{\alpha_j}\left[\frac{\alpha_i}{K_i}\left\{F(1,\beta_i) - F(y_i,\beta_i)\right\}\right]^{\alpha_j/\alpha_i} \qquad \text{B.2}$$

given a set of cross-sectional data, $y_{i(n)}$, $y_{j(n)}$.

Fit of data to anisometry equation

The problem is to determine the following six parameters:

$$1/a_1 = K_i/\alpha_i$$

$$a_2 = K_j/\alpha_j$$

$$a_3 = \alpha_j/\alpha_i$$

$$a_4 = \beta_i$$

$$a_5 = \beta_j$$

$$a_6 = Y_{jf}$$

Given a collection of points, YI(N), YJ(N), find the equation

$$F(y_j,\beta_j) = F(y_{jf},\ \beta_j) - \frac{K_j}{\alpha_j}\left[\frac{\alpha_i}{i}\left\{F(1,\beta_i) - F(y_i,\beta_i)\right\}\right]^{\alpha_j/\alpha_i} \qquad B.3$$

It is necessary to provide estimates of the coefficients

AE (A estimate)

AE (6) = YJ (K), K being the index number of the last pair of data points.

AE (5) = 0.10

AE (4) = 0.10

AE (3) = 1.0

AE (2) = F J 1 - F (YJ (1), 0.10)

AE (1) = 1. (F 1 - F (YI(1), 0.10)

In fitting growth data to equation 2.3.3.14:

$$F(y,a_5) = F(a_6,a_5) - a_2\left[a_1\left\{F(1,a_4) - F(x,a_4)\right\}\right]^{a_3} \qquad \text{B.4}$$

Then, taking partial derivatives with respect to each of the 6 parameters a_i:

$$\frac{\partial F(y,a_5)}{\partial a_1} = -a_2\, a_3\, a_1^{a_3-1}\left\{F(1,a_4) - F(x,a_4)\right\} \qquad \text{B.5}$$

from where:

$$\frac{\partial y}{\partial a_1} = \frac{a_2\, a_3\, a_1^{a_3-1}\left\{F(1,a_4) - F(x,a_4)\right\}^{a_3}}{F'_{\alpha K}(y,a_5)} \qquad \text{B.6}$$

$$\frac{\partial y}{\partial a_2} = \frac{\left[a_1\left\{F(1,a_4) - F(x,a_4)\right\}\right]^{a_3}}{F'_{\alpha K}(y,a_5)} \qquad \text{B.7}$$

$$\frac{\partial y}{\partial a_3} = -\frac{a_2\left[a_1\left\{F(1,a_4) - F(x,a_4)\right\}\right]^{a_3} \ln\left[a_1\left\{F(1,a_4)-F(x,a_4)\right\}\right]}{F'_{\alpha K}(y,a_5)} \qquad \text{B.8}$$

$$\frac{\partial F(y,a)}{\partial a_4} = -a_2\, a_3\, a_1^{a_3}\left\{F(1,a^4) - F(x,a^4)\right\}^{a_3-1} F'(x,a_4) \qquad \text{B.9}$$

$$\frac{\partial y}{\partial a_4} = \frac{-a_1^{a_3}\, a_2\, a_3\left\{F(1,a_4) - F(x,a_4)\right\}^{a_3-1} F'(x,a_4)}{F'\alpha_K(y,a_5)} \qquad \text{B.10}$$

$$\frac{\partial F(y,a_5)}{\partial a_5} = \frac{\partial F(a_6,a_5)}{\partial a_5} \qquad \frac{\partial y}{\partial a_5} = \frac{F'(y,a_5) - F'(a_6,a_5)}{F'_{\alpha K}(y,a_5)} \qquad \text{B.11}$$

$$\frac{\partial F(y,a_5)}{\partial a_6} = \frac{\partial F(a_6,a_5)}{\partial a_6} = F'_{\alpha K}(a_6, a_5) \qquad \text{B.12}$$

$$\frac{\partial y}{\partial a_6} = \frac{F'_{\alpha K}(a_6,a_5)}{F'_{\alpha K}(y,a_5)} \qquad \text{B.13}$$

Where
$$F'_{\alpha K}(y,\beta) = \frac{1}{y} + \beta + \frac{\beta^2 y}{2!} + \ldots + \frac{\beta^n y^{n-1}}{n!} + \ldots + \qquad \text{B.14}$$

and
$$F'(y,\beta) = 1 - y + \frac{\beta(1-y^2)}{2!} + \ldots + \frac{\beta^{n-1}(1-y^n)}{n!} + \ldots + \qquad \text{B.15}$$

I-C) Program listings

These programs are listed here only for the benefit of those who would like to apply the double-damped equation for growth or the anisometry equation directly. The programs require a subroutine for matrix inversion like subroutine MATINV in Bevington (1969)

```
      PROGRAM GROFIT (INPUT,OUTPUT,TAPE5=INPUT,TAPE6=OUTPUT)
C     THIS PROGRAM FITS THE PARAMETERS OF THE DOUBLE-DAMPED GROWTH
C     EQUATION TO LONGITUDINAL GROWTH DATA. THE PROGRAM IS SET UP TO
C     GENERATE THE GROWTH DATA FROM THE EQUATION AND THEN DO A FIT
C     TO THESE THEORETICAL DATA, TO ILLUSTRATE THE DOUBLE-DAMPED
C     GROWTH EQUATION. TO FIT ACTUAL DATA ,LOOP 50 SHOULD BE
C     ELIMINATED AND T(N)-TIME AND Y(N)-SIZE READ IN.
C     THE METHOD USES MARQUARDT,S ALGORITHM FOR STEEPEST DESCENT,
C     WITH LINEARIZATION IN THE NEIGHBOURHOOD OF THE SOLUTION.
C     ALL FUNCTIONS AND SUBROUTINES NEEDED WITH THE EXCEPTION
C     OF MATINV ARE LISTED WITH PROGRAM ANSFIT.
  101 FORMAT (2F5.2)
  102 FORMAT (1H1,5X,1HI,10X,4HT(I),10X,4HY(I),7X,7HYFIT(I),7X,4HT(I+,I2
     1,1H),7X,4HY(I+,I2,1H),4X,7HYFIT(I+,I2,1H),21H    ORIGINAL ALPHA =
     2,F4.2,11H    BETA = F4.2//)
  103 FORMAT ((5X,I2,5F14.4))
  105 FORMAT (1H0,5X,59HCRITICAL DATA FOR GROWTH CURVE WITH PARAMETERS..
     1.  ALPHA = ,F5.3,10H   BETA = ,F5.3,7H   C = ,F7.4/7X,7HAT T = ,F8
     2.4,14H AND SIZE Y = ,F7.5,29H MAXIMUM GROWTH RATE YPMAX = ,F8.6,23
     3H      TMAX = T(.999) = ,F8.4/5X,11HSIGALPHA = ,F6.3,5X,10HSIGBETA
     4 = ,F6.3,6X,9HSIGMAC = ,F6.3,6X,9HCHISQR = ,F8.4//)
      DIMENSION T(100),Y(100),A(3),SIGMAA(3),YFIT(100)
      Y(1) = 0.10     $    FMIN1 = EXP(-1.0)      $    T(1) = 0.0
    1 READ (5,101) ALPHA,BETA
      IF (ALPHA.GT.10.0) GO TO 888
      ASAVE = ALPHA     $    BSAVE = BETA
      DELYMX = -1000.          $    KAKA = 0
      F1 = F(1.,BETA)
      CA = F1-F(Y(1),BETA)     $    C = CA*ALPHA
      SOL = Y(1)
      K = 100
      DO 50 N=2,100
      T(N) = 1.5*FLOAT(N-1)      $    TI = T(N)
      CALL SODOM (0,BETA,CA,BETAJ, TI ,ALPHA,F1,FJ1,YI,0.05,SOL)
      Y(N) = SOL      $    YI = Y(N)
      DELY = YI - Y(N-1)
      IF (DELY.LE.DELYMX) GO TO 48
C        YDELMX = SIZE AT WHICH GROWTH IS MAXIMUM
      DELYMX = DELY     $    YDELMX = YI
   48 IF (YI .GT. 0.99) GO TO 49
      GO TO 50
    4 K = N     $   GO TO 51
   50 CONTINUE
   51 FLAMDA = 0.001
      A(1) = 4./FLOAT(K)    $    A(2) =(-.038024262+SQRT(.038024262**2-4.*
     1.000866241*(YDELMX-FMIN1)))/2.*.000866241
      A(3) =A(1)*(F(1.,A(2)) - F(Y(1),A(2)))
   52 KAKA = KAKA + 1
      CALL CURFIT (T,Y,SIGMAY,K,3,0,A,SIGMAA,FLAMDA,YFIT,CHISQR)
      IF (CHISQR.GT.0.0001.OR.KAKA.LE.10) GO TO 52
      J = FLOAT(K/2) + 0.5
      WRITE (6,102) J,J,J,ASAVE,BSAVE
      WRITE(6,103)(I,T(I),Y(I),YFIT(I),T(I+J),Y(I+J),YFIT(I+J),I=1,J)
      ALPHA = A(1)    $    BETA = A(2)    $    C = A(3)    $    CA = C/ALPHA
      F1 = F(1.,BETA)
      TMAX = -ALOG(F1 - F(.999,BETA)/CA)/ALPHA
      YYPMAX = FMIN1 - .038024262*BETA - .000866241*BETA**2
      TYPMAX = -ALOG((F1 - F(YYPMAX,BETA))/CA)/ALPHA
      YPMAX = C*YYPMAX*EXP(-ALPHA*TYPMAX-BETA*YYPMAX)
```

```
      PROGRAM ANSFIT (INPUT,OUTPUT,TAPE5=INPUT,TAPE6=OUTPUT)
  101 FORMAT (6F5.2)
  102 FORMAT (1H1,5X,1HI,10X,4HY(I),9X,5HYJ(I),6X,8HYJFIT(I),7X,4HY(I+,I
     12,1H),6X,5HYJ(I+,I2,1H),3X,8HYJFIT(I+,I2,1H)//)
  103 FORMAT ((5X,I2,6F14.4))
  104 FORMAT (1H0,1X,29HORIGINAL PARAMETERS...  CA = ,F5.2,11H    CJAJ =
     1 ,F5.2,11H    AJAI = ,F5.2,11H    BETA = ,F5.2,12H    BETAJ = ,F5.
     22/10X, 6HYJF = ,F5.2,10H    YJ0 = ,F5.3/1X,29HCALCULATED PARAMETER
     3S.. CA = ,F6.3,10H   CJAJ = ,F6.3,10H   AJAI = ,F6.3,10H   BETA =
     4,F6.3,11H   BETAJ = ,F6.3/9X,6HYJF = ,F6.3,9H   YJ0 = ,F6.3,8H   Y
     50 = ,F5.3//)
  106 FORMAT (1H0,5X,9HCHISQR = ,F8.5,33H    STANDARD DEVIATIONS...  CA
     1= ,F6.3,11H    CJAJ = ,F6.3,11H    AJAI = ,F6.3/30X, 7HBETA = ,F6.
     23,12H    BETAJ = ,F6.3,10H    YJF = ,F6.3)
      DIMENSION Y(100),YJ(100),SIGMAY(100),A(6),SIGMAA(6),YFIT(100)
      YSTEP = 1.0/110.    $   EMIN1 = EXP(-1.0)
    1 READ (5,101) ALPHA,BETA,ALPHAJ,BETAJ,CJAJ,YJF
      IF (ALPHA.GT.10.) GO TO 888
      F1 = F(1.,BETA)   $   FJ1 = F(YJF,BETAJ)    $   YJA = 0.10
      CA = F1 -  F(0.1,BETA)
      AJAI = ALPHAJ/ALPHA    $   YJ0 = 0.10
      CALL SODOM (0,BETAJ,CJAJ,BETAJ,0.0,0.0,FJ1,FJ1,YI,0.03,YJ0)
      CASAVE = CA   $   CJSAVE = CJAJ   $   AJSAVE = AJAI
      BSAVE = BETA   $   BJSAVE = BETAJ   $   YJFSAV = YJF
      YJOSAV = YJ0   $   K = 100   $   Y(1) = 0.1   $   YJ(1) = YJ0
      DO 50 N=2,100
      Y(N) = 0.1 + FLOAT(N-1)*YSTEP    $   YI = Y(N)
      CALL SODOM (1,BETA,CA,BETAJ,CJAJ,AJAI,F1,FJ1,YI,0.05,YJA)
      IF (YJA.GT.1.5) GO TO 49    $   GO TO 50
   49 K = N-1   $   GO TO 51
   50 YJ(N) = YJA
   51 FLAMDA = 0.001    $   KAKA = 0
      A(1) = 1./(F1 - F( Y(1),0.10))   $   A(2) = FJ1 - F(YJ(1),0.10)
      A(3) = 1.0   $   A(4) = 0.1   $   A(5) = 0.1   $   A(6) = YJ(K)
   52 KAKA = KAKA + 1
      CALL CURFIT(Y,YJ,SIGMAY,K,6,0,A,SIGMAA,FLAMDA,YFIT,CHISQR)
      IF (CHISQR.GT.0.01.OR.KAKA.LT.5) GO TO 52
      J = FLOAT(K/2) + 0.5   $   IF (2*J-K) 53,53,54
   54 J = J - 1
   53 WRITE (6,102) J,J,J
      WRITE(6,103)(I,Y(I),YJ(I),YFIT(I),Y(I+J),YJ(I+J),YFIT(I+J),I=1,J)
      CA = 1./A(1)   $   CJAJ = A(2)   $   AJAI = A(3)   $   BETA = A(4)
      BETAJ = A(5)   $   YJF = A(6)   $   F1 = F(1.,BETA)
      FJ1 = F(YJF,BETAJ)      $   Y0 = 0.098
      CALL SODOM (0,BETA,CA,BETAJ,     0.0,0.0,F1,FJ1,0.,0.03,Y0)
      CALL SODOM (0,BETAJ,CJAJ,BETAJ,     0.0,0.0,FJ1,FJ1,0.,0.03,YJ0)
      WRITE (6,104) CASAVE,CJSAVE,AJSAVE,BSAVE,BJSAVE,YJFSAV,YJOSAV,CA,
     1CJAJ,AJAI,BETA,BETAJ,YJF,YJ0,Y0
      WRITE (6,106) CHISQR, (SIGMAA(I), I=1,6)
      GO TO 1
  888 STOP
      END
      SUBROUTINE CURFIT (X,Y,SIGMAY,NPTS,NTERMS,MODE,A,SIGMAA,FLAMDA,
     1 YFIT,CHISQR)
      DIMENSION X(100),Y(100),SIGMAY(100),A(6),SIGMAA(6),YFIT(100),DERIV
     1(6),WEIGHT(100),BETA(6),B(6),ALPHA(6,6),ARRAY(6,6)
      NFREE = NPTS - NTERMS    $   IF (NFREE) 13,13,20
   13 CHISQR = 0.    $   GO TO 110
   20 DO 30 I=1,NPTS
```

```
 21 IF (MODE) 22,27,29
 22 IF (Y(I)) 25,27,23
 23 WEIGHT(I) = 1./Y(I)          $    GO TO 30
 25 WEIGHT(I) = 1./(-Y(I))       $    GO TO 30
 27 WEIGHT(I) = 1.               $    GO TO 30
 29 WEIGHT(I) = 1./SIGMAY(I)**2
 30 CONTINUE
 31 DO 34 J=1,NTERMS             $    BETA(J) = 0.
    DO 34 K=1,J
 34 ALPHA(J,K) = 0.
 41 DO 50 I=1,NPTS               $    YVAL = Y(I)
    IF (NTERMS.GT.3) GO TO 35
    CALL FDERIV (X,Y,I,A,DERIV)        $    GO TO 36
 35 CALL FDARIV (X,Y,I,A,DERIV)
 36 DO 46 J=1,NTERMS
    BETA(J) = BETA(J) + WEIGHT(I)*(Y(I)-FUNCTN(X,I,NTERMS,A,YVAL))*DER
   1IV(J)
    DO 46 K=1,J
 46 ALPHA(J,K) = ALPHA(J,K) + WEIGHT(I)*DERIV(J)*DERIV(K)
 50 CONTINUE
 51 DO 53 J=1,NTERMS
    DO 53 K=1,J
 53 ALPHA(K,J) = ALPHA(J,K)
 61 DO 62 I=1,NPTS
    YVAL = Y(I)
 62 YFIT(I) = FUNCTN (X,I,NTERMS,A,YVAL)
 63 CHISQ1 = FCHISQ(Y,SIGMAY,NPTS,NFREE,MODE,YFIT)
 71 DO 74 J=1,NTERMS
    DO 73 K=1,NTERMS
 73 ARRAY(J,K) = ALPHA(J,K)/SQRT(ALPHA(J,J) * ALPHA(K,K))
 74 ARRAY(J,J) = 1. + FLAMDA
 80 CALL MATINV (ARRAY,NTERMS,DET)
 81 DO 84 J=1,NTERMS
    B(J) = A(J)
    DO 84 K=1,NTERMS
 84 B(J) = B(J) + BETA(K)*ARRAY(J,K)/SQRT(ALPHA(J,J)*ALPHA(K,K))
 91 DO 92 I=1,NPTS
    YVAL = Y(I)
 92 YFIT(I) = FUNCTN (X,I,NTERMS,B,YVAL)
 93 CHISQR = FCHISQ (Y,SIGMAY,NPTS,NFREE,MODE,YFIT)
    IF (CHISQ1-CHISQR) 95,101,101
 95 FLAMDA = 10.*FLAMDA     $    GO TO 71
101 DO 103 J=1,NTERMS
    A(J) = B(J)
103 SIGMAA(J) = SQRT(ARRAY(J,J)/ALPHA(J,J))
    FLAMDA = FLAMDA/10.
110 RETURN
    END
    SUBROUTINE FDARIV (X,Y,I,A,DERIV)
    DIMENSION X(1),Y(1),A(6),DERIV(6)
    XI = X(I)     $     YI = Y(I)
    FIX = F(1.,A(4)) - F(XI,A(4))
    FPAY = FPAK(YI,A(5))
    DERIV(1) = -A(2)*A(3)*(A(1)*FIX)**(A(3)-1.)*FIX/FPAY
    DERIV(2) = -(A(1)*FIX)**A(3)/FPAY
    DERIV(3) = -A(2)*(A(1)*FIX)**A(3)*ALOG(A(1)*FIX)/FPAY
    DERIV(4) = -A(1)*A(2)*A(3)*(A(1)*FIX)**(A(3)-1.)*FP(XI,A(4))/FPAY
    DERIV(5) = (FP(YI,A(5))-FP(A(6),A(5)))/FPAY
```

```
      DERIV(6) = FPAK(A(6),A(5))/FPAY
      RETURN
      END
      SUBROUTINE SODOM (MODE,BETA,CA,BETAJ,CJAJ,AJAI,F1,FJ1,YI,YIN,ROOT)
         TO USE IN MODE 0, PUT ALPHA IN AJAI, T(N) IN CJAJ.
      Y1 = ROOT - YIN    $    Y2 = ROOT + YIN       $    J = 1
    5 IF (Y1.LE.0.0) Y1=0.001    $    IF (MODE) 1,2,3
    1 PY1=EXP(-BETA*Y1)*(1.-BETA*Y1)*(F1 - F(Y1,BETA)) - 1.
      PY2=EXP(-BETA*Y2)*(1.-BETA*Y2)*(F1 - F(Y2,BETA)) - 1.
      GO TO 4
    2 PY1 = F1-F(Y1,BETA) - CA*EXP(-AJAI*CJAJ)
      PY2 = F1-F(Y2,BETA) - CA*EXP(-AJAI*CJAJ)    $    GO TO 4
    3 PY1 = FJ1 - F(Y1,BETAJ)- CJAJ*((F1-F(YI,BETA))/CA)**AJAI
      PY2 = FJ1 - F(Y2,BETAJ)- CJAJ*((F1-F(YI,BETA))/CA)**AJAI
    4 IF (PY1*PY2) 11,12,13
   13 Y2 = Y2 + YIN  $  Y1 = Y1 - YIN
      J = J + 1     $    IF (J.GT.10) GO TO 23    $    GO TO 5
   23 WRITE (6,130) MODE,Y1,Y2,YI,PY1,PY2,BETA,BETAJ,CA
  130 FORMAT (80H FUNCTION VALUES WITH INITIAL Y VALUES ARE NOT OF OPPOS
     1ITE SIGNS. CHANGE INPUTS./5X,7HMODE = ,I2,10H      Y1 = ,F5.3,10H
     2    Y2 = ,F5.3,10H      YI = ,F5.3,11H      PY1 = ,F8.4, 9H     PY2 =
     3,F8.4/10X,  7HBETA = ,F5.3,13H      BETAJ = ,F5.3, 11H       CA = ,F
     45.3/)
      ROOT = Y1                          $    RETURN
   12 IF (PY1) 14,15,14
   15 WRITE (6,150) Y1   $    ROOT = Y1                                $  RETURN
  150 FORMAT (22H THE INPUT VALUE, Y = ,F6.3,27H IS A ROOT OF THE EQUATI
     1ON.)
   14 IF (PY2) 16,17,16
   17 WRITE (6,150) Y2
      ROOT = Y2                          $  RETURN
   16 WRITE (6,160)
  160 FORMAT (54H ERROR.PY1 AND PY2 NOT ZERO THOUGH PRODUCT TESTS ZERO.)
      ROOT = Y1                          $    RETURN
         BEGIN INTERVAL HALVING PROCESS. LIMIT TO 25 TIMES.
   11 DO 30 I=1,25
      Y = (Y1 + Y2)/2.
      IF (MODE) 31,32,33
   31 PY =EXP(-BETA*Y )*(1.-BETA*Y )*(F1 - F(Y,BETA)) - 1.
      GO TO 34
   32 PY  = F1 - F(Y,BETA) - CA*EXP(-AJAI*CJAJ)    $    GO TO 34
   33 PY  = FJ1 - F(Y,BETAJ) - CJAJ*((F1-F(YI,BETA))/CA)**AJAI
   34 IF (ABS(PY )-.001)  18,18,19
   19 IF (PY1*PY ) 20,21,22
   20 Y2 = Y    $    GO TO 30
   22 Y1 = Y    $    PY1 = PY
   30 CONTINUE
      WRITE (6,204)
  204 FORMAT (33H NON-CONVERGENT IN 25 ITERATIONS.)
      WRITE (6,106) Y,PY,Y1,Y2,PY2
  106 FORMAT (8H AT Y = ,F10.7,8H P(Y) = ,F10.6,10H      Y1 = ,F8.6,10H
     1    Y2 = ,F8.6,11H      PY2 = ,F10.6)
      ROOT = Y                           $    RETURN
   21 WRITE (6,205)
  205 FORMAT (7H ERROR.)
   18 ROOT = Y                           $    RETURN
      END
      FUNCTION F(X,BETA)
```

```
 99 FORMAT (1H0,10X,29HATROCIOUS ERROR.          X = ,F10.5,10X,7HBETA
   1= ,F10.5//)
100 FORMAT (1H ,10X,3(F10.6,5X),14HNOT CONVERGENT)
    IF (X) 1,1,2
  1 WRITE (6,99) X,BETA
    F = 0.1      $     RETURN
  2 LFACT=1               $                 SUM = 0.0
    DO 10 L=1,20
    TERM = (BETA*X)**L/FLOAT(L*L*LFACT)
    IF (ABS(TERM) - .0001)  20,20,10
 10 SUM = SUM + TERM
    WRITE (6,100) X,BETA,TERM
 20 F = ALOG(X) + SUM
    RETURN
    END
    FUNCTION FCHISQ (Y,SIGMAY,NPTS,NFREE,MODE,YFIT)
    DIMENSION Y(NPTS),SIGMAY(NPTS),YFIT(NPTS)
 11 CHISQ = 0.
 12 IF (NFREE) 13,13,20
 13 FCHISQ = 0.          $      GO TO 40
 20 DO 30 I=1,NPTS
 21 IF (MODE) 22,27,29
 22 IF (Y(I)) 25,27,23
 23 WEIGHT = 1./Y(I)              $     GO TO 30
 25 WEIGHT = 1./(-Y(I))           $     GO TO 30
 27 WEIGHT = 1.                   $     GO TO 30
 29 WEIGHT = 1./SIGMAY(I)**2
 30 CHISQ = CHISQ + WEIGHT*(Y(I)-YFIT(I))**2
 31 FREE = NFREE
 32 FCHISQ = CHISQ/FREE
 40 RETURN
    END
    FUNCTION FP (Y,BETA)
  3 FORMAT (1H0,5X,23HNONCONVERGENT      SUM = ,F8.4,12H      TERM = ,F8
   1.6,9H      Y = ,F6.4,12H      BETA = ,F6.4,12H           FP)
    FP  = 0.    $   LFACT = 1
    DO 1 L=1,20
    TERM = BETA**(L-1)*(1.-Y**L)/FLOAT(LFACT*L)
    IF (ABS(TERM) - .0001)  2,2,1
  1 FP = FP + TERM
    WRITE (6,3) SUM,TERM,Y,BETA
  2 RETURN
    END
    FUNCTION FPAK (Y,BETA)
  3 FORMAT (1H0,5X,23HNONCONVERGENT      SUM = ,F8.4,12H      TERM = ,F8
   1.6,9H      Y = ,F6.4,12H      BETA = ,F6.4,12H          FPAK)
    SUM = 0.    $   LFACT = 1
    DO 1 L=1,20
    TERM = (BETA**L)*Y**(L-1)/FLOAT(LFACT*L)
    IF (ABS(TERM) - .0001)  2,2,1
  1 SUM = SUM + TERM
    WRITE (6,3) SUM,TERM,Y,BETA
  2 FPAK = 1./Y + SUM
    IF (FPAK) 4,5,6
  4 IF (FPAK.GT.-0.001) FPAK = -0.001     $   GO TO 7
  5 FPAK = 0.001     $     GO TO 7
  6 IF (FPAK.LT.0.001) FPAK= 0.001
  7 RETURN
```

```
      WRITE (6,105) ALPHA,BETA,C,TYPMAX,YYPMAX,YPMAX,TMAX,SIGMAA(1),SIGM
     1AA(2),SIGMAA(3),CHISQR
      GO TO 1
  888 STOP
      END
```

```
END
FUNCTION FUNCTN (X,I,NTERMS,A,YVAL)
DIMENSION X(1),A(6)
XI = X(I)
CA = 1./A(1)    $    CJAJ = A(2)    $    AJAI = A(3)    $    BETA = A(4)
BETAJ = A(5)    $    YJF = A(6)    $    FJ1 = F(YJF,BETAJ)
F1 = F(1.,BETA)
CALL SODOM (1,BETA,CA,BETAJ,CJAJ,AJAI ,F1,FJ1,XI,0.05,YVAL)
FUNCTN = YVAL
RETURN
END
```